NATURAL KILLER CELL ANTIBODY RECEPTOR ENGAGEMENT IN ANTIBODY-MEDIATED ALLOGRAFT REJECTION

By

MICHAEL DAVID PARKES

A thesis submitted in partial fulfillment of the requirements for the degree of

MASTER OF SCIENCE

DEPARTMENT OF MEDICINE
UNIVERSITY OF ALBERTA

Page left intentionally blank

ABSTRACT

Background: NK cells are a key cellular component of antibody-mediated rejection (ABMR), but their role in ABMR has not been identified. We postulated that NK cells are stimulated through their CD16a antibody receptors by donor-specific anti-HLA antibodies in ABMR. There is currently no direct evidence supporting this phenomenon, although it is often assumed to occur. Given some of the similarities between NK cells and CD8 effector T cells that drive T cell-mediated rejection (TCMR), we further hypothesized that some CD16a-inducible NK cell transcripts are also induced by T cell receptor (TCR) stimulation of CD8 T cells in TCMR.

Methods: We characterized transcripts that were CD16-inducible in NK primary human NK cells *in vitro*, and studied their expression in human kidney transplant biopsies with ABMR. We used an extended human cell panel to determine these transcripts' selectivity for NK cells. We also examined these transcripts' expression in primary human CD8 T cells stimulated *in vitro* through CD3/TCR. *In vitro* soluble mediator production by CD16a-stimulated NK cells and CD3/TCR-stimulated CD8 T cells was assessed using a multiplex platform.

Results: 276 transcripts were increased in CD16a-stimulated versus unstimulated NK cells (FC>2x, FDR<0.05), including *IFNG, TNF, CSF2,* multiple proinflammatory chemokines (e.g. *CCL3, CCL4, XCL1*) and modulators of NK cell effector functions (e.g. *TNFRSF9, CRTAM, CD160*). Many CD16a-inducible

transcripts were also CD3/TCR-inducible in CD8 T cells. Multiplex analysis of 30 different soluble mediators in stimulated NK cell and CD8 T cell culture supernatants revealed that both produced CCL3, CCL4, IFNG, TNF, and CSF2, but not the other 25 mediators. Eight of the top 30 CD16a inducible transcripts were strongly associated with ABMR, including NK-selective transcripts *CD160* and *XCL1*. Many NK cell transcripts such as *GNLY* and *SH2D1B* were increased in ABMR but were not CD16a-inducible, probably reflecting NK cell localization. 12 of the top 30 CD16a-inducible transcripts were highly associated with TCMR, and six of these were strongly associated with ABMR as well.

Conclusions: The association of NK cell-selective transcripts with ABMR provides direct evidence of CD16a-mediated NK cell activation in ABMR. The overlap in CD3/TCR-inducible and CD16a-inducible transcripts and soluble mediators illustrates shared effector potential between NK cells and CD8 T cells. Top CD16a-inducible ABMR-associated NK cell transcripts are also associated with TCMR because they are strongly inducible in CD8 T cells following CD3/TCR stimulation.

PREFACE

Parts of this work have been submitted for publication in peer-reviewed journals. A paper for which I was the primary author was submitted to *Transplantation* and is pending review at the time of writing of this work, and another is in preparation for submission to the same journal. Drs. Phil Halloran and Luis Hidalgo provided significant guidance in study design and content review for both papers. I was responsible for data collection, analysis, and writing these papers. The submitted paper presents evidence of CD16a-mediated NK cell activation in ABMR, and contains data pertaining to some of the analyses in chapter 5, specifically **Tables 5.2, 5.3,** and **5.4**, and **Figures 5.1** and **5.3**. The paper in preparation for submission deals with the overlap between CD16a-inducible NK cell transcripts in ABMR and CD3/TCR-inducible CD8 T cell transcripts in TCMR, and contains data pertaining to all analyses outlined in chapter 6. **Figure 7.1** is my own work and has been published in Nature Reviews Nephrology volume 12 (September 2016), page 541.

Approval by the University of Alberta ethics review board was obtained for a collection of blood and biopsy samples and their use in this study ("Diagnostic and Therapeutic Applications of Microarrays in Kidney Transplantation", Pro00022226, 2013).

For Roberta and Elsie Parkes, and their boundless love and commitment to my success.

ACKNOWLEDGEMENTS

Thanks to Luis Hidalgo and Phil Halloran who provided guidance throughout my graduate education, and immense gratitude towards the people who made each day conducive to learning through their support, services, and winning personalities. In no particular order: Jeff Venner, Jeff Reeve, Konrad Famulski, Jessica Chang, Vido Ramassar, Anna Hutton, Michelle Ryan, and all others whose names I've missed. Special thanks to Brandon MacIsaac and Gina Sykes—training you was a valuable learning experience.

Table of Contents

List of Tables

List of Figures

Abbreviations

Antibody-mediated rejection, ABMR; antibody-dependent cell-mediated cytotoxicity, ADCC; Alberta Transplant Applied Genomics Centre, ATAGC; baculoviral IAP repeat containing 3, BIRC3; CC chemokine ligand, CCL; cytotoxic and regulatory T cell molecule, CRTAM; granulocyte-macrophage colony stimulating factor, CSF2; donor-specific antibody, DSA; extracellular-signal-regulated kinase, ERK; immunoglobulin molecule crystallizable fragment, Fc; Fc receptor-like 3, FCRL3; false discovery rate, FDR; granulysin, GNLY; G-protein-coupled receptor 18, GPR18; growth factor receptor-bound protein 2, GRB2; human umbilical vein endothelial cell, HUVEC; interferon gamma, IFNG; International Collaborative Microarray Study, INTERCOM; interferon regulatory factor 4, IRF4; immunoreceptor tyrosine-based activation motif, ITAM; killer lectin-like receptor F1, KLRF1; lipopolysaccharide, LPS; mitogen-activated protein kinase kinase, MEK; V-Myb avian myeloblastosis viral oncogene homolog-like 1, MYBL1; nuclear factor of activated T cells, NFAT1; natural killer cell, NK; nuclear receptor subfamily 4, NR4A2; peripheral blood mononuclear cell, PBMC; phosphatidylinositol 4-phosphate 5-kinase, PIP5K; phospholipase A1, PLA1A; serine protease E2, SERPINE2; SH2 domain containing 1B, SH2D1B; Son of Sevenless, SOS; stAR-related lipid transfer domain containing 4, STARD4; spleen tyrosine kinase, SYK; T cell-mediated rejection, TCMR; T cell receptor, TCR; tumor necrosis factor, TNF; tumor necrosis factor receptor superfamily member 9,

TNFRSF9; units, U; chemokine (C motif) ligand 1, XCL1; zeta-chain TCR associated protein kinase 70kDa, ZAP70; zinc finger BED-type containing 2, ZBED2.

CHAPTER 1
Background

1.1 Introduction

Allograft rejection occurs when an organ recipient's immune system mounts a defense against donated organs. There are two major types of allograft rejection: antibody-mediated rejection (ABMR), and T cell-mediated rejection (TCMR). Whereas the incidence of T cell mediated rejection is effectively mitigated by immunosuppression, ABMR remains difficult to control and is thus the major cause of late allograft failure (1). TCMR is perpetuated by the effects of T cell-derived soluble mediators and cell lysis mediated by CD8 T cells (CTL) against targets bearing donor antigens on class I HLA. Conversely, ABMR is caused by cellular responses to donor-specific anti-HLA antibodies (DSA). Cells that express Fc receptors can be activated by DSA directly. NK cells express the activating Fc receptor CD16a, and it is well-established that NK cells are present in biopsies diagnosed with ABMR (2;3). A role for CD16a activation of NK cells in ABMR has been suggested, but has not yet been demonstrated. Evidence of CD16a-mediated NK cell activation in ABMR would be a significant finding because it would establish NK cells as major effectors in ABMR.

There are striking parallels between activated NK cells and activated T cells. For example, stimulated CD8 T cells and NK cells are potent producers of

proinflammatory cytokines IFNγ and TNF, which have distinct effects on other cells. NK cells activated through CD16a by IgG-opsonized target cells can lyse those cells *in vitro* in a process called antibody-dependent cell-mediated cytotoxicity (ADCC). Thus, NK cells are similar to CD8 T cells in that they produce some of the same mediators and have cytolytic functions. In allograft rejection, this means that CD16a-stimulated NK cells could perform similar immunologic functions in ABMR as do CD8 T cells in TCMR, such as encouraging immune cell recruitment and activation, and allogeneic target cell lysis.

1.2 NK cells

NK cells in allograft rejection and other diseases

In the 1970s, researchers identified a new type of cell that was capable of lysing murine leukemia cells without prior sensitization (4). These "Natural Killer" cells have since been implicated in various other biological processes. NK cells are thought to support pregnancy by facilitating extravillous trophoblast invasion and arterial remodelling (5). In viral infections, NK cells are an important early source of IFNG. IFNG supports antiviral immune responses by enhancing antigen processing and increasing class I and II MHC expression on cells, stimulating production of proinflammatory and chemotactic mediators in other cells, hampering cellular and thus viral proliferation, and promoting microbicidal activities by immune cells (6). NK cells possess natural cytotoxicity receptors that activate cytotoxicity against some virally infected targets as well as tumor cells (7). For

example, NKp46 can recognize influenza hemagglutinin on infected cells, and therefore gives NK cells an important role in defending against influenza infection (8). A 2010 study by Hidalgo *et al.* identified NK cell involvement in ABMR. The study found six NK-associated transcripts that were selectively expressed in DSA-positive clinically indicated biopsies and highly expressed in ABMR but not TCMR. Biopsy immunostaining revealed that NK cells, but not T cells, were increased in ABMR compared to TCMR (2). These data were corroborated by the later finding that a handful of NK-associated transcripts are differentially expressed in ABMR compared to other diagnoses, and further suggested a possible role for CD16a activation in ABMR (9). The six NK-associated DSA-selective transcripts identified in the Hidalgo paper was a subset of 132 transcripts associated with DSA positive status (FDR < 0.005). Strikingly, of the initial 132 DSA-associated transcripts, at least ten were expressed in NK cells and CD8 T cells alike. This finding raises the possibility that NK cells and CD8 T cells share effector functions in ABMR and TCMR, respectively, although more detailed study is needed to explore this possibility.

Regulation of NK cell activation

The earliest model of NK cell activation—the "missing self" hypothesis—holds that NK cells are responsive to reduced or absent MHC expression on host cells. This was in response to the finding that NK cells would lyse tumor cells with absent or reduced endogenous MHC expression, but did not lyse tumor cells that expressed self-MHC (10). Given that transformed and virally infected cells often

downregulate class I MHC expression (11), the missing-self hypothesis was an appealing explanation for how NK cells could be self-tolerant, yet kill compromised cells in a seemingly non-specific manner. But this early model was not without faults: it failed to explain scenarios where NK cells lysed tumors or virally infected targets with sustained MHC expression (12). The discovery of activating receptors against tumor- and virus-associated ligands led to the current consensus that NK cell activation is regulated by the balance of inhibitory and stimulatory inputs from diverse ligands (13). Thus, it is possible for NK cells to be activated and kill targets even when those targets express class I MHC, if activating stimuli outweigh inhibitory signals from MHC.

While individual NK cells within the same host express different repertoires of receptors, most NK cells always have at least one inhibitory receptor against class I MHC (14). Some NK cell inhibitory receptors recognize non-MHC ligands such as E-, N-, and R-cadherins, α-2,8 disialic acid, collagen, and CD66 (13). Non-MHC ligands may play a role in inhibiting NK cell activation in tissues that normally express low or no class I MHC, such as neurons and erythrocytes (15). Inhibitory NK cell receptors take two forms: C-type lectin-like receptors, and immunoglobulin superfamily receptors. Killer immunoglobulin-like receptors (KIR) and leukocyte immunoglobulin-like receptors (LILRs) comprise the immunoglobulin superfamily receptors on human NK cells (13). Most inhibitory receptors contain one or more immunoreceptor tyrosine-based inhibitory motifs (ITIM), which get phosphorylated when the inhibitory receptor binds its ligand. Tyrosine

phosphatases SHP-1 or SHP-2, or lipid phosphatase SHIP-1 docks at the phosphorylated tyrosine residues on the ITIMs and dephosphorylate substrates associated with activation pathways. In essence, by recruiting phosphatases in the presence of sufficiently inhibitory stimuli, inhibitory receptors prevent cytokine release, cytotoxicity, and proliferation of NK cells (15). KLRC1 (NKG2A) and KLRD1 (CD94) are two well-studied inhibitory receptors. KLRD1 recognizes non-classical HLA-E, and complexes with KLRC1, which contains two ITIMs. Several studies have shown that KLRD1/C1 recognition of peptides presented on HLA-E attenuates NK cell cytotoxicity (16-18). It is thought that peptide presentation on HLA-E is an indication of a target cell's ability to process and present antigens. NK cells might use this as a proxy for cell health, as some virally infected and transformed cells have reduced ability to present antigens on class I HLA (13). The repertoire of antigens presented by HLA-E is not known, although both pathogenic and self peptides could be presented (19).

Some receptors are inhibitory under specific conditions, but activating under others. 2B4 (CD244/SLAMF4) is a signaling lymphocyte activation molecule (SLAM) family receptor that encodes multiple immunoreceptor tyrosine-based switch motifs (ITSM). In human NK cells, 2B4 interacts with CD48 (SLAMF2) and results in different outcomes depending on the NK cell's developmental stage and availability of ligands and intracellular signaling molecules. SH2D1A (SAP), SHP-1, SHP-2, and SHIP-1 compete to bind four ITSMs on human 2B4 (20). SH2D1A recruits Src family kinase Fyn, and thus initiates a signal cascade that culminates

in IFNG production, cytotoxicity, and granule exocytosis. Alternatively, as is seen in X-linked lymphoproliferative syndrome (XLP) patients with mutated SH2D1A, ITSMs recruit phosphatases and serve an inhibitory function (21). In mature NK cells, 2B4 normally acts as an activating receptor, but in immature NK cells it acts as an inhibitory receptor (22), perhaps because of late acquisition of SH2D1A during development. It is theorized that CD48 ligand density and SH2D1A availability both play a role in determining whether the net signal from 2B4 engagement is inhibitory or stimulatory (20). To further complicate the narrative, human NK cells can express two isoforms of 2B4 which differ in their affinity for CD48 and in their ability to mediate cytotoxicity (23).

Stimulatory NK cell receptors signal through immunoreceptor tyrosine-based activating motifs (ITAMs). The ITAMs are encoded in the cytoplasmic domains of transmembrane DAP12, CD3ζ, and FcεRIγ associated with the activating receptors (13). CD16a, for example, couples with CD3ζ homodimers, CD3ζ-FcεRIγ heterodimers, or FcεRIγ homodimers, and the ITAMs on these complexes are phosphorylated by Src-family kinases to initiate signalling that leads to cytokine production, degranulation, and cytotoxicity (24). These outcomes are shared between many activating NK cell receptors that signal through the same homo- or heterodimeric ITAM-bearing protein complexes. For example, NKp46, a natural cytotoxicity receptor (NCR) that can recognize influenza hemagglutinin (8) and heparan sulfate on tumor cells (25), also signals through CD3ζ to mediate cytotoxicity and cytokine release. NCRs NKp30 and NKp44 function similarly to

NKp46; however, while both recognize heparan sulfate, only NKp44 and NKp46 recognize viral hemagglutinin (26), and NKp44 signals through DAP12 whereas NKp30 and NKp46 signal through CD3ζ (27). Consequently, NK cells engage their effector functions upon activation of several functionally redundant pathways. While engagement of predictable effector functions in response to various receptor-ligand interactions benefits defense against tumors and intracellular pathogens, in transplantation the absence of inhibitory endogenous class I HLA on allogeneic target cells and the presence of DSA on donor HLA for CD16a ligation may have serious negative consequences for graft health because it would tip the balance in favor of NK cell activation.

CD16a Signaling in NK cells

As previously mentioned, CD16a is an activating receptor that recognizes the Fc portions of IgG antibodies. Structurally, it is a 234 amino acid transmembrane glycoprotein with a 190 amino acid extracellular region in the form of two Ig-like domains, and a 25 amino acid cytoplasmic tail (28). CD16a preferentially binds IgG3 and IgG1, and has minimal affinity for IgG4 and IgG2 subclasses. The affinity of CD16a for all IgG subclasses is affected by a 158V/F polymorphism in the IgG-binding domain, where CD16a-158V is the higher affinity phenotype (29). The transmembrane character of CD16a is determined by a phenylalanine residue at position 203. Through its transmembrane domain, CD16a associates with disulfide-bonded FcεRIγ/CD3ζ homo- or heterodimers. The interaction between CD16a and FcεRIγ/CD3ζ hinges on an aspartic acid residue in the transmembrane domains of

FcεRIγ and CD3ζ (30). The cytoplasmic domain of CD16a contains an RSSTR motif which is phosphorylatable by PKC on one of the serine residues. CD16a RSSTR phosphorylation increases CD16a-mediated cytokine production, calcium influx, and Syk-mediated tyrosine phosphorylation of signaling proteins; however, phosphorylated CD16a also interacts with S100A4 in a calcium-dependent manner, and phosphorylation by PKC is attenuated by S100A4 binding (31). Thus, the cytoplasmic RSSTR motif may play an important role in modulating CD16a-mediated activation.

Phosphorylation of the ITAMs on CD16a-associated FcεRIγ/CD3ζ is mediated by Src-family kinases such as Lck. ITAM phosphorylation permits binding of protein kinase ZAP70, which Lck also phosphorylates. Syk also binds phosphorylated ITAMs on FcεRIγ/CD3ζ. Together, ZAP70 and Syk phosphorylate subsequent substrates in the CD16a signal cascade (32). In general, downstream signaling branches into pathways with effects on the cell membrane, or with effects on gene expression. Gene expression changes are induced by convergence of two main branches. The first involves phosphorylation of LAT by Syk and ZAP70 (33), which localizes PLCγ. PLCγ hydrolyzes PIP_2 into DAG and IP3. IP3 binds to receptors at the endoplasmic reticulum and stimulates exodus of calcium ions from the endoplasmic reticulum to the cytoplasm (34). Cytoplasmic calcium binds calmodulin and regulatory calcineurin B, which activates catalytic calcineurin A. Calcineurin A dephosphorylates cytoplasmic transcription factor NFATp (NFAT1), permitting its translocation to the nucleus. The related transcription factor NFATc

(NFAT2) is similarly affected, but NFATc is only expressed after CD16a stimulation, and thus plays a delayed role in CD16a signaling (35). NFATp and NFATc interact with nuclear factors associated with the second major branch that affects gene expression following CD16a activation. The second branch involves Shc and GRB2 localization at FcεRIγ /CD3ζ. This localizes SOS GDP/GTP exchange factor, which participates in the signaling cascade that involves H-Ras, c-Raf-1, MEK, and ERK (36;37). This leads to formation of the AP-1 transcription factor complex, which cooperates with NFAT to alter gene expression (38;39). Membrane effects such as actin rearrangement and exocytosis are mediated through numerous branches of CD16a pathways, whose activities include localization and activation of phospholipase A2 (37), PLD1 lipid phosphatase (40), Rac1 GTPase (41), PIP5K1A lipid kinase, and generation of various phospholipid second messengers (42).

Given the signaling pathways involved in CD16a-mediated NK cell activation, the key functions of NK cells in ABMR might include proinflammatory mediator production and ADCC against graft endothelial cells. Although ADCC through CD16a is demonstrable *in vitro* (43), it is uncertain whether it actually drives ABMR pathogenesis, as endothelial cell lysis is not observed in histopathologic examination of biopsies diagnosed with ABMR (44;45). For example, a distinct feature of ABMR is the formation of basement membrane multilayering and/or intimal arteritis in the absence of necrosis (46). In severe TCMR, there is sometimes intimal arteritis with medial smooth muscle cell necrosis; however, these lesions are not unique to TCMR, and can be found in acute

kidney injury and ABMR (46-48). There is probably a role for IFNG in ABMR, evidenced by the prominence of IFNG-inducible transcripts in biopsies diagnosed with ABMR (9). CD16a may shape ABMR pathogenesis through production of IFNG and other soluble mediators that have marked effects on endothelial cells. As we learn more about NK cell activation in ABMR, we will surely find it is not a straightforward process. CD16a-mediated NK cell activation may be modulated by other receptors and motifs richly expressed by NK cells. Although modulation of CD16a activation of NK cells in rejection is not the focus of the present study (we have yet to show that CD16a activation occurs at all in ABMR), modulators could include the CD16a RSSTR motif, which may fine-tune CD16a activation in combination with the polymorphisms at position 158, and KLRC1/D1, which could attenuate NK cell activation in response to peptides presented on HLA-E on target cells with functional proteasomes.

1.3 T cells

As its name suggests, T cell-mediated rejection (TCMR) is driven by T cell responses to donor alloantigens. Recipient T cells may recognize alloantigens presented on the recipient's own antigen presenting cells (APCs), or they may react to non-self MHC on donor APCs that reside in donated tissue (49). T cell activation by host APCs constitutes "indirect recognition", and activation by donor APCs is termed "direct recognition." Under the influence of proinflammatory cytokines (e.g. IL-1ß, IL-6, IL-13, IL-15, TNF, etc.) (50), APCs mature and migrate from the allograft to the paracortex of lymph nodes where they interface with T cells. T cells

activated by donor antigens migrate to the allograft and perpetuate inflammation through the release of proinflammatory cytokines and chemokines.

T cell activation

Unlike NK cells, which are activated depending on a balance of activating and inhibitory inputs, T cell activation is dominated by input from the T cell receptor (TCR) and has a requirement for costimulation which NK cells lack. The TCR consists of two disulfide-linked glycoprotein chains (TCRα and TCRβ) that recognize antigenic peptides presented on MHC complexes (51). The TCR chains associate with a cluster of CD3 proteins comprised of CD3γ, CD3δ, CD3ε, and homodimeric CD3ζ. CD3-p21 is sometimes disulfide-linked to CD3ζ (52). CD3ζ is a critical signaling unit in the TCR complex. When CD3ζ is absent, T cell receptor signaling is blocked, although phosphatidylinositol hydrolysis and IL-2 production still occur (53). TCR stimulation engages many of the same downstream signaling pathways as CD16a because signaling is mediated by CD3ζ in both receptor systems. The CD16a signaling elements described earlier in this chapter are also involved in TCR signaling. A non-exhaustive selection of downstream signaling molecules employed by both CD16a and TCR is illustrated in **Figure 1.1**. Some of the effector responses activated by both CD16a and TCR are thus similar: degranulation, cytotoxicity, and production of certain soluble mediators.

In order to acquire a full complement of effector functions, naïve T cells must first be primed by antigen presenting cells. Dendritic cells, for example, present

exogenous alloantigens to CD4 T cells on class II MHC, or cross-present exogenous antigens to CD8 T cells on class I MHC (54). The capacity of B cells and macrophages to prime both CD4 and CD8 naïve T cells cannot be excluded; however, reports on the ability of non-dendritic cells to cross-present antigen to CD8 T cells suggest that dendritic cells are by far the most effective at activating naïve T cells (55). In a process called dendritic cell "licensing," CD4 helper T cells activate dendritic cells that present compatible antigens through interactions between CD40L on T cells and CD40 on dendritic cells (56). In response, dendritic cells increase expression of costimulatory ligands and produce cytokines such as IL-12 that act as secondary and tertiary activation signals for T cells (57;58). Well-studied costimulatory ligands on dendritic cells include CD80 and CD86 (B7-1 and B7-2), which both interact with T cell coreceptors CD28 and CTLA4. Different coreceptors elicit different responses from T cells. For instance, CD28 is just one of many coreceptors that promote T cell effector responses, survival, and proliferation. Conversely, CTLA4 and several others inhibit effector responses and favor exhaustion and apoptosis. Once primed by licensed APCs, effector T cells can be activated by target cells without costimulation (59).

Classically, it was thought that CD8 T cells require stimulation by APCs that had been licensed by CD4 helper T cells. However, we now know that dendritic cell licensing is not an absolute requirement for CD8 T cell activation. High antigen load may lessen the requirement for costimulation (60), and in some infections, pathogens can prime dendritic cells through pattern recognition receptors,

bypassing the need for T cell help altogether. However, whereas CD8 T cells can become competent effectors this way, they do not become competent memory cells (61).

T cell activation, costimulation, and effector function in TCMR

If CD4-independent activation of naïve CD8 T cells occurs in transplant rejection, the mode is unclear. In fact, hematopoietic APCs may not even be solely responsible for T cell priming in transplantation. There is some evidence that allogeneic endothelial cells can prime CD8 T cells to differentiate into effector cells (62-64). A number of studies have also demonstrated CD4 T cell priming by allogeneic endothelial cells expressing IFNG-induced class II MHC (65-67), although one study was unable to reproduce this phenomenon (68). This is relevant to rejection because allograft microcirculation is largely donor-derived, with sporadic instances of replacement by recipient cells in association with vascular rejection (69). Ultimately, the details of how CD4 T cells support CD8 T cell activation in allograft rejection—whether through dendritic cells, macrophages, B cells, endothelial cells with cytokine-induced class II MHC expression, or sometimes not at all—remain unclear (70).

CD4 and CD8 T cells are capable of independently mediating allograft rejection (71-73), and costimulation requirements appear to differ between CD4 and CD8 T cells in animal models of allograft rejection. In some murine models, CD40L blockade is effective against CD4 T cell-mediated rejection, but not CD8 T cell-

mediated rejection (71). Similarly, blocking the CD28/B7 costimulatory pathway is effective against CD4 T cell-mediated rejection but not necessarily CD8 T cell-mediated rejection (74;75). Caution is warranted in interpreting these results because CD40/CD28-independent CD8 T cell-mediated rejection is not consistent between different genetic strains of mice. In one skin allograft study, CD40/CD28 blockade resulted in median survival times beyond 100 days in C3H/HeJ mice with no generation of allospecific CD8 T cells. On the other hand, median survival times were as low as 20 days for C57BL/6 mice treated with CD40/CD28 blockade, and unlike the C3H/HeJ mice, the C57BL/6 mice generated allospecific CD8 T cells (76). It is unclear why the latter generated CD8 T cells against the allograft whereas the former did not, but decreased sensitivity of CD8 T cells to costimulation blockade could partially explain why the CD57BL/6 mice experienced worse outcomes.

In humans, costimulation blockade is used clinically to suppress TCMR, and because T cell costimulation is a key step preceding antibody production by B cells, it also has an indirect suppressive effect on ABMR pathogenesis. One group devised an experimental system that crosslinked CTLA4 using membrane-bound anti-CTLA4 antibodies on allogeneic target cells injected into mice. They found that CTLA4 ligation prevented T cell-mediated lysis of these allogeneic cells (77). Although there are currently no soluble CTLA4 crosslinking agents available for clinical use, there are clinically available agents that compete for costimulation ligands. Belatacept is a CTLA4-Ig fusion protein that binds CD80 and CD86, which are both ligands for CD28 and CTLA4. While belatacept effectively prolongs graft

survival in animal models—especially in combination with CD40/CD40L blockade (78)—it does not completely prevent acute TCMR in humans, possibly because of differences in costimulation requirements between various T cell subsets (79). In support of this notion, the proinflammatory CD4 T cell Th17 subset appears to be resistant to belatacept treatment. Acute rejection episodes in patients treated with belatacept are associated with higher frequencies of Th17 cells compared to belatacept-treated patients without acute rejection, and compared to Th1 cells and resting memory Th17 cells, stimulated memory Th17 cells express more CTLA4 and expand *in vitro* despite belatacept treatment (80). This is in contrast to Th1 cells, which are more effectively suppressed by belatacept. These findings illustrate that individual subsets of T cells active in TCMR may respond to costimulation differently from one another.

Ultimately, relatively little is known about how T cell subsets mediate rejection mechanistically. A major effector mechanism of CD8 T cells is targeted cytotoxicity, and there is some evidence supporting a role for CD8 T cell-mediated cytolysis of allogeneic tissue. Pathologic examination of human heart transplants reveals perforin-containing cells in coronary artery subendothelial spaces with perforin-containing granules often polarized toward adjacent endothelial cells (81). Additionally, CD8 T cell-mediated cytolysis of human aortic endothelial cells and human umbilical vein endothelial cells is mitigated by granzyme B inhibition *in vitro* (82). In an islet rejection study that utilized an adoptive T cell transfer model, it was shown that CD8 T cells were able to mediate allograft rejection when

allograft Fas expression or CD8 T cell perforin expression were independently disrupted, but allograft rejection was usually prevented when Fas and perforin were simultaneously disrupted (83). However, the same was not observed in murine kidneys: Einecke *et al.* showed that epithelial deterioration and tubulitis (indicative of TCMR) occurred independently of Fas, perforin, and granzymes (84). Thus, there appears to be some role for cytotoxicity in TCMR; however, cytotoxicity does not appear to be necessary for rejection to occur in all circumstances, and its significance might vary between different tissues.

Phenotypic changes can also be caused directly and indirectly by proinflammatory cytokines, chemokines, and growth factors from activated CD4 and CD8 T cells. IFNγ is a prime example, although other mediators also contribute to rejection pathogenesis. The effects of IFNγ on various cell types are well-documented. It can cause ultrastructural changes in tissues; for example, IFNγ affects barrier function of intestinal epithelial cells by inducing tight junction internalization (85). IFNγ can also contribute to vascular dysfunction by dysregulating NO expression (86), altering extracellular matrix composition, and affecting expression of genes involved in vascular remodeling (87). In transplantation, cytokine-induced changes in allograft tissue may encourage loss of graft function. IFNG itself is robustly associated with TCMR (88). However, the impact of IFNG in TCMR is unclear. In TCMR, IFNγ may suppress CD8 cytotoxic T cell responses to allogeneic tissues in acute rejection, as *Ifng*(-/-) mice that receive heart and kidney allografts have more immunologically-mediated allograft necrosis

than wild-type hosts (89). On the other hand, IFN γ also affects expression of many proinflammatory cytokines and chemokines implicated in rejection, and some of these IFNG-inducible mediators are T cell chemoattractants. For example, expression of the IFNG-inducible lymphokine CXCL9 is compromised *Ifng*(-/-) mice, and while CXCL9 deficiency delays acute allograft rejection and reduces T cell infiltration in these mice, it does not prevent rejection, probably because its effects are redundant with other chemokines (90). Thus, untangling the contribution of IFNG and other soluble mediators to rejection pathogenesis has yet to be done. The *in vivo* effects of T cell-derived proinflammatory mediators on TCMR pathogenesis are most likely influenced by many other factors, including regulation by various receptors, functional redundancy of many chemokines and cytokines, and synergism or antagonism between soluble mediators.

1.4 CD8 T cells and NK cells: A comparison

NK cells and T cells are phenotypically similar. Using gene expression microarray analysis, we previously looked for transcripts that selectively differentiate between CD4 T cells, CD8 T cells, and NK cells (91). Surprisingly, we found that CD4 and CD8 T cells did not express any transcripts that selectively set them apart from both NK cells and each other. That is not to say that there were no differences in expression of some transcripts between CD4 and CD8 T cells. For example, granzymes, perforin, and granulysin were not exclusive to CD8 T cells, but they were expressed more highly in CD8 T cells than in CD4 T cells and were

therefore relatively more selective for CD8 T cells. Transcripts that differentiated between CD4 and CD8 T cells were not strictly selective, as they were also expressed by NK cells: several NK cell KIR and lectin-like receptors were expressed by NK cells and CD8 T cells, but not CD4 T cells. In contrast, CD4 T cells did not express any transcripts that uniquely identified them compared to CD8 T cells.

The phenotypic similarity between CD8 T cells and NK cells extends to activation by TCR and CD16a. CD16a and TCR employ many of the same signaling elements and generate similar downstream responses. Both receptors signal through CD3ζ, which recruits protein tyrosine kinases Syk and ZAP70 to ITAMs encoded in its cytoplasmic domain. These molecules are phosphorylated by various src-family kinases such as Lck. These interactions are illustrated in **Figure 1.1**. Recruitment of these proteins to CD3ζ ITAMs results in common calcium-dependent and -independent pathways being engaged in NK cells and T cells. In both cells, calcium-dependent signaling begins with LAT phosphorylation and subsequent catalysis of PIP_2 into IP3 and DAG, and culminates with calcineurin A activation and NFATp/NFATc translocation to the nucleus. Shared calcium-independent signaling mechanisms include activation of the SOS/RAS/MEK/ERK axis, as well as VAV1/RAC1-utilizing signaling pathways that lead to actin rearrangement and degranulation. Although many signaling molecules found in T cells are also found in NK cells, their importance in NK cell CD16a signaling has yet to be fully understood. The contribution of various signaling molecules to CD16a responses is not straightforward because NK cells express many functionally redundant

signaling molecules that, while sometimes critical for T cell signaling, do not necessarily impair NK cell activation when absent. For instance, Syk and ZAP70 deletion have no significant adverse effects on NK cell development and cytotoxic function (92), but ZAP70-deficient patients have severe combined immunodeficiency because their T cells cannot respond to TCR stimulation (93).

Transcription factors mobilized by CD16a and TCR also overlap. Major examples are NFATc, NFATp, AP-1, and NF-κB. In NK cells, NFATp is constitutively present in the cytosol, and immediately translocates to the nucleus upon CD16a activation. NFATc is not constitutively present in NK cells; it is expressed following CD16a activation. In the NK cell nucleus, NFATp and NFATc can interact with AP-1. NFAT and AP-1 transcription factors can act independently, but in genes whose promoters contain adjacent consensus sequences for NFAT and AP-1, combinatorial enhancement adds an extra level of complexity to gene regulation (94). AP-1 can be dimers of c-Jun, c-Fos, or ATF. In NK cells, AP-1 is a c-Jun/c-Fos heterodimer (35). Regulation of c-Fos (and therefore AP-1) in NK cells relies on IL-2. IL-2 signaling activates cAMP response element binding protein, CREB, which in turn regulates c-fos gene expression (95). CREB is also present in T cells, where it is phosphorylated by MSK1/2 at the end of the ERK/MAPK signaling axis (96). In resting T cells and NK cells, cytoplasmic NF-κB is complexed with IκB, which prevents NF-κB from translocating to the nucleus. In stimulated T cells, TCR/CD28 signaling initiates a PKCθ-mediated pathway that activates IκB kinase, which phosphorylates and releases IκB from NF-κB, freeing it to translocate to the

nucleus. In NK cells, the pathways of NF-κB activation are unknown, but data support a role for IL-2-mediated NF-κB nuclear translocation (97).

Because many of the same transcription factors are activated following CD16a and TCR activation, some of the gene expression changes may be shared. The *IFNG* gene contains consensus sequences for binding by many transcription factors activated by CD16a and TCR. NFAT, NF-κB, and AP-1 are all able to bind enhancer elements in the *IFNG* promoter, and regulate its expression in NK cells and T cells (98;99). Indeed, NK cells and T cells are major suppliers of IFN γ during immune responses. TNF is also produced by both cell types. In T cells, the *TNF* promoter is regulated by ATF-2/Jun and NFATp, as well as other transcription factors (100;101). It is unclear whether the same transcription factors are used to regulate *TNF* in NK cells. NK cells and T cells also have similar cytotoxic abilities when stimulated through CD16a and TCR. Through pathways that rely on many overlapping signaling branches, including the VAV1/RAC1 axis, T cell and NK cells initiate actin rearrangements that lead to the release of cytolysin-containing granules. Thus, two major axes of effector function that overlap between NK cells and cytotoxic T cells are soluble mediator release, and cytotoxic degranulation.

Although we don't know the fine details of how NK cells and effector T cells contribute to rejection pathogenesis, the similarities between CD16a and TCR signaling propose an interesting parallel between these cells in ABMR and TCMR, respectively. This project explores the parallel by investigating some of the overlap

between CD16a-mediated NK cell responses in ABMR and TCR-mediated CD8 T cell responses in TCMR.

1.5 Rejection pathology and pathogenesis

Pathological classification of rejection

Histologic characterization of transplant biopsies is currently the global standard for diagnosis of ABMR and TCMR. The current reference standard for kidney transplant rejection is the Banff classification system. The most recent revisions to the Banff system were made in 2013, and divide ABMR into acute/active and chronic/active categories (102). For a diagnosis of acute/active ABMR, biopsies must have histologic evidence of acute tissue injury, current or recent antibody interaction with vascular endothelium, and patient serum must be DSA-positive. Histologic findings in ABMR may include microvascular inflammation, intimal or transmural arteritis, acute thrombotic microangiopathy, and acute tubular injury that is not associated with other causes. Evidence of antibody interactions is described as any one of the following: immunostaining of peritubular capillaries for C4d (although C4d negative ABMR is common (103)), evidence of moderate microvascular inflammation, or identification of transcripts in biopsies associated with endothelial injury. DSA positivity is assessed with crossmatching assays designed to test reactivity of recipient antibodies against donor HLA molecules. For a diagnosis of chronic/active ABMR, all the above criteria must be met, plus histologic evidence of a more advanced state of injury: transplant

glomerulopathy in the absence of chronic thrombotic microangiopathy, severe multilayering of the peritubular capillary basement membrane, or arterial intimal fibrosis. Overall, the pathology of ABMR is predominantly microvascular.

TCMR classification is also divided into acute and chronic designations. Acute TCMR is subtyped based on histopathological findings: significant interstitial infiltration and moderate focal tubulitis (type I), mild to severe intimal arteritis (type II), and transmural arteritis or arterial fibrinoid change accompanied by lymphocytic inflammation and medial smooth muscle necrosis (type III). Notably, intimal arteritis may also be a characteristic of acute/active ABMR, and our group has shown that intimal arteritis is non-diagnostic (104). Overall, TCMR pathology is largely characterized by interstitial changes and tubulitis.

Molecular classification of rejection

One of the greatest shortcomings of histopathologic classification of rejection is the fact that it suffers from variability in the subjective assessments of individual pathologists, and different centres use difference classification systems. Even Banff is semi-quantitative (classification criteria are scored, but the scores may be based on qualitative assessments). Furthermore, pathology is only relevant when the disease has progressed to the point of visible tissue injury, and thus does not accurately reflect the true nature of progression to graft failure. In many patients, rejection can be rapid or drawn out, and visual evidence of diseases lag their causative molecular mechanisms. Subclinical rejection leads to unhelpful

classifications such as "borderline" where biopsies do not have visible abnormalities, but may nonetheless be undergoing rejection at the molecular level.

To address some of these shortcomings, our group has focused on developing a classification of rejection reliant on characterization of gene expression changes (105). Using gene expression microarray analysis, we previously studied kidney transplant biopsies and identified sets of transcripts that are differentially expressed in ABMR or TCMR (9;88;106). In ABMR, we found that typifying transcripts were related to endothelial cell responses to IFNG, NK cells, possible CD16a signaling, and angiogenesis. In TCMR, the identifying gene expression changes were associated with T cell signaling and costimulation (e.g. *CD28*, *CTLA4*), and APC activation (e.g. *CD86, PDL1, ADAMDEC1, ANKRD22, AIM2*). *IFNG* itself was robustly associated with TCMR compared to other diagnoses. Other associations with TCMR included inflammasome activation, cytotoxicity, and parenchymal injury.

Several of the key features of ABMR and TCMR identified in the molecular studies agree with pathological findings in biopsies: ABMR transcripts associated with endothelial injury correspond to microcirculation inflammation, and TCMR-associated transcripts related to T cell/APC activation and parenchymal injury are compatible with the extensive interstitial mononuclear cell infiltrate in TCMR. Although the ABMR molecular landscape study found a correlation between ABMR, NK cells, and CD16a, it did not show whether NK cell CD16a was actually being activated in ABMR or if it was simply present due to increased NK cell burden. We

propose that, through their CD16a Fc receptors, NK cells recognize DSA bound to donor HLA on allograft endothelium, thereby becoming activated and contributing to ABMR pathogenesis possibly through cytotoxicity and/or proinflammatory mediator release. The primary aim of the present study was to find evidence that NK cells are activated through CD16a in ABMR. The secondary aim was to explore overlap in gene expression between CD16a-stimulated NK cells and TCR/CD3-stimulated CD8 T cells. We hypothesized that some CD16a-inducible NK cell transcripts would be associated with ABMR. We further hypothesized that, given the overlap between the CD16 and TCR signaling systems, some gene expression changes would also overlap between NK cells and T cells stimulated this way, and would be present in ABMR and TCMR. To address these hypotheses, we asked the following questions:

1. What gene expression changes occur in NK cells following CD16 stimulation?
2. Are CD16a-inducible gene expression changes associated with ABMR?
3. Are any of the top CD16a-inducible NK cell transcripts TCR-inducible in CD8 T cells, and associated with TCMR?

We address these questions herein. Reaching a better understanding of how ABMR pathogenesis is mediated by the immune cells involved may generate new approaches to risk stratification and prevention of ABMR.

FIGURES & TABLES

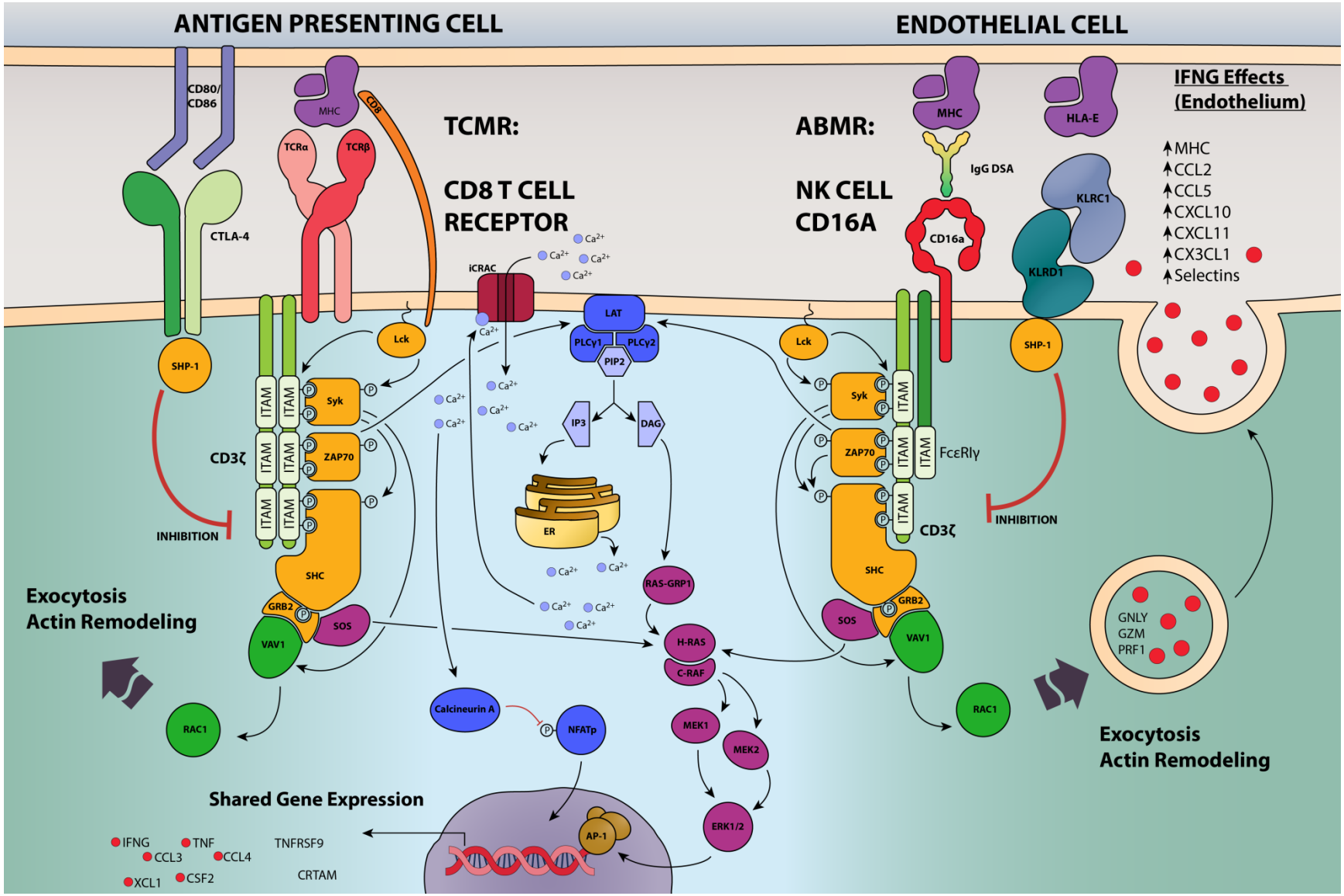
ANTIGEN PRESENTING CELL
ENDOTHELIAL CELL
CD80/
CD86
CTLA-4
MHC
CD8
TCRα
TCRβ
TCMR:
CD8 T CELL
RECEPTOR
ABMR:
NK CELL
CD16A
MHC
IgG DSA
CD16a
HLA-E
KLRC1
KLRD1
IFNG Effects
(Endothelium)
MHC
CCL2
CCL5
CXCL10
CXCL11
CX3CL1
Selectins
iCRAC
Ca2+
LAT
PLCγ1
PLCγ2
PIP2
IP3
DAG
ER
SHP-1
Lck
Syk
ZAP70
ITAM
CD3ζ
FcεRIγ
INHIBITION
SHC
GRB2
SOS
VAV1
RAS-GRP1
H-RAS
C-RAF
MEK1
MEK2
ERK1/2
Calcineurin A
NFATp
AP-1
RAC1
Exocytosis
Actin Remodeling
GNLY
GZM
PRF1
Shared Gene Expression
IFNG
TNF
CCL3
CCL4
XCL1
CSF2
TNFRSF9
CRTAM

Figure 1.1 (previous page) – Some shared elements of CD16a and TCR signaling. Some of the signaling molecules that overlap between TCR signaling (left) and CD16a signaling (right) are depicted. Calcium-dependent and -independent branches leading to activation of nuclear transcription factors are illustrated centrally: signaling molecules fundamental to the calcium-dependent signaling axis are shown in blue, and the calcium-independent ERK1/2 axis is depicted in purple. Vav1 and Rac1 are involved in a vast network of molecules that signal actin rearrangements, represented in green. CTLA4 and KLRC1/D1 are examples of systems that employ protein tyrosine phosphatases to negatively regulate TCR and CD16a signaling, respectively, by dephosphorylating ITAMs in the CD3 ζ chain.

CHAPTER 2
Materials & Methods

2.1 Overview

An overview of the analyses performed in this study is outlined in **Table 2.1.**

The aim of this project was to find evidence of CD16a-mediated NK cell triggering in ABMR, and identify overlap between gene expression changes induced by CD16a signaling in NK cells in ABMR and TCR signaling in CD8 effector T cells in TCMR. As such, we used gene expression microarrays to study the effect of CD16a or TCR/CD3 stimulation on cultures of primary human NK cells and CD8 T cells. The quality of the *in vitro* system was ensured using flow cytometry to determine cell purity and cytokine ELISAs to verify that the cells were activated. Soluble mediator production by cultured cells was profiled using a multiplex platform for one of the experiments in this study.

Gene expression microarrays of total RNA from the cell cultures were analyzed to identify lists of transcripts with various characteristics (e.g. highly CD16a-inducible in NK cells, highly expressed in unstimulated NK cells, highly TCR/CD3-inducible in CD8 T cells). Transcripts from these lists were looked up in gene expression microarray results from 703 histologically classified kidney transplant biopsies, and their associations with ABMR or TCMR versus other diagnoses were calculated. We used previously collected microarray data for a

primary human cell panel of various immune cells, endothelial cells, and epithelial cells with or without IFNG treatment to determine the selectivity of transcripts for NK cells, and to study the effect of IFNG on transcripts' associations with ABMR.

2.2 Materials & Methods

Patient Population and Biopsy Collection

As previously described (88), a set of 703 kidney transplant biopsies collected from 579 patients at six kidney transplant centres were histologically classified to include C4d- ABMR and the changes outlined in the Banff 2013 report (102). Patient demographics and clinical details for this set have been published (107;108). Biopsy collection for this study was approved by the institutional review boards of participating centres. Some biopsies were collected as part of the INTERCOM study (ClinicalTrials.gov NCT01299168).

Transcript Expression in Biopsies

RNA extraction from biopsies, subsequent labeling, and hybridization to HG-U133 Plus 2.0™ GeneChip® human gene expression arrays (Affymetrix, Santa Clara, CA) was performed as previously described (108). CEL files were generated with Affymetrix GeneChip® Command Console® Software version 4.0. Platforms used in analysis include GeneSpring GX 13.0 (Agilent Technologies, Santa Clara, CA), Microsoft Office Excel (Redmond, WA), and "R" software. Biopsy RNA extraction, labelling, quality control, and microarray data acquisition were

performed by Anna Hutton and Vido Ramassar. All biopsies used in this study were previously collected and the data were housed in a database kept in the Alberta Transplant Applied Genomics Centre (ATAGC).

Transcript Expression in Cultured Cells

We used a Ficoll-Paque™ (GE Healthcare Life Sciences, Baie-D'Urfé, Quebec, Canada) density gradient to isolate peripheral blood mononuclear cells (PBMCs) from the blood of healthy volunteers. Cells were purified using EasySep™ negative selection kits (Stem Cell Technologies, Vancouver, BC, Canada), which use dextran-coated magnetic particles which bind tetramers of antibodies directed against markers on unwanted cell types. Following incubation of cell suspensions in a magnetic chamber, the supernatant is enriched for the desired cell type while the unwanted cells are pulled to the walls of the test tube. Purity was assessed by flow cytometry. Cells were cultured as specified below.

NK cells: Cells were purified from PBMCs using an EasySep™ Human NK Cell Enrichment Kit. These kits operate on immunomagnetic negative selection using antibodies against markers on unwanted cell types: CD3, CD4, CD14, CD19, Cd20, CD36, CD66b, CD123, HLA-DR, and glycophorin A. Data was obtained from three separate cultures of NK cells from three different donors. Purity of CD45+/CD3-/CD56+ cells as a percent of all viable cells was 80-99%. Stimulated NK cell cultures were prepared in 24-well plates that were coated overnight with 5µg goat anti-mouse IgG $F(ab')_2$ (Jackson ImmunoResearch, West Grove, PA) in 500µL PBS, which was

used to cross link anti-CD16a antibodies on the NK cells; unstimulated cells were cultured in uncoated wells. Cells were stimulated with 1μg per million NK cells of mouse anti-human CD16a Low Endotoxin, Azide-Free (LEAF)™ antibodies (BioLegend, San Diego, CA) for 10 minutes at room temperature prior to adding them to the $F(ab')_2$-coated 24-well plates to ensure complete coating of the NK cells with the anti-CD16a. Cells were cultured for 4 hours in 1mL of RPMI 1640 supplemented with 10% fetal bovine serum (Thermo-Fisher Gibco, Waltham, MA) and 200 units (U) per mL recombinant human IL-2 (Affymetrix eBioscience, San Diego, CA). IFNG and TNF ELISAs were performed on cell-free supernatants to confirm activation. Cells were lysed in TRIzol® Reagent (Life Technologies Inc., Burlington, ON, Canada) and their total RNA was collected for analysis on Affymetrix PrimeView™ GeneChip® human gene expression arrays according to manufacturer-recommended procedures. Gene expression data were averaged across the three cultures for each condition for analysis. I performed RNA isolation and quality control, Anna Hutton and Vido Ramassar acquired the microarray data, and I performed all subsequent data analyses.

CD8 T cells: Cells were purified from PBMCs using an EasySep™ Human CD8 T Cell Enrichment Kit. This immunomagnetic negative selection kit utilizes a cocktail of antibodies that bind markers on unwanted cells: CD4, CD14, CD16, CD19, CD20, CD36, CD56, Cd123, TCRγ/δ, and glycophorin A. Data was obtained from three separate cultures of T cells from three different donors. Purity of CD45+/CD3+/CD8a+ cells as a percent of all viable cells was 93-96%. Stimulated

CD8 T cell cultures were prepared in 24-well plates that were coated overnight with 5µg goat anti-mouse IgG $F(ab')_2$ (Jackson ImmunoResearch, West Grove, PA) in 500µL PBS, which was used to cross link anti-CD3 antibodies on the T cells; unstimulated cells were cultured in uncoated wells. Cells were stimulated with 1µg per million T cells of mouse anti-human CD3 antibodies (Affymetrix eBioscience, San Diego, CA) for 10 minutes prior to adding them to the $F(ab')_2$-coated 24-well plates. Cells were cultured for 4 hours in 1mL of RPMI 1640 supplemented with 10% fetal bovine serum (Thermo-Fisher Gibco, Waltham, MA) and 200 units (U) per mL recombinant human IL-2 (Affymetrix eBioscience, San Diego, CA). IFNG and TNF ELISAs were performed on cell-free supernatants to confirm activation. Cells were lysed in TRIzol® Reagent (Life Technologies Inc., Burlington, ON, Canada) and their total RNA was collected for analysis on Affymetrix PrimeView™ GeneChip® human gene expression arrays according to manufacturer-recommended procedures. Gene expression data were averaged across the three cultures for each condition for analysis. I performed RNA isolation and quality control, Anna Hutton and Vido Ramassar acquired the microarray data, and I performed all subsequent data analyses.

Monocytes: Cells were purified from PBMCs of a single donor using an EasySep™ Human Monocyte Enrichment Kit without CD16a Depletion. This immunomagnetic negative selection kit utilizes a cocktail of antibodies that bind markers on unwanted cells: CD2, CD3, CD19, CD20, CD56, CD66b, CD123, and glycophorin A. Purity of CD45+/CD3-/CD14+ as a percent of all viable cells was

82%. Cells were stimulated with 500U/10^6 cells recombinant human IFNG (Affymetrix eBioscience). Cells were cultured in 1mL RPMI 1640 with 10% fetal bovine serum in non-$F(ab')_2$-coated 24-well plates and were harvested at 2, 4, and 8 hour time points. IL-6 and TNF ELISAs were performed on cell-free supernatants to confirm activation at each time point. Cells were lysed in TRIzol® Reagent and their total RNA was collected for analysis on Affymetrix PrimeView™ GeneChip® human gene expression arrays according to manufacturer-recommended procedures. Gene expression data were averaged across the three time points. I performed RNA isolation and quality control, Anna Hutton and Vido Ramassar acquired the microarray data, and I performed all subsequent data analyses.

Extended Cell Panel*:* We used existing Affymetrix HG-U133™ GeneChip® gene expression data for a panel of primary human B cells, immature and LPS-treated mature primary human dendritic cells, primary human monocytes, allostimulated primary human CD4 and CD8 T cells, HUVECs (ATCC, Manassas, VA) +/- IFNG treatment, human RPTECs (Lonza, Inc., Allendale, NJ) +/- IFNG, and primary human macrophages +/- IFNG isolated and cultured as previously described (2).

Cytokine & Chemokine Profiling

Following the technique for NK cells and CD8 T cells described above, primary human NK cells and CD8 T cells were cultured unstimulated or stimulated with anti-CD16a (NK cells) or anti-CD3 (T cells) at a concentration of 500,000

cells/mL. Cell-free supernatants were harvested at 2, 4, 8, and 24 hours. Using a Meso Scale Discovery® V-PLEX Human Cytokine 30-Plex Kit (Rockville, MD), we profiled supernatants for CCL2, CCL3, CCL4, CCL13, CCL17, CCL22, CSF2, CXCL10, Eotaxin, Eotaxin-3, Flt-1/VEGFR1, IFNG, IL-10, IL-12/IL-23p40, IL-12p70, IL-13, IL-15, IL-16, IL-17A, IL-1α, IL-1β, IL-2, IL-4, IL-5, IL-6, IL-7, IL-8, TNF, TNF-β, VEGF-A, and VEGFR-2. This experiment was performed once with cells from a single donor for each time point and stimulation condition, but each sample on the multiplex plate was run in triplicate.

Gene expression analysis of transcripts in cultured cells

Gene expression data were pre-processed using robust multi-array average normalization to remove background noise, array effects, and combine probe intensities across arrays. For analysis, we used the geometric mean of non-log-transformed expression for each probeset across all available replicates for a given sample.

NK cells: We identified probe sets increased >2x across 3 CD16a-stimulated versus 3 unstimulated NK cells (Benjamini-Hochberg FDR<0.05) and with <500 expression across 4 control nephrectomies. Transcripts with low expression in stimulated NK cells (<200) were also removed. To avoid the possibility that increased transcripts were coming from trace amounts of IFNG-stimulated contaminating monocytes in the NK cell cultures, we excluded transcripts that were increased >2x in IFNG-stimulated versus unstimulated monocyte cultures. Probe

sets for redundant transcripts were eliminated. From the remaining probe sets, we identified the top 30 CD16a-inducible transcripts with the highest fold change in CD16a-stimulated versus unstimulated NK cells. Transcripts with the highest expression in unstimulated NK cells were identified after removing transcripts with >500 expression in control nephrectomies and removing probe sets for redundant transcripts. The top 30 with the highest expressed in unstimulated NK cells were selected from the remaining transcripts.

CD8 T cells: We identified probe sets increased >2x across 3 TCR/CD3-stimulated versus 3 unstimulated CD8 T cell cultures (Benjamini-Hochberg FDR<0.05) and with <500 expression across 4 control nephrectomies. To avoid the possibility that increased transcripts were coming from trace amounts of IFNG-stimulated contaminating monocytes in the T cell cultures, we excluded transcripts that were increased >2x in IFNG-stimulated versus unstimulated monocyte cultures. Probe sets for redundant transcripts were eliminated.

Biopsies & extended cell panel: Biopsy and extended cell panel data were obtained using HG-U133™ chips, but top CD16a-inducible NK cell transcripts, top highly expressed resting NK cell transcripts, and top TCR/CD3-inducible transcripts were identified using PrimeView™ chip data. The PrimeView™ chips are a newer version of gene chip than the HG-U133™ chips, and are annotated with different probe set IDs. To permit comparison between these chips' different probe set IDs, HG-U133™ probe set IDs representing the gene symbols on each PrimeView™-based transcript list were selected on the basis of sequence consensus

with PrimeView™ probe sets, probe set selectivity, and signal intensity in the extended cell panel. The same HG-U133™ probe set equivalents were used consistently throughout this study.

FIGURES & TABLES

Table 2.1 – Overview of analyses performed in this study

Characterize gene expression changes in CD16a-stimulated NK cells	Gene expression microarray analysis of total RNA from 4 hour cultures of primary human NK cells +/- CD16a stimulation.
Identify top 30 CD16a-inducible NK cell transcripts	Criteria: - *Increased >2x in stimulated (N = 3) vs. unstimulated (N = 3) NK cells (FDR<0.05)* - *Has >200 geometric mean expression in stimulated NK cells* - *Has <500 geometric expression in normal kidneys (N = 4)* - *Increased <2x in IFNG-stimulated vs. unstimulated primary human monocytes at 2, 4, and 8 hours (N = 1 per time point)* The top 30 were selected by decreasing fold change in stimulated versus unstimulated NK cells.
Identify top 30 highly expressed transcripts in resting NK cells	Criteria: - *Has < 500 geometric mean expression in normal kidneys (N = 8)* The top 30 were selected by decreasing expression in unstimulated NK cells.
Determine association of top 30 CD16a-inducible and highly expressed resting NK cell transcripts with ABMR	Calculate fold change and p values for transcripts in biopsies with ABMR compared to all other diagnoses except TCMR and mixed rejection.
Determine selectivity of CD16a-inducible and highly expressed resting transcripts for NK cells	Study transcript expression in a primary human cell panel comprised of cultured monocytes, B cells, allostimulated CD4 & CD8 T cells, macrophages +/- IFNG treatment, renal proximal tubule epithelial cells +/- IFNG treatment, human umbilical vein endothelial cells +/- IFNG, immature dendritic cells, and mature LPS-treated dendritic cells.
Characterize gene expression changes in TCR/CD3-stimulated CD8 T cells	Gene expression microarray analysis of total RNA from 4 hour cultures of primary human CD8 T cells +/- CD3 stimulation.
Study soluble mediator production in stimulated and unstimulated NK cells and CD8 T cells	30-plex analysis of cytokines, chemokines, and growth factors in 2, 4, 8, and 24 hour cultures of CD16a-stimulated (N=1 per time point) and unstimulated (N=1 per time point) NK cells, and TCR/CD3-stimulated (N=1 per time point) and unstimulated (N= 1 per time point) CD8 T cells
Identify transcripts that are CD16a-inducible in NK cells and TCR/CD3-inducible in CD8 T cells	Criteria: - *Increased >2x in stimulated (N = 3) vs. unstimulated (N = 3) NK cells (FDR<0.05)* - *Increased >2x in stimulated (N = 3) vs. unstimulated (N = 3) CD8 T cells (FDR<0.05)* - *Has <500 geometric mean expression in normal kidneys (N = 4)* - *Increased <2x in IFNG-stimulated vs. unstimulated primary human monocytes (N = 3)* Also determined expression of the top 30 CD16a-inducible transcripts in TCR/CD3-stimulated vs. unstimulated CD8 T cells.
Determine association of top 30 CD16a-inducible transcripts with TCMR	Calculate fold change and p values for transcripts in biopsies with TCMR compared to all other diagnoses except ABMR and mixed rejection.

CHAPTER 3
Establishing the Experimental System

3.1 Overview

In this study we characterized global gene expression changes in freshly isolated primary human NK cells following CD16a stimulation *in vitro.* We tried three different methods of CD16a stimulation before choosing one to use for gene expression studies. This chapter documents the results of each method. As a measure of the reliability of each stimulation method, activation was assessed by IFNG and TNF ELISAs. The first method stimulated CD16a with commercially available purified polyclonal human IgG cross-linked by solid phase goat anti-human IgG $F(ab')_2$. The second method used Jurkat or MOLT-4 T cells as targets. The targets were coated with positive control serum (PCS), which is pooled serum from highly sensitized patients. The PCS is reactive against all HLA types encountered by the HLA laboratory at the University of Alberta Hospitals. The PCS was used to coat HLA molecules on the T cell targets, allowing crosslinking of CD16a on primary NK cell effectors. The final system we tested used a monoclonal human CD16a-specific IgG antibody of mouse origin to trigger NK cells. The anti-CD16a antibody was cross-linked by plate-bound goat anti-mouse IgG $F(ab')_2$. This final system was used for gene expression microarrays.

3.2 NK CD16a engagement by solid-phase crosslinked polyclonal human IgG

Well plates were coated overnight with goat anti-human IgG F(ab')2, which was used to crosslink polyclonal human IgG on NK cell CD16a. $1x10^6$ freshly isolated human NK cells were coated for 10 minutes with 2.0µg of polyclonal IgG, resuspended in 1mL medium, and cultured for 2, 4, 8, or 24 hours. 200U/mL recombinant human IL2 was added to each well. Unstimulated controls were prepared in uncoated wells without IgG for each time point. Activation was assessed by TNF and IFNG ELISAs using cell-free supernatants from each time point (**Figure 3.1**). In retrospect, the serially diluted standards used to calculate the cytokine concentrations generated very clean standard curves, but they were probably degraded because of age and likely did not provide readings that accurately reflected the concentrations they were meant to represent. This conclusion is based on our observation that those standard curves were much lower than readouts from freshly prepared standards at the same concentrations. Therefore, the concentrations of cytokines in cell-free culture supernatants reported in **Figure 3.1** are probably higher than the true concentrations. NK cells produced TNF earlier than IFNG, but TNF levels tapered after 8 hours. In contrast, IFNG levels increased throughout the time course, with highest levels observed at 24 hours. Later time points were not tested.

3.3 NK CD16a engagement by target T cells coated with anti-HLA antibodies

Primary NK cells were cultured with Jurkat (HLA I type A24,25, B7,41) or MOLT-4 (HLA I type A1, A25, B18, B57) targets that had been coated with PCS pooled from patients with HLA-reactive antibodies. The PCS contains antibodies against a broad range of HLA types and was the source of IgG ligands for NK cell CD16a. Target cells were to be coated with diluted PCS prior to coculture with NK cells. The appropriate range of serum dilutions to coat target cells in experiments was determined by running a flow-cytometry-based titration curve for 1/20, 1/40, 1/80, 1/160, and 1/320 dilutions of PCS compared to uncoated negative control targets, where 500,000 targets in 100µL of wash buffer received 20µL of each dilution. PCS on targets was detected using a FITC-conjugated goat anti-human IgG secondary antibody. A FITC conjugated pan-class I HLA antibody (W6/32) was used as a positive control. The median fluorescence intensity shift for each dilution compared to uncoated negative controls was calculated as (MFI dilution – MFI uncoated). This titration curve was performed three times, and the MFI shifts for each replicate are plotted together in **Figure 3.2**.

800,000 Jurkats or MOLT4 were incubated with 1/20, 1/40, or 1/80 PCS for 20 minutes at room temperature prior to coculture with 400,000 primary human NK cells in 1 mL culture medium. Cocultures were incubated for 4 or 8 hours with 200U of recombinant human IL2 per mL of medium. Cell-free supernatants were harvested for IFNG and TNF ELISAs. Controls included NK cells incubated without targets, NK cells incubated with uncoated targets, or NK cells stimulated

with solid-phase crosslinked polyclonal human IgG. Cytokine production was strong with all three PCS dilutions (**Figure 3.3**). Uncoated T cell targets elicited strong signals from NK cells, presumably because these are immortalized tumor lines that might express antigens for NK cell activating receptors other than CD16a. In contrast, NK cells incubated without targets were quiescent. Thus, CD16a was not solely responsible for NK cell activation in this system. The polyclonal IgG stimulation performed alongside the PCS stimulation was weaker than expected based on previous results from polyclonal IgG stimulation.

3.4 Direct stimulation of NK cells with solid-phase crosslinked anti-CD16a antibody

Plates were coated overnight with goat anti-mouse $F(ab')_2$ fragments, which were used to cross-link murine anti-human CD16a antibodies on the surface of primary NK cells. Freshly isolated NK cells were incubated for ten minutes with 1.0ug per million cells of anti-CD16a, and were added to coated plates and cultured for 4 hours before harvesting cell-free supernatants for IFNG and TNF ELISA analysis. The ELISA results for the NK cell stimulation is shown in **Figure 3.4.** Compared to negative controls that did not receive any anti-CD16a antibodies, NK cells stimulated this way consistently provided strong activation signals.

FIGURES & TABLES

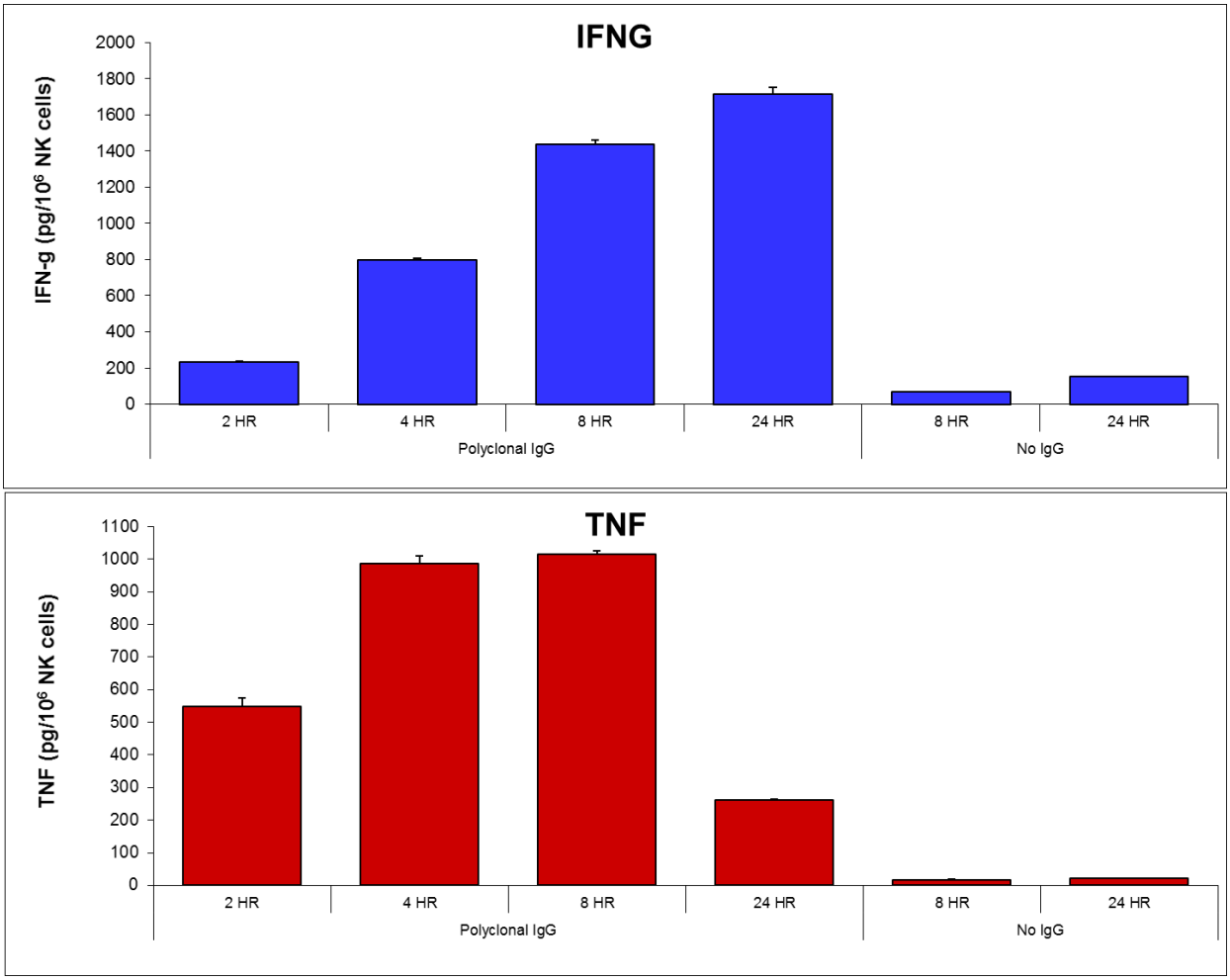

Figure 3.1 – IFNG and TNF production by NK cells stimulated with polyclonal human IgG in vitro. ELISAs were performed on cell-free supernatants of primary human NK cells cultured for 2, 4, 8, or 24 hours with polyclonal human IgG crosslinked by plate-bound goat anti-human IgG F(ab')2. Unstimulated controls were cultured for 8 or 24 hours. Concentrations are given in picograms per million NK cells. Each sample denoted by the bars was analyzed in triplicate, and error bars show the standard deviation between the replicates. Data are taken from a single experiment.

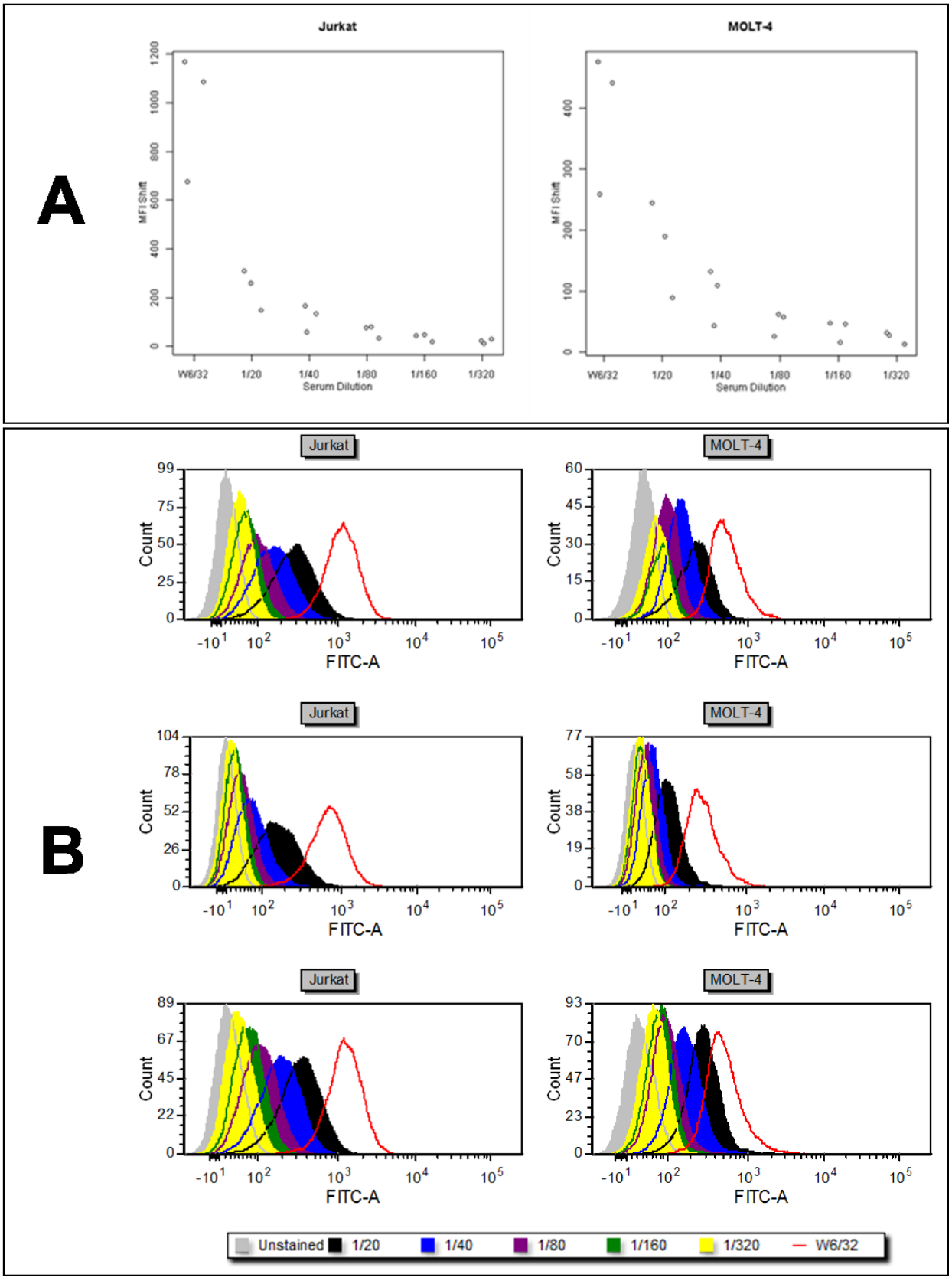
A
Jurkat
MOLT-4
MFI Shift
Serum Dilution
W6/32
1/20
1/40
1/80
1/160
1/320
B
Count
FITC-A
Unstained
1/20
1/40
1/80
1/160
1/320
W6/32

Figure 3.2 (previous page) – Titration curve and flow cytometry histograms for positive control serum dilutions used to coat Jurkat and MOLT-4 T cell target HLA. 500,000 cells in 100uL of wash buffer were incubated with 20uL of each PCS dilution. W6/32 antibody binds all class I HLA and was used as a positive control. (A) MFI (median fluorescence intensity) shift is calculated as (MFI of antibody coated targets – MFI of unstained cells), and is plotted for each PCS dilution. The shift calculations for each sample were based on the flow cytometry results shown in panel B. Data for three independent replicates are plotted for each dilution. The slight horizontal deviation of each point from dilution markers on the x axis does not represent variation in the dilution factor; it is simply a visual effect applied by the graphing software to visually separate clusters of points. (B) Flow cytometry data for PCS dilutions for each target cell sample. Three replicates are shown for each cell type.

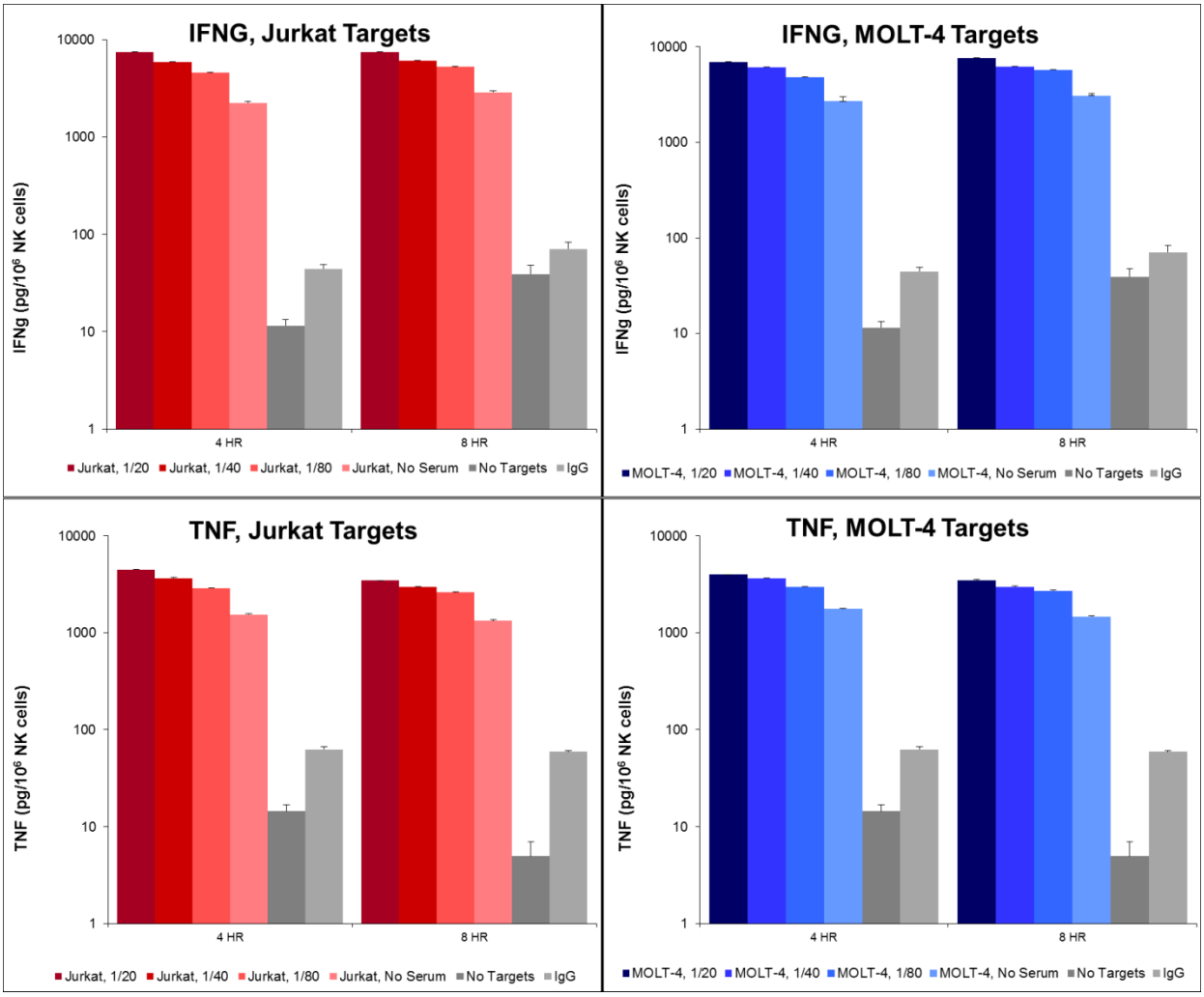

Figure 3.3 – IFNG and TNF production by NK cells stimulated with anti-HLA antibody-coated T cell targets. Cytokine concentrations were detected with ELISAs on cell-free supernatants. 800,000 Jurkat or MOLT-4 targets were coated with 1/20, 1/40, or 1/80 positive control serum and cultured with 400,000 primary human NK cell responders for 4 or 8 hours (dark to light coloured bars in order of decreasing serum concentration). Controls included uncoated targets (lightest coloured bars), NK cells without targets (dark grey bars), and NK cells stimulated with polyclonal human IgG (light grey bars). Concentrations are given per million NK cells. Each sample denoted by the bars was run in triplicate, and the error bars show the standard deviation between the replicates.

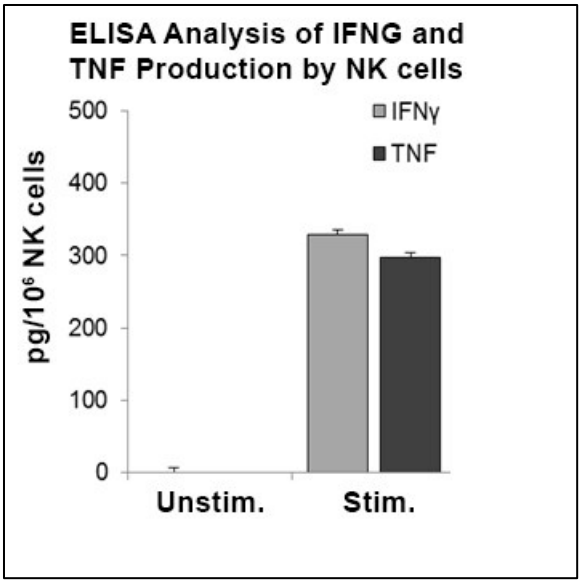

Figure 3.4 – IFNG and TNF production by NK cells stimulated with anti-CD16a antibodies. Primary NK cells were stimulated with 1.0μg per million cells of anti-CD16a antibody, cross-linked by plate-bound goat anti-human IgG $F(ab')_2$. Results from a single experiment are shown. Concentrations are given in pictograms per million NK cells. Each sample denoted by the bars was analyzed in triplicate, and the error bars show standard deviation between the replicates.

CHAPTER 4
Troubleshooting the Experimental System

4.1 Overview

In this project, we used total RNA from primary immune cells to generate gene expression microarray data about how NK cells express transcripts following CD16a stimulation, and how CD8 T cells respond to TCR/CD3 stimulation. Freshly isolated primary human NK cells were stimulated with murine anti-human CD16a crosslinked by plate-bound goat anti-mouse IgG $F(ab')_2$. Primary human CD8 T cell activation was similarly achieved with mouse anti-human CD3 IgG antibodies crosslinked by plate-bound goat anti-mouse IgG $F(ab')_2$. The isolated cells had to be pure if they were to be used for microarray analysis. Purity was frequently suboptimal, so we optimized the isolation procedure to achieve higher purities more consistently.

4.2 Determining purity of freshly isolated immune cells

Primary NK cell and CD8 T cell isolations were performed by separating PBMCs from whole blood using a Ficoll density gradient centrifugation, followed by immunomagnetic negative selection of the cells of interest. Purity was assessed by flow cytometry. Gene expression microarray data on CD16a-stimulated NK cells and CD3-stimulated T cells (see chapters 5 & 6) were derived from three

independent cultures for each cell type using three different donors. The purity analyses for the NK cells used for microarrays are shown in **Figure 4.1,** and the purity analyses for the CD8 T cells used for microarrays are shown in **Figure 4.2**. NK cells were identified as CD45+/CD3-/CD56+ events; CD8 T cells were identified as CD45+/CD3+/CD8a+ events (CD45 staining was not performed on T cells from the 09-30 donor). NK cells from the 08-11 (**Figure 4.1A-D**) and 08-25 (**Figure 4.1E-H**) donors were obtained before the isolation protocol was optimized, and are anomalous in that they were atypically pure compared to most isolates obtained prior to optimization. NK cells from the 12-04 donor were isolated using the optimized isolation protocol. Similarly, the 09-30 T cell sample (**Figure 4.2A-C**) was obtained prior to optimization, whereas the 12-10 (**Figure 4.2D-G**) and 12-11 (**Figure 4.2H-K**) samples were obtained with the optimized protocol. **Figure 4.1M** shows that only 41% of the viable cells in the 08-25 NK cell sample were CD56+; however, the CD56 profile is suspicious in light of the scatter profile, which is dominated by CD3- lymphocyte-like events. We gated CD45+/CD3- events that had a lymphocyte-like forward scatter (FSC)/side scatter (SSC) profile and treated this as a more reliable assessment of NK cell purity (**Figure 4.1H**). Using this strategy, the purity of viable cells in the 08-25 NK cell sample is between 80% and 92%, although we cannot rule out CD45+/CD3- B cells or CD45+/CD3- innate lymphoid cells (that are not NK cells) in this population.

We encountered two major problems with most of our cell isolations prior to optimization. Firstly, undesirable types of PBMCs often contaminated the isolates.

Secondly, these samples contained large proportions of small events with low FSC and SSC values (i.e. dead cells, debris, platelets). This is illustrated in final columns of the tables in **Figures 4.1M** and **4.2L**, which list percentages of NK cells (**Figure 4.1M**) and CD8 T cells (**Figure 4.2L**) relative to the combined total of viable and non-viable events collected for each sample. 85% of events in the 09-30 CD8 T cell sample were debris, compared to ca. 10-20% debris in the optimized 12-10 and 12-11 CD8 T cell samples. Likewise, the 12-04 NK cell sample was performed with an optimized protocol, and fewer than 10% of the events collected were debris.

4.3 Optimization of primary cell isolations

Prior to optimization, the Ficoll centrifugation was performed by diluting no more than 16mL of blood with 20mL calcium and magnesium-free HBSS in a 50mL conical, followed by addition of 12mL of the Ficoll solution. The preparations were centrifuged for 20 minutes at 2000 RPM (850xg). The PBMC layer was collected in a fresh 50mL conical, topped up with HBSS and washed once at 1600 RPM (544xg) for 15 minutes before proceeding with immunomagnetic isolation. The immunomagnetic isolation was performed with only a single magnetic step. To improve purity, we performed two additional magnetic steps in optimized protocol. This reduced the frequency of undesirable PBMC populations in our preparations, but there was still a large amount of small FSC/SSC events in our samples.

The immunomagnetic isolation kits we used contained antibodies against most undesired cell types, but they did not contain antibodies against platelet

markers. We therefore assumed that the debris in our preparations were platelets. We optimized the Ficoll process to reduce platelet contamination. We tested several variables, including using 8mL of whole blood versus 16mL of whole blood per 50mL conical, adjusting the number of washes, and adjusting the speed of the washes. Centrifuging 8mL of whole blood per conical slightly improved yield. Adjustments to the washes made the most meaningful impact on purity. Two additional 8 minute washes with at least one equivalent of room-temperature calcium and magnesium-free HBSS at 200xg (much slower than the original 1600 RPM/544xg) eliminated most of the platelets, but cost considerable cell loss. Based on the results of our troubleshooting, we modified the cell isolation protocol. We collected more blood to compensate for cell loss during washes, performed a 2000 RPM 10-minute wash to maximize recovery following the PBMC collection, performed two additional 200xg washes to eliminate debris and platelets, and increased the number of magnetic steps in the negative selection from one to three to exclude unwanted cell populations. After optimization, our NK cell and CD8 T cell isolations were typically 90-99% pure.

4.4 Determining purity of NK cell and CD8 T cell cultures used in multiplex analysis of soluble mediators

NK cells and CD8 T cells used in the multiplex analyses of soluble mediator production (see chapter 6) were cultured separately from those used for microarray analysis of gene expression changes. The purity assessment for the cells used in the

multiplex analysis is shown in **Figure 4.3**. In the NK cell sample, at least 89% of viable events were CD45+/CD3-/CD56+. In the CD8 T cell sample, at least 88% of viable events were CD45+/CD3-/CD8a+. These cells were isolated using the optimized protocol.

4.5 Identifying IFNG-inducible monocyte transcripts in NK cell and T cell culture microarray data

Stimulated NK cells and CD8 T cells produced IFNG *in vitro*. In pilot experiments, we observed that small numbers of contaminating monocytes in NK and T cell cultures were sufficient to introduce IFNG-inducible monocyte transcripts. These transcripts were highly responsive in monocytes but did not necessarily reflect sole induction by CD16a in NK cells or TCR/CD3 in CD8 T cells. Thus, we cultured primary human monocytes from a single donor to identify IFNG-inducible transcripts in stimulated NK cell and T cell cultures contaminated with monocytes. Monocyte purity was 82% (**Figure 4.4**). $1.3x10^6$ monocytes were cultured with 1000U/mL recombinant human IFNG in 1.5mL medium for 2, 4, 8, 24, and 48 hours. We also stimulated monocytes with polyclonal human IgG crosslinked by plate-bound goat anti-human IgG $F(ab')_2$ in the presence or absence of 1000U/mL IFNG to gauge the contribution of Fc receptor cross-linking to monocyte activation in NK and T cell cultures. IL-6 and TNF ELISAs were performed on cell-free supernatants to confirm activation (**Figure 4.5**). IFNG was a potent activator, but IgG alone was not. IgG and IFNG in combination stimulated greater cytokine

production than IFNG alone. The 2, 4, and 8 hour unstimulated and IFNG-only cultures were analyzed with gene expression microarrays. We pooled microarray data for the 2, 4, and 8-hour time points and took raw gene expression as the average signal across all three time points for each series. Gene expression microarray data from NK cell and T cell cultures were filtered to exclude transcripts that were increased more than two-fold in IFNG-stimulated versus unstimulated monocytes (see chapter 5).

FIGURES & TABLES

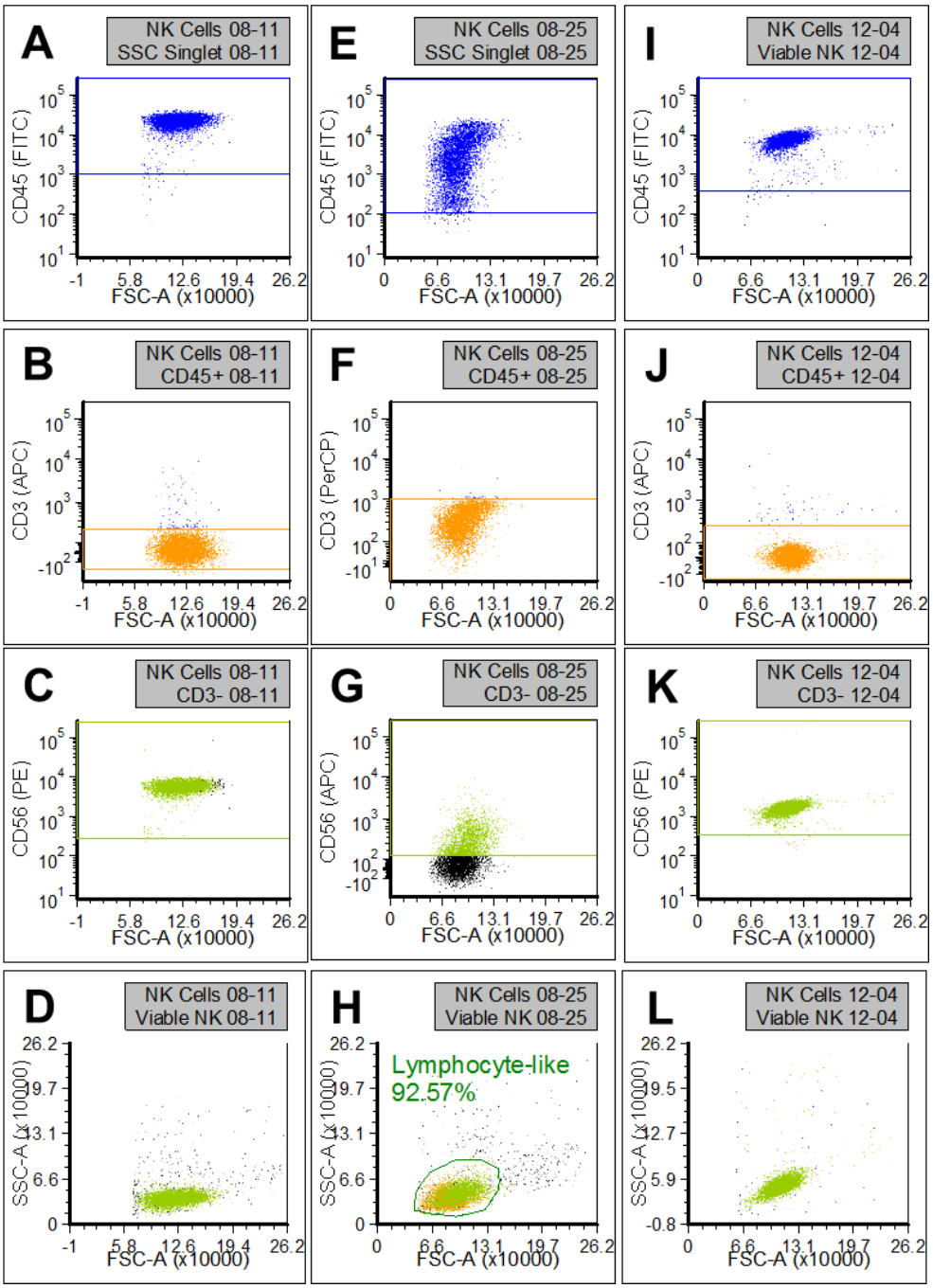
A
NK Cells 08-11
SSC Singlet 08-11
CD45 (FITC)
FSC-A (x10000)
E
NK Cells 08-25
SSC Singlet 08-25
CD45 (FITC)
FSC-A (x10000)
I
NK Cells 12-04
Viable NK 12-04
CD45 (FITC)
FSC-A (x10000)
B
NK Cells 08-11
CD45+ 08-11
CD3 (APC)
FSC-A (x10000)
F
NK Cells 08-25
CD45+ 08-25
CD3 (PerCP)
FSC-A (x10000)
J
NK Cells 12-04
CD45+ 12-04
CD3 (APC)
FSC-A (x10000)
C
NK Cells 08-11
CD3- 08-11
CD56 (PE)
FSC-A (x10000)
G
NK Cells 08-25
CD3- 08-25
CD56 (APC)
FSC-A (x10000)
K
NK Cells 12-04
CD3- 12-04
CD56 (PE)
FSC-A (x10000)
D
NK Cells 08-11
Viable NK 08-11
SSC-A (x10000)
FSC-A (x10000)
H
NK Cells 08-25
Viable NK 08-25
Lymphocyte-like
92.57%
SSC-A (x10000)
FSC-A (x10000)
L
NK Cells 12-04
Viable NK 12-04
SSC-A (x10000)
FSC-A (x10000)

NK cells, 08-11

Gate	Number of Events	Percent of Gated Cells	Percent of All Cells
SSC Singlet	9076	100.00	33.90
CD45+	9043	99.64	33.78
CD3-	8898	98.04	33.24
CD56+	8895	98.01	33.23

NK cells, 08-25

Gate	Number of Events	Percent of Gated Cells	Percent of All Cells
SSC Singlet	8232	100.00	82.32
CD45+	8141	98.89	81.41
CD3-	8096	98.35	80.96
CD56+	3365	40.88	33.65

NK cells, 12-04

Gate	Number of Events	Percent of Gated Cells	Percent of All Cells
Viable NK	9849	100.00	92.46
CD45+	9818	99.69	92.17
CD3-	9740	98.89	91.44
CD56+	9704	98.53	91.10

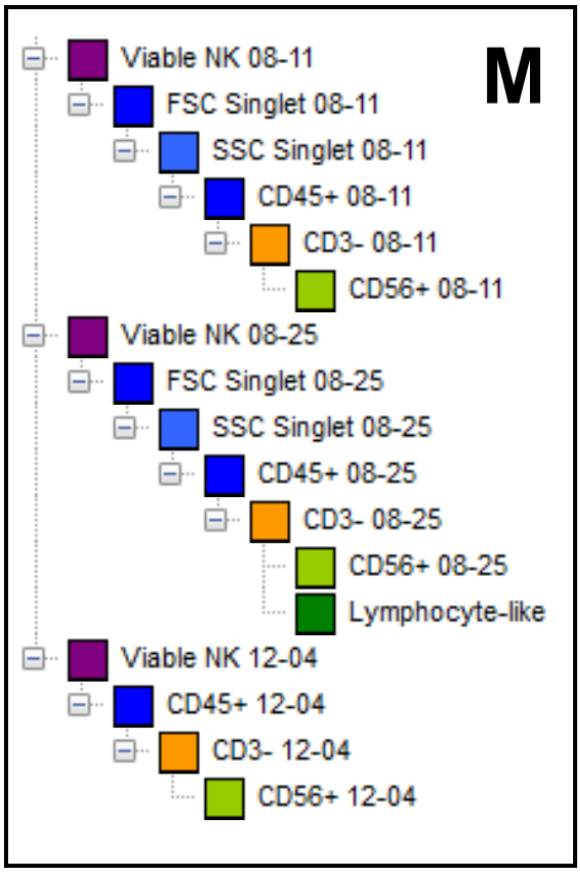

Figure 4.1 – Flow cytometry purity assessment of primary human NK cell samples used for microarray analysis. (A-D) NK cells from donor 1. (E-H) NK cells from donor 2. (I-L) NK cells from donor 3. Viable cells are gated hierarchically as depicted in panel M. Singlet discrimination was performed using FSC-H/W and SSC-H/W data when available. The purity of CD45+/CD3-/CD56+ events are highlighted in red text in the tables in panel M as a percent of all viable cells. The "lymphocyte-like" gate in panel H captures viable events with lymphocyte-like FSC/SSC properties, and the percentage in the lymphocyte-like gate text is relative to the total number of viable events collected for that sample. The 08-11 and 08-25 NK cells were collected before the Ficoll procedure had been optimized. Gate is indicated on the second plot title line in A-L. Mouse isotypes: CD3-APC IgG1, CD3-PerCP IgG2a, CD45-FITC IgG1, CD56-APC IgG1, CD56-PE IgG2a.

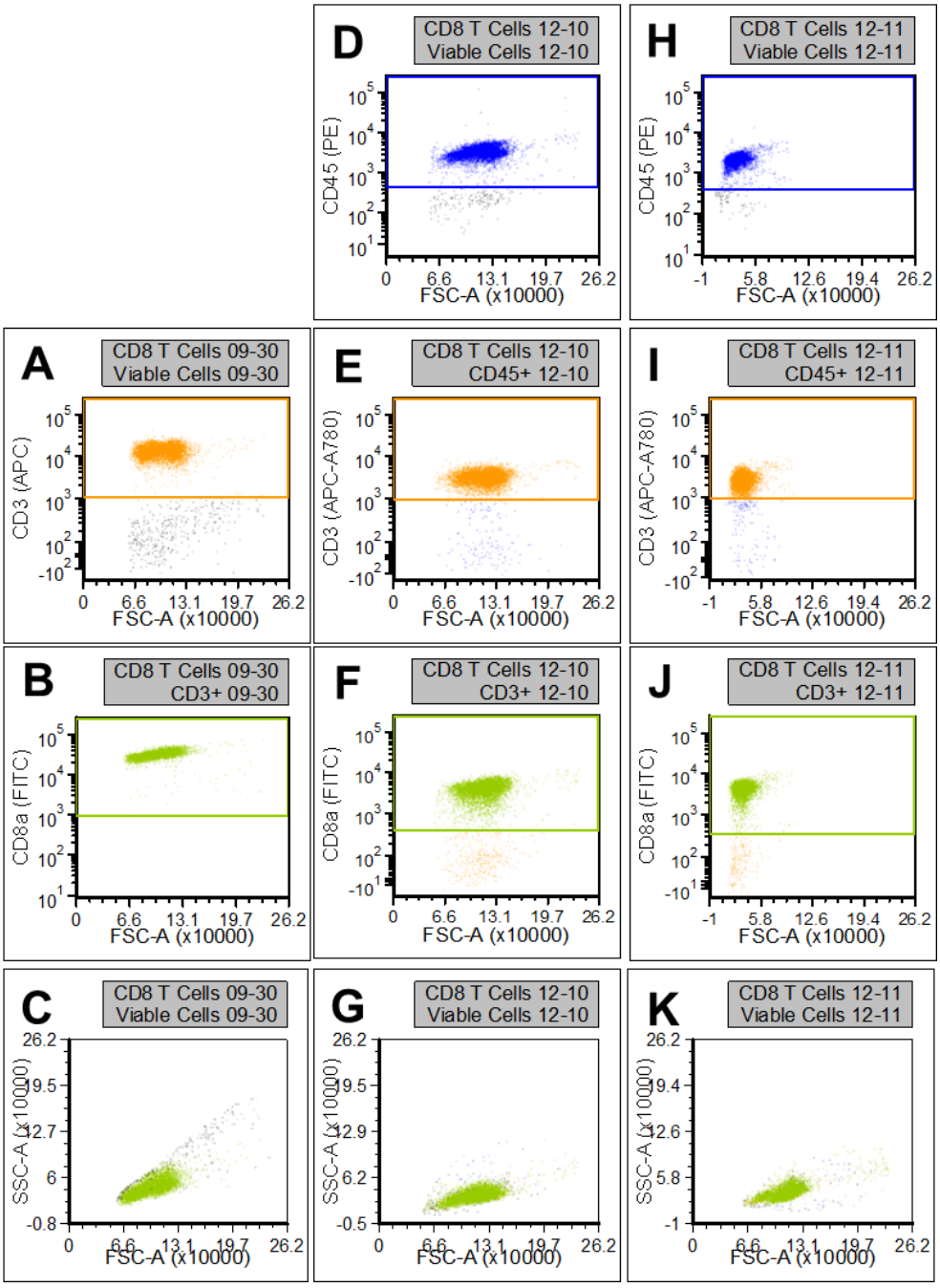
A
CD8 T Cells 09-30
Viable Cells 09-30
CD3 (APC)
FSC-A (x10000)
B
CD8 T Cells 09-30
CD3+ 09-30
CD8a (FITC)
FSC-A (x10000)
C
CD8 T Cells 09-30
Viable Cells 09-30
SSC-A (x10000)
FSC-A (x10000)
D
CD8 T Cells 12-10
Viable Cells 12-10
CD45 (PE)
FSC-A (x10000)
E
CD8 T Cells 12-10
CD45+ 12-10
CD3 (APC-A780)
FSC-A (x10000)
F
CD8 T Cells 12-10
CD3+ 12-10
CD8a (FITC)
FSC-A (x10000)
G
CD8 T Cells 12-10
Viable Cells 12-10
SSC-A (x10000)
FSC-A (x10000)
H
CD8 T Cells 12-11
Viable Cells 12-11
CD45 (PE)
FSC-A (x10000)
I
CD8 T Cells 12-11
CD45+ 12-11
CD3 (APC-A780)
FSC-A (x10000)
J
CD8 T Cells 12-11
CD3+ 12-11
CD8a (FITC)
FSC-A (x10000)
K
CD8 T Cells 12-11
Viable Cells 12-11
SSC-A (x10000)
FSC-A (x10000)

CD8+ T cells, 09-30			
Gate	Number of Events	Percent of Gated Cells	Percent of All Cells
Viable Cells	8545	100.00	16.14
CD3+	8189	95.83	15.47
CD8a+	8188	95.82	15.47

CD8+ T cells, 12-10			
Gate	Number of Events	Percent of Gated Cells	Percent of All Cells
Viable Cells	9475	100.00	73.87
CD45+	9301	98.16	72.52
CD3+	9151	96.58	71.35
CD8a+	8824	93.27	68.80

CD8+ T cells, 12-11			
Gate	Number of Events	Percent of Gated Cells	Percent of All Cells
Viable Cells	9747	100.00	90.82
CD45+	9664	99.15	90.05
CD3+	9522	97.69	88.73
CD8a+	9298	95.39	86.64

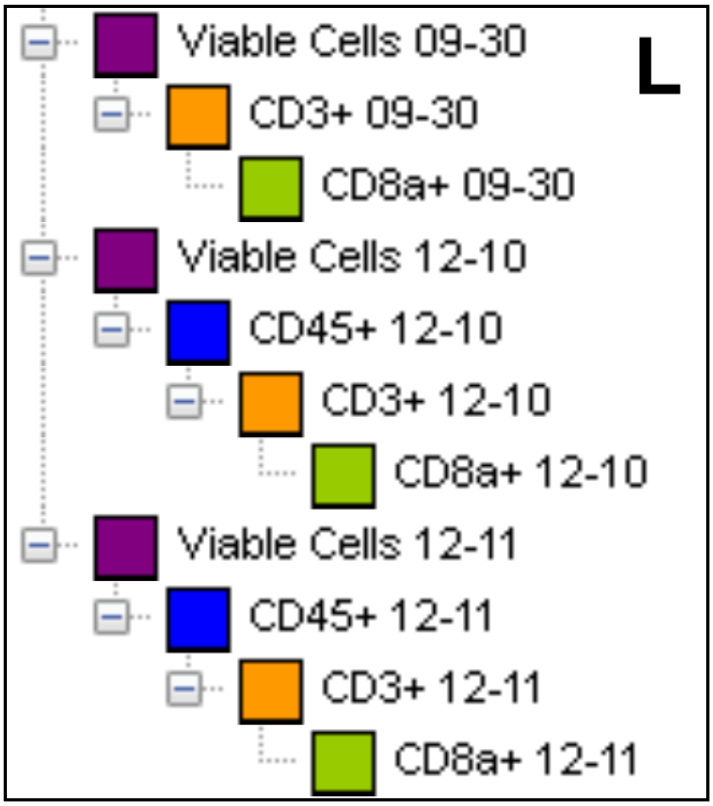

Figure 4.2 – Flow cytometry purity assessment of primary human CD8 T cell samples used for microarray analysis. (A-C) CD8 T cells from donor 1. CD45 staining was not performed with cells from donor 1. (D-G) CD8 T cells from donor 2. (H-K) CD8 T cells from donor 3. Viable cells are gated hierarchically as depicted in panel L. The purity of CD45+/CD3+/CD8a+ events are highlighted in red text in the tables in panel L as a percent of all viable cells. The 09-30 T cells were collected before the Ficoll procedure had been optimized. Mouse isotypes: CD3-APC IgG1, CD3-APC-A780 IgG1, CD45-PE IgG1, CD8a-FITC IgG1.

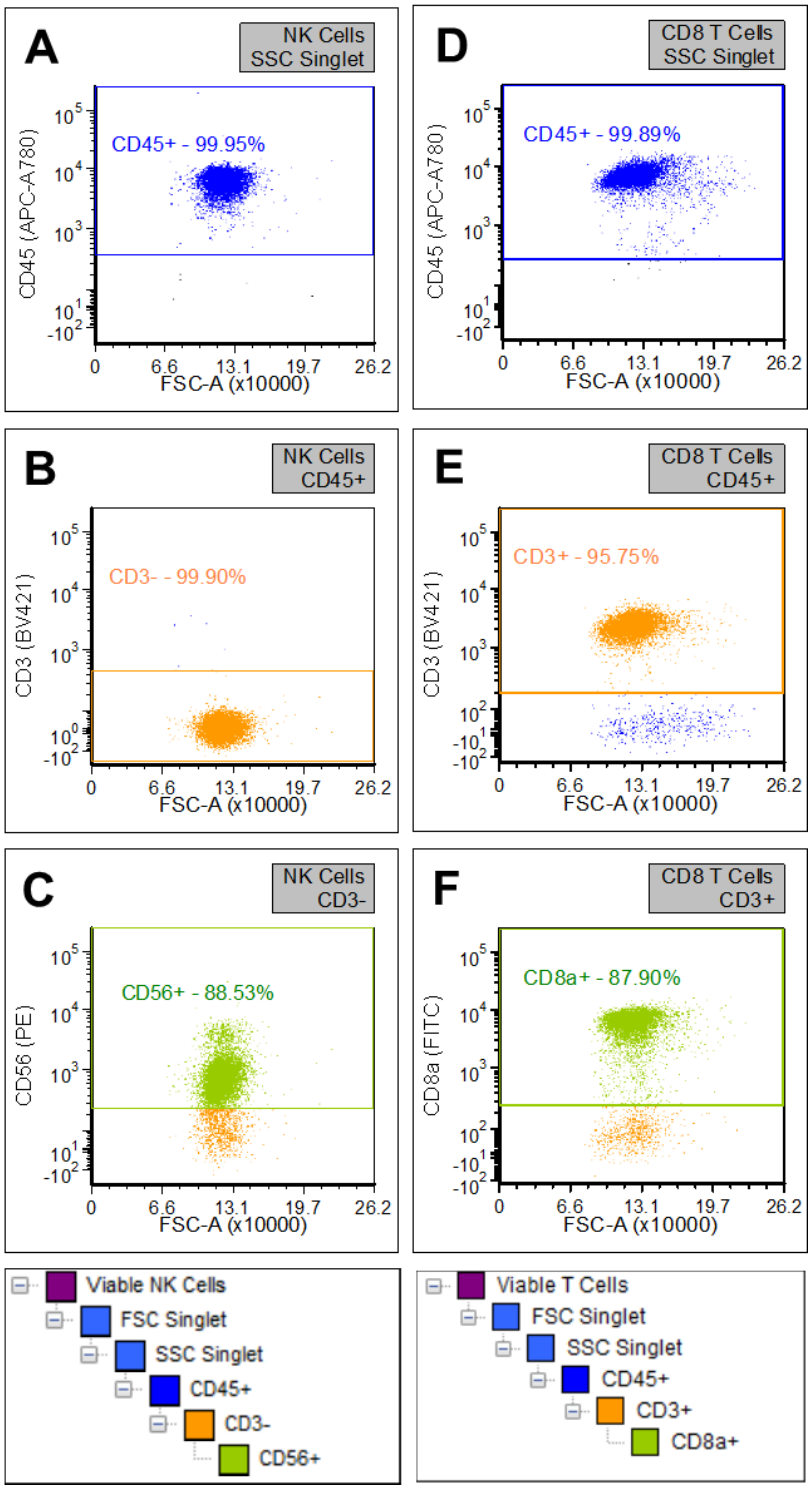
A
NK Cells
SSC Singlet
CD45+ - 99.95%
CD45 (APC-A780)
FSC-A (x10000)
D
CD8 T Cells
SSC Singlet
CD45+ - 99.89%
CD45 (APC-A780)
FSC-A (x10000)
B
NK Cells
CD45+
CD3- - 99.90%
CD3 (BV421)
FSC-A (x10000)
E
CD8 T Cells
CD45+
CD3+ - 95.75%
CD3 (BV421)
FSC-A (x10000)
C
NK Cells
CD3-
CD56+ - 88.53%
CD56 (PE)
FSC-A (x10000)
F
CD8 T Cells
CD3+
CD8a+ - 87.90%
CD8a (FITC)
FSC-A (x10000)
Viable NK Cells
FSC Singlet
SSC Singlet
CD45+
CD3-
CD56+
Viable T Cells
FSC Singlet
SSC Singlet
CD45+
CD3+
CD8a+

Figure 4.3 (previous page) – Flow cytometry purity assessment of primary NK cells and CD8 T cells used for multiplex analysis of soluble mediator production. (A-C) NK cell sample, showing CD56+ as a percentage of viable CD45+/CD3- events; (D-F) CD8 T cell sample, showing CD8+ as a percentage of CD45+/CD3+ events. Mouse isotypes: CD3-BV421 IgG2a, CD45-APC-A780 IgG1, CD56-PE IgG2a, CD8a-FITC IgG1.

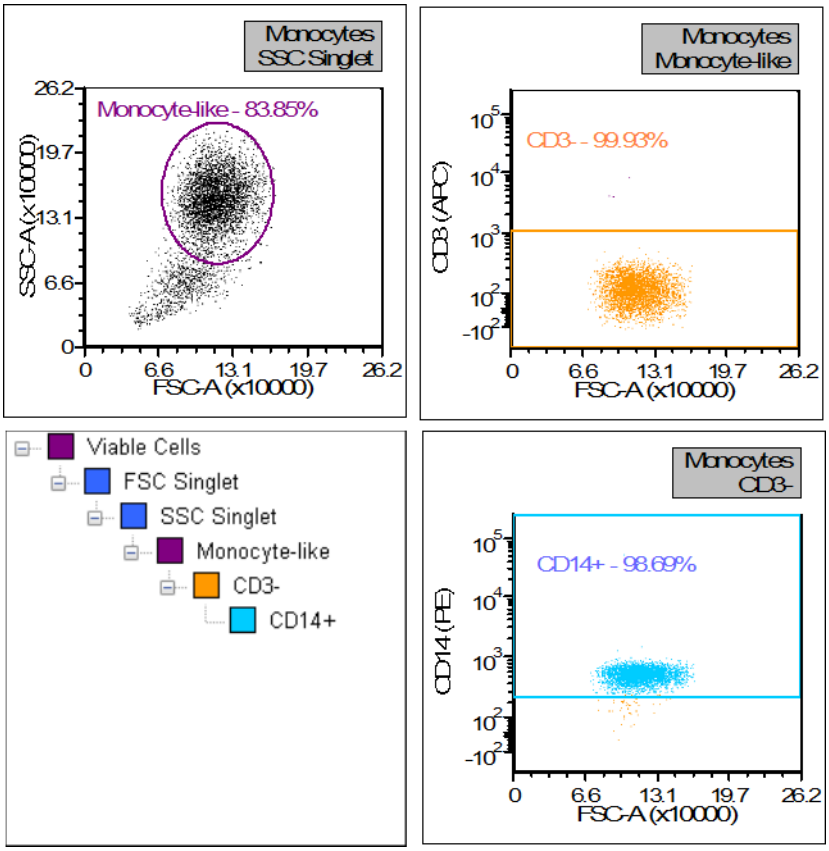

Figure 4.4 – Flow cytometric analysis of purity of monocytes used in the IFNG stimulation time course. The gating strategy is depicted in the bottom-left panel. Events in the monocyte-like gate are described as a percentage of all viable singlet events. The CD3- and CD14+ events are described as a percentage of events in the monocyte-like gate. CD3-/CD14+ monocyte-like events accounted for 82.75% of all viable singlet events. Data was derived from a single sample of primary monocytes from a single donor. Mouse isotypes: CD3-APC IgG1, CD14-PE IgG1.

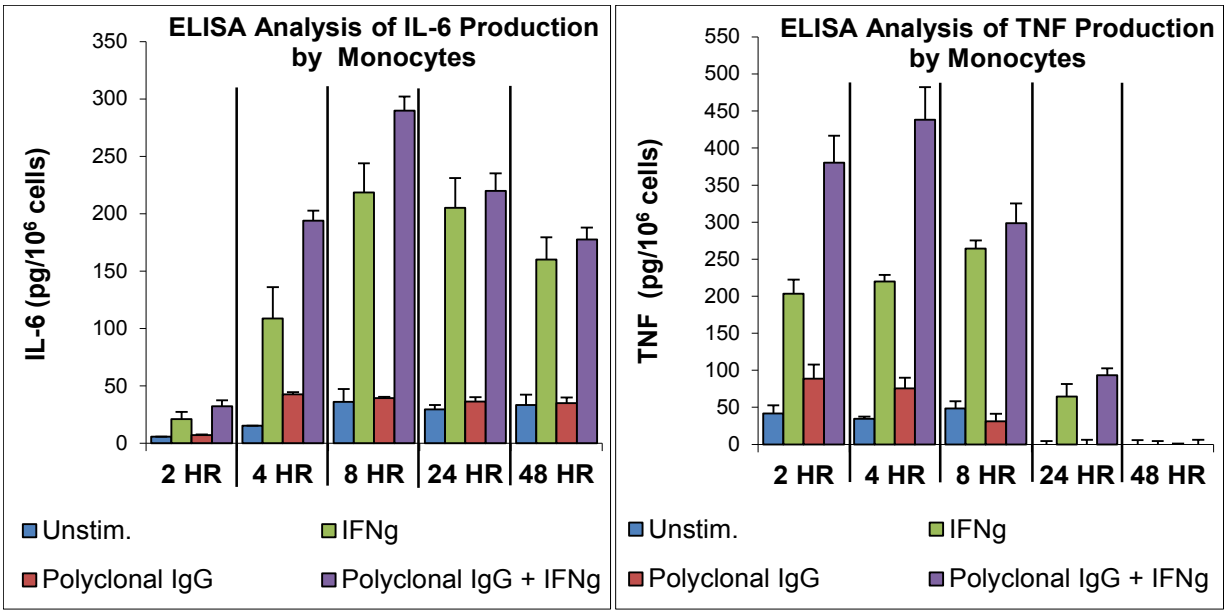

Figure 4.5 – ELISA detection of supernatant levels of IL-6 and TNF produced by IFNG-stimulated primary human monocytes. Concentrations are given in picograms per million monocytes. Unstimulated (blue), IFNG-stimulated (green), polyclonal IgG-stimulated (red), and polyclonal IgG + IFNG-stimulated (violet) monocytes were assessed. IFNG was given at a concentration of 1153U per million monocytes. Polyclonal IgG stimulation was achieved by cross-linking the IgG on monocyte Fc receptors with plate-bound goat anti-human IgG $F(ab')_2$. Results are derived from a single experiment using monocytes from a single donor. Each sample denoted by the bars was analyzed in triplicate, and the error bars show the standard deviation between the triplicates.

CHAPTER 5
CD16a-Inducible NK Cell Transcripts in ABMR

5.1 Overview

We cultured primary human NK cells *in vitro* and stimulated them directly through CD16a using plate-bound anti-CD16a antibodies as described in chapter 3. We analyzed global gene expression changes in CD16a-stimulated versus unstimulated NK cells using microarrays and identified the top 30 most highly increased CD16a-inducible NK cell transcripts, as well as the 30 most highly expressed (but not necessarily CD16a-inducible) transcripts in unstimulated NK cells. To find evidence of CD16a-mediated NK cell activation in ABMR, we studied these transcripts' expression levels in a set of 703 histologically classified, clinically indicated human kidney transplant biopsies. A handful of the top CD16a-inducible transcripts were strongly associated with ABMR compared to other diagnoses, and several associated weakly with ABMR. Many transcripts that were weakly associated with ABMR were promiscuously expressed in other cell types in a primary human cell panel. We identified at least one ABMR-associated transcript that was selective for CD16a-stimulated NK cells, providing evidence of CD16a-mediated NK cell activation.

5.2 Identifying top CD16a-inducible NK cell transcripts

Three replicate cultures of primary human NK cells from three separate donors were either left unstimulated or were stimulated for 4 hours with anti-CD16a antibodies crosslinked by plate-bound $F(ab')_2$. Successful activation of each replicate was confirmed by IFNG and TNF ELISAs (see chapter 3). To determine which transcripts were most highly increased following CD16a stimulation in NK cells, we analyzed gene expression microarray data from stimulated and unstimulated NK cell cultures. First, we identified transcripts that were increased more than two-fold in stimulated versus unstimulated NK cells (FDR < 0.05). We removed transcripts with >500 mean expression across four control nephrectomies, as these transcripts would be highly expressed in all kidney biopsies and would not be useful in identifying CD16a activity in ABMR. In pilot experiments we observed that small numbers of contaminating monocytes can alter transcript lists by introducing transcripts inducible by IFNG from stimulated NK cells. To mitigate the influence of monocytes, transcripts that were increased more than two-fold in IFNG-stimulated versus unstimulated primary human monocytes were removed from the list of CD16a-inducible NK cell transcripts.

A total of 455 probe sets representing 276 unique transcripts were increased more than two-fold in stimulated versus unstimulated NK cells (FDR < 0.05). Of these, we selected the top 30 most increased transcripts (by fold change versus unstimulated NK cells) that had >200 expression in stimulated NK cells (**Table 5.1**). Notable transcripts included cell surface markers associated with effector cell

function *CRTAM, TNFRSF9* (4-1BB), and *CD160*; chemokines *CCL3* (MIP-1α), *CCL4* (MIP-1β), and *XCL1* (lymphotactin); and effector cytokines *CSF2* (GM-CSF) and *IFNG*, among others. CCL3, CCL4, IFNG, and CSF2 production was later confirmed in 30-plex analysis of soluble mediators produced by CD16a-stimulated NK cells (see chapter 6). Thus, CD16a-stimulated NK cells produce proinflammatory mediators that may affect tissue phenotypes and shape immune responses in ABMR pathogenesis.

5.3 CD16a-inducible NK cell transcripts' associations with ABMR

Next, we studied expression of the top CD16a-inducible NK cell transcripts in703 clinically indicated histologically classified biopsies and asked whether they are differentially expressed in ABMR compared to other diagnoses. As outlined in the materials and methods, these biopsies were originally analyzed on microarrays in previous studies, and the data is preserved in a local database. **Figure 5.1** shows the fold change and association strengths of transcripts with ABMR compared to all other diagnoses except TCMR and mixed rejection. Including TCMR and mixed rejection in the comparator could weaken the *p* values of some CD16a-inducible transcripts in ABMR because CD16a and TCR signaling are similar processes that might induce expression of shared transcripts in NK cells and T cells. By excluding TCMR and mixed rejection from the comparator, we could identify transcripts that may have been overlooked had TCMR and mixed rejection been included in the comparator.

Transcripts satisfying $p < 5x10^{-6}$ were considered strongly associated with ABMR. In decreasing order of association, these were *CCL4, CD160, CCL3, XCL1, CRTAM, FCRL3, TNFRSF9,* and *STARD4.* The remaining transcripts were weakly associated with ABMR. Interestingly, despite robust expression by CD16a-stimulated NK cells *in vitro*, *IFNG* was increased in ABMR but only modestly associated with ABMR ($p = 4.6x10^{-3}$), probably because it is induced in multiple forms of tissue injury (109).

5.4 DSA-selective NK associated transcripts that identified NK cell involvement in ABMR are not CD16a-inducible

Our group previously published a set of six NK cell transcripts that were selectively associated with DSA-positive patient status and provided evidence of NK cell involvement in human ABMR: *GNLY, SH2D1B, KLRF1, CX3CR1, MYBL1,* and *FGFBP2*. None of these DSA-selective transcripts (DSASTs) were represented among the top 30 most highly CD16a-inducible NK cell transcripts, yet they are among the most strongly ABMR-associated NK cell transcripts. The paper that discussed these DSASTs did not examine whether these transcripts are CD16a-inducible in NK cells, so we examined their expression in CD16a-stimulated versus unstimulated NK cells. **Table 5.2** shows that these transcripts are highly expressed in both resting and stimulated NK cells, but they are not strongly CD16a-inducible. *GNLY* expression was unaffected by CD16a activation; *KLRF1* and *SH2D1B* were slightly increased; and *FGFBP2, MYBL1,* and *CX3CR1* decreased following CD16a

stimulation. Thus, these transcripts' associations with ABMR are driven by increased NK cell localization in ABMR compared to other diagnoses, not by CD16a stimulation alone.

5.5 Many highly expressed but non-CD16a inducible NK cell transcripts are associated with ABMR

Pursuing the notion that some NK cell transcripts are associated with ABMR by virtue of high expression in NK cells and increased NK cell burden in ABMR, we identified a list of the top 30 most highly expressed transcripts in unstimulated NK cells (**Table 5.3**). Four of the six DSASTs were represented on this list: *GNLY, KLRF1, SH2D1B,* and *FGFBP2*. Cytolysins *GZMB, GNLY,* and *PRF1* were among the most highly expressed transcripts in resting and CD16a-stimulated NK cells, reflecting a state where cytolysin transcripts are constitutively expressed but not transcriptionally regulated by CD16a. Some transcripts were both highly expressed in resting NK cells and were CD16a-inducible. *CCL4* and *KLRD1* are examples. *AUTS2*, *RASA3*, *SLA2,* and a few others decreased in response to CD16a stimulation.

We examined expression of these 30 highly expressed transcripts in ABMR compared to all other diagnoses except TCMR and mixed rejection (**Figure 5.2**). Twenty-two highly expressed resting NK cell transcripts were strongly associated with ABMR versus eight CD16a-inducible transcripts ($p < 5 \times 10^{-6}$). All six DSASTs were strongly associated with ABMR. As was the case with the top 30 CD16a-

inducible transcripts, some of the top highly expressed transcripts were weakly associated with ABMR. We hypothesized that transcripts' *p* values in ABMR could be explained by expression in other cell types in other diagnoses.

5.6 Determining the selectivity of transcripts for NK cells

We observed that many highly expressed and CD16a-inducible NK cell transcripts were not strongly associated with ABMR, and postulated that the weak *p* values could be explained by promiscuous expression of transcripts by non-NK cells. We studied expression of the top highly expressed unstimulated NK cell transcripts (listed in **Table 5.3**) and the top CD16a-inducible NK cell transcripts (listed in **Table 5.1**) in an extended primary human cell panel. The cell panel included cultures of human umbilical vein endothelial cells (HUVECs) +/- IFNG treatment, renal proximal tubule epithelial cells (RPTECs) +/- IFNG treatment, immature dendritic cells, mature LPS-treated dendritic cells, monocytes, macrophages +/- IFNG treatment, B cells, allostimulated CD4+ T cells, and allostimulated CD8+ T cells. The effect of IFNG treatment on HUVECs, RPTECs, and macrophages was studied because CD16a-stimulated NK cells produce IFNG, and we wanted to determine whether NK cell transcripts that were associated with ABMR were also IFNG-inducible in other cell types, which would potentially boost their association with ABMR. Details of the composition and culture conditions that were used in the generation of this cell panel were previously described (9).

Figure 5.3 shows the expression of the top 30 CD16a-inducible NK cell transcripts in the extended human cell panel. **Figure 5.4** shows expression of DSASTs and the top highly expressed resting NK cell transcripts in the extended human cell panel. In analyzing expression of these transcripts in other cells we described transcripts with expression >200 (7.64 in log2 format in **Figure 5.3** and **5.**4) as moderately expressed in a given cell type. Transcripts with expression >500 (8.97 in log2 format in **Figure 5.3** and **5.4**) were described as highly expressed. We did not include expression data for NK cells in **Figure 5.3** and **Figure 5.4** because NK cell gene expression was studied using Affymetrix PrimeView™ gene chips, whereas the extended cell panel data were obtained using Affymetrix HG-U133™ gene chips. A transcript's expression in a microarray chip can be described quantitatively in relation other transcripts reported by the same type of chip, and cross-platform comparisons of the qualitative trends overlying those quantitative descriptions are valid because these qualitative trends are preserved across different chip platforms. However, because raw expression values are reported differently between different types of chips, different chip platforms cannot be directly compared on a quantitative basis.

Many of the top CD16a-inducible transcripts were expressed in other cell types besides NK cells (**Figure 5.3**). Only *CD160* appeared selective for NK cells based on these data, and provides the most compelling evidence of CD16a-mediated NK cell activation in ABMR. Of the eight most highly ABMR-associated CD16a-inducible transcripts ($p < 5\text{x}10^{-6}$), *CCL3, CCL4, STARD4,* and *CRTAM* were IFNG-

inducible in one or more cell types. All four were IFNG-inducible in macrophages. *STARD4* was IFNG-inducible in HUVECs, and was highly expressed by all cells on the extended panel except monocytes. *CCL3* and *CCL4* were IFNG-inducible in macrophages, and also highly expressed in unstimulated macrophages. *CCL3* was highly expressed by unstimulated monocytes, CD8+ T cells, and dendritic cells, and moderately expressed by allostimulated CD4+ T cells. *CCL4* was moderately expressed by unstimulated monocytes, and highly expressed by allostimulated CD4+ T cells, CD8+ T cells, and dendritic cells. *FCRL3* was highly expressed by B cells. *XCL1* was highly expressed by allostimulated CD8+ T cells, and moderately expressed by allostimulated CD4+ T cells. *TNFRSF9* was moderately expressed by macrophages and mature dendritic cells, and decreased in macrophages treated with IFNG. Characteristics of the top 8 most highly ABMR-associated CD16a-inducible transcripts are summarized in **Table 5.4.**

CD16a-inducible transcripts that were not strongly associated with ABMR were often highly expressed in other cell types. Transcripts that were at least moderately expressed in HUVECs or RPTECs but not IFNG-inducible in these cells were weakly associated with ABMR (e.g. *SERPINE2, FAM3C, RILPL2, MYC, RRAD, TBC1D4, NAB2, SPRY1, SPRY2)*. Transcripts that were preferentially expressed by B cells and stimulated NK cells were at least mildly associated with ABMR (e.g. *CD72, GPR18, FCRL3*). Non-IFNG inducible transcripts that were expressed in multiple types of leukocytes were weakly associated with ABMR (e.g. *NR4A2, NR4A3, IRF4*).

Expression of the DSASTs and the top highly expressed unstimulated NK cell transcripts was examined in the same cell panel (**Figure 5.4**). As we observed with the top CD16a-inducible NK cell transcripts, top highly expressed resting NK cell transcripts that were IFNG-inducible in other cell types were more strongly associated with ABMR than promiscuously expressed transcripts that were not IFNG-inducible. *HLA-F* exemplified this phenomenon: it was intensely expressed by all cells in the extended cell panel, but it gained impressive expression in all cells treated with IFNG. In contrast, CD44 was similarly highly expressed by all cells in the extended cell panel, but it decreased in all cells that received IFNG treatment. *HLA-F* was strongly associated with ABMR ($p = 3.8 \times 10^{-18}$), whereas CD44 was not ($p = 1.3 \times 10^{-2}$). Strikingly, most of the transcripts that were highly expressed in resting NK cells were also strongly expressed in CD4+ and CD8+ T cells. *EOMES, KLRD1, GZMH,* and *FGFBP2* were highly expressed by CD8+ T cells, but not CD4+ T cells. Only *KLRF1*, *SH2D1B*, *CX3CR1*, *IL23A*, *TARP*, and *MYBL1* were at most modestly expressed by either type of T cell. Note that the data for *IL23A* and *TARP* in the extended cell panel and biopsy analyses may be unreliable because the signal gain displayed by these probe sets is minimal on the HG-U133™ gene chips. This was not the case with the PrimeView™ chips used to identify *IL23A* and *TARP* as highly expressed NK cell transcripts in the first place.

In summary, *CD160* was NK selective and provided evidence of CD16a triggering in ABMR. ABMR-associated transcripts that were highly expressed but not CD16a-inducible in NK cells support increased NK cell burden in ABMR

compared to other diseases. Promiscuous expression in other cell types tended to weaken transcripts' associations with ABMR, presumably because the proportion of NK cells relative to some other cell types is low in ABMR and because other cells that express the same transcripts are often present in biopsies with other diagnoses. A key exception was transcripts that were IFNG-inducible in other cell types. These transcripts were more strongly associated with ABMR than promiscuously expressed transcripts that were not IFNG-inducible, corroborating studies that reported a preponderance of IFNG-inducible transcripts in ABMR (9;107;110). Given that some of the most highly CD16a-inducible transcripts in NK cells are proinflammatory chemokines and cytokines (*IFNG* among them), these results support the concept that NK cells play a major role orchestrating the immune response in ABMR.

FIGURES & TABLES

Table 5.1 Top 30 CD16a-inducible transcripts in primary human NK cells in vitro, by decreasing fold change in CD16a-stimulated NK cells

Gene Symbol	Gene Title	Alias	NK Cells, Unstimulated Raw Expression	NK Cells, Anti-CD16α Stimulated Raw Expression	Fold Change (Stimulated vs. Unstimulated)
CRTAM	Cytotoxic and regulatory T cell molecule	CD355	45	7361	164.7
IFNG	Interferon, gamma	-	59	6484	110.0
TNFRSF9	Tumor necrosis factor receptor superfamily, member 9	4-1BBR	43	3835	90.1
SPRY2	Sprouty homolog 2 (Drosophila)	IGAN3	19	895	46.1
CCL4	Chemokine (C-C motif) ligand 4/ 4-like 1 / 4-like 2	MIP-1B	289	12522	43.4
CD72	CD72 molecule	LYB2	20	667	33.5
CSF2	Colony stimulating factor 2 (granulocyte-macrophage)	GM-CSF	34	1093	32.3
CCL3	Chemokine (C-C motif) ligand 3/ 3-like 1 / 3-like 3	MIP-1A	322	7433	23.1
ZBED2	Zinc finger, BED-type containing 2	-	15	332	22.7
FEZ1	Fasciculation and elongation protein zeta 1 (zygin I)	-	119	2624	22.0
RGS16	Regulator of G-protein signaling 16	RGSR	50	831	16.8
XCL1	Chemokine (C motif) ligand 1	LTN	93	1344	14.4
NR4A2	Nuclear receptor subfamily 4, group A, member 2	NOT	141	1888	13.4
TRAF1	TNF receptor-associated factor 1	-	55	628	11.5
NR4A3	Nuclear receptor subfamily 4, group A, member 3	CHN	20	220	11.3
IRF4	Interferon regulatory factor 4	LSIRF	157	1749	11.2
NAB2	NGFI-A binding protein 2 (EGR1 binding protein 2)	YGL122C	45	479	10.6
CD160	CD160 molecule	BY55	481	4602	9.6
FCRL3	Fc receptor-like 3	CD307c	275	2568	9.3
PTPN6	Protein tyrosine phosphatase, non-receptor type 6	SHP1	93	836	9.0
SERPINE2	Serpin peptidase inhibitor, clade E (nexin, plasminogen activator inhibitor type 1), member 2	GDN	105	791	7.6
SPRY1	Sprouty homolog 1, antagonist of FGF signaling (Drosophila)	-	38	235	6.1
RRAD	Ras-related associated with diabetes	RAD	56	339	6.0
GPR18	G protein-coupled receptor 18	-	606	3641	6.0
TBC1D4	TBC1 domain family, member 4	-	49	293	5.9
STARD4	StAR-related lipid transfer (START) domain containing 4	-	108	643	5.9
RILPL2	Rab interacting lysosomal protein-like 2	RLP2	96	556	5.8
FAM3C	Family with sequence similarity 3, member C	ILEI	209	1196	5.7
BIRC3	Baculoviral IAP repeat containing 3	c-IAP2	157	892	5.7
MYC	V-myc myelocytomatosis viral oncogene homolog (avian)	MRTLC	287	1616	5.6

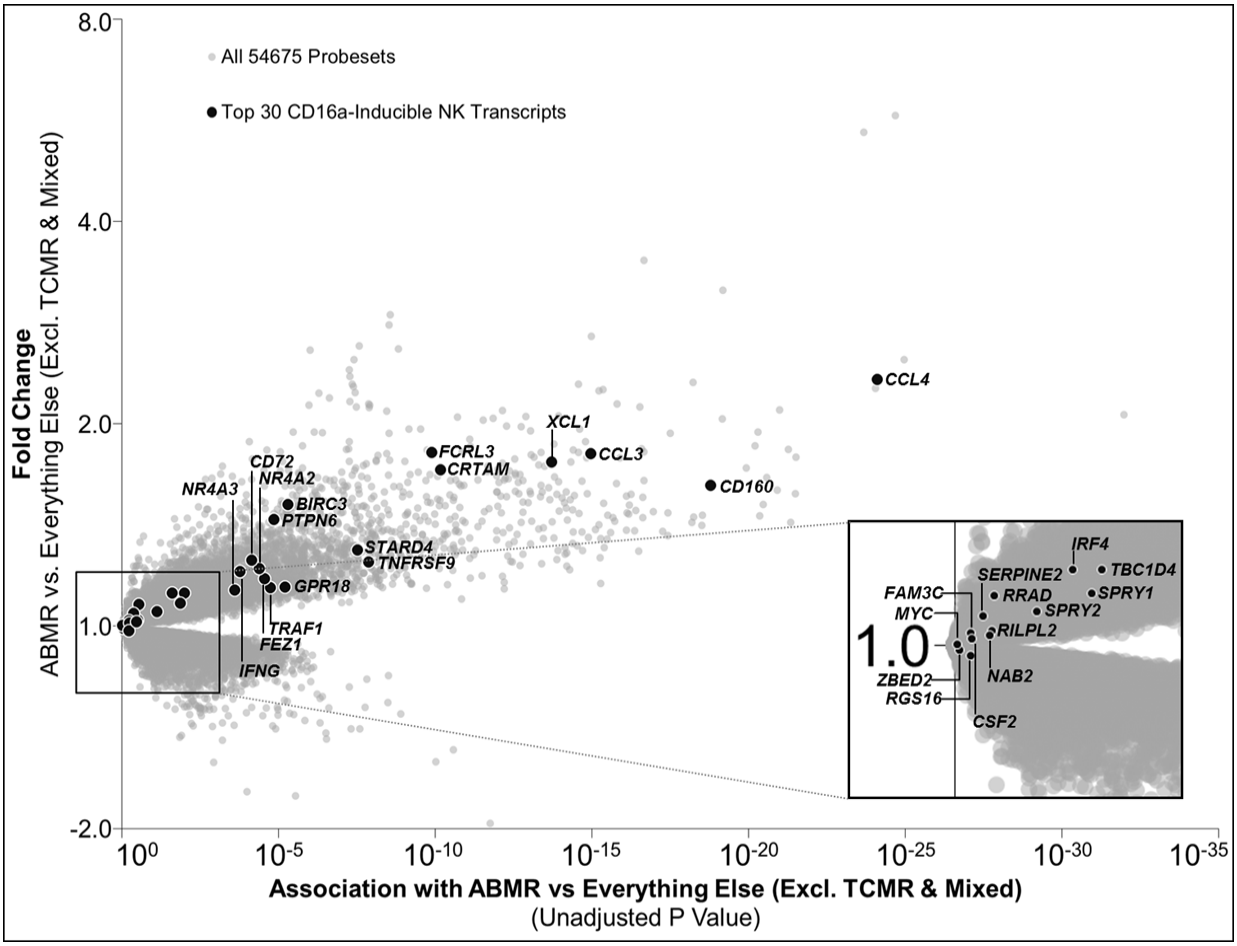

Figure 5.1 – Association of the top 30 CD16a-inducible NK cell transcripts with histologically classified ABMR versus all other diagnoses except TCMR and mixed rejection. Probe sets are plotted by fold change and association with 110 histologically classified ABMR biopsies versus 498 biopsies without histologically classified TCMR or mixed rejection.

Table 5.2 – Expression of DSA-selective NK associated transcripts in CD16a-stimulated and unstimulated NK cells, sorted by decreasing association with ABMR

Gene Symbol	Gene Title	NK Cells, Unstim. Raw Expression	NK Cells, Anti-CD16α Stim. Raw Expression (FC vs Unstim.)	P Value, ABMR vs. Everything Except TCMR, Mixed
GNLY	Granulysin	15676	15049 (0.96)	9.12×10^{-25}
FGFBP2	Fibroblast growth factor binding protein 2	10404	5410 (0.52)	5.45×10^{-22}
SH2D1B	SH2 domain containing 1B	6512	8402 (1.29)	1.21×10^{-21}
CX3CR1	Chemokine (C-X3-C motif) receptor 1	4154	2825 (0.68)	3.25×10^{-18}
KLRF1	Killer cell lectin-like receptor subfamily F, member 1	6886	7988 (1.16)	2.26×10^{-17}
MYBL1	v-myb myeloblastosis viral oncogene homolog (avian)-like 1	3800	2888 (0.76)	4.33×10^{-14}

Table 5.3 – Top 30 most highly expressed transcripts in unstimulated primary human NK cells by decreasing expression in unstimulated NK cells

Gene Symbol	Gene Title	Alias	NK Cells, Unstimulated Raw Expression	NK Cells, Anti-CD16α Stimulated Raw Expression	Fold Change (Stimulated vs. Unstimulated)
GZMB	Granzyme B	-	16897	19938	1.2
GNLY	Granulysin	-	15694	15049	1.0
IL2RB	Interleukin 2 receptor, beta	-	15493	14489	0.9
PRF1	Perforin 1 (pore forming protein)	-	11203	10383	0.9
GZMA	Granzyme A	-	11169	8318	0.7
CCND2	Cyclin D2	-	10634	9901	0.9
LCP1	Lymphocyte cytosolic protein 1 (L-plastin)	L-Plastin	10433	9073	0.9
FGFBP2	Fibroblast growth factor binding protein 2	KSP37	10369	5410	0.5
FCGR3A/FCGR3B	Fc fragment of IgG receptor, low affinity IIIa/IIIb	CD16a/b	10001	9289	0.9
PTPRC	Protein tyrosine phosphatase, receptor type, C	CD45	9666	10237	1.1
CCL4	Chemokine (C-C motif) ligand 4 /4-like 1 /4-like 2	MIP-1B	9219	19312	2.1
GNG2	Guanine nucleotide binding protein (G protein), gamma 2	-	8516	8193	1.0
GIMAP7	GTPase, IMAP family member 7	IAN7	7988	3463	0.4
CLEC2B	C-type lectin domain family 2, member B	AICL	7978	7320	0.9
CD44	CD44 molecule (Indian blood group)	-	7895	6382	0.8
CXCR4	chemokine (C-X-C motif) receptor 4	CD184	7668	5279	0.7
KLRF1	Killer cell lectin-like receptor subfamily F, member 1	NKp80	6916	7988	1.2
EOMES	Eomesodermin	TBR2	6705	4587	0.7
SH2D1B	SH2 domain containing 1B	EAT2	6534	8401	1.3
KLRD1	Killer cell lectin-like receptor subfamily D, member 1	CD94	6520	10848	1.7
TRBC1	T cell receptor beta constant 1	-	6151	4723	0.8
SLA2	Src-like-adaptor 2	-	6049	3016	0.5
GZMH	Granzyme H	-	5960	3366	0.6
IL23A	Interleukin 23, alpha subunit p19	-	5941	5389	0.9
CCL5	Chemokine (C-C motif) ligand 5	RANTES	5884	7471	1.3
TARP/TRGC2	TCR gamma alternate reading frame protein /T cell receptor gamma constant 2	-	5747	7293	1.3
NKG7	Natural killer cell group 7 sequence	GIG1	5671	4861	0.9
RASA3	RAS p21 protein activator 3	-	5654	3049	0.5
HLA-F	Major histocompatibility complex, class I, F	-	5645	7193	1.3
KLRB1	Killer cell lectin-like receptor subfamily B, member 1	NKRP1A	5568	5115	0.9

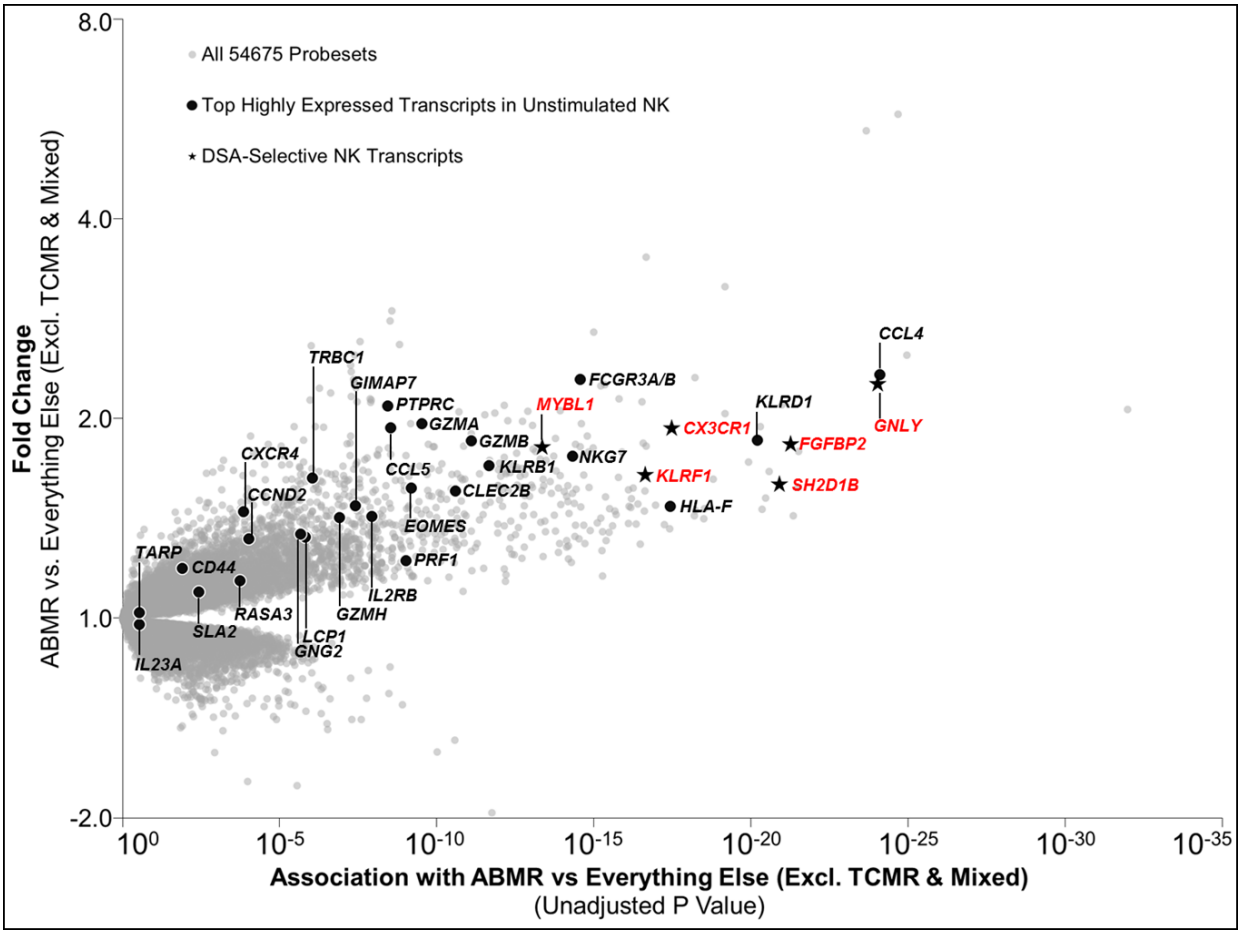

Figure 5.2 – Association of the top 30 most highly expressed unstimulated NK cell transcripts and DSA-selective NK cell transcripts with histologically classified ABMR versus all other diagnoses except TCMR and mixed rejection. Probe sets are plotted by fold change and association with 110 histologically classified ABMR biopsies versus 498 biopsies without histologically classified TCMR or mixed rejection. DSA-selective NK transcripts that provided initial evidence of NK cell involvement in ABMR are highlighted in red.

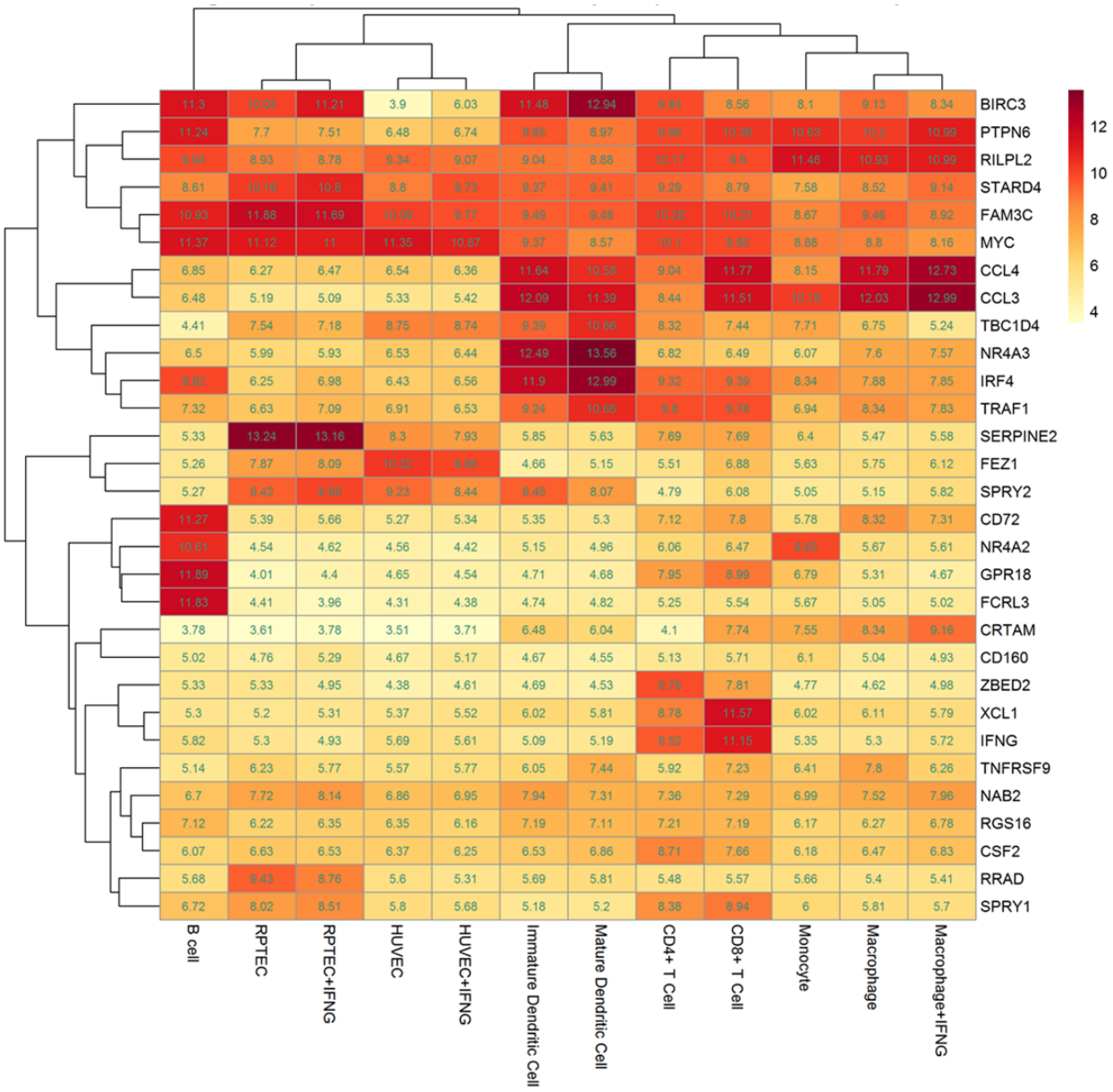

Figure 5.3 – Top 30 CD16a-inducible transcripts' expression in an extended human cell panel. Geometric mean expression for each transcripts' representative probe set was calculated for each cell type. Geometric mean expression values are given in base-2 logarithmic format in each heatmap cell. Color is mapped to the logarithmic geometric mean expression values. Clustering was calculated using a Euclidean distance matrix. NK cell data is not shown, as the gene expression data for NK cells was obtained on a different chip platform (PrimeView™) than the cells shown in this figure (HG-U133™).

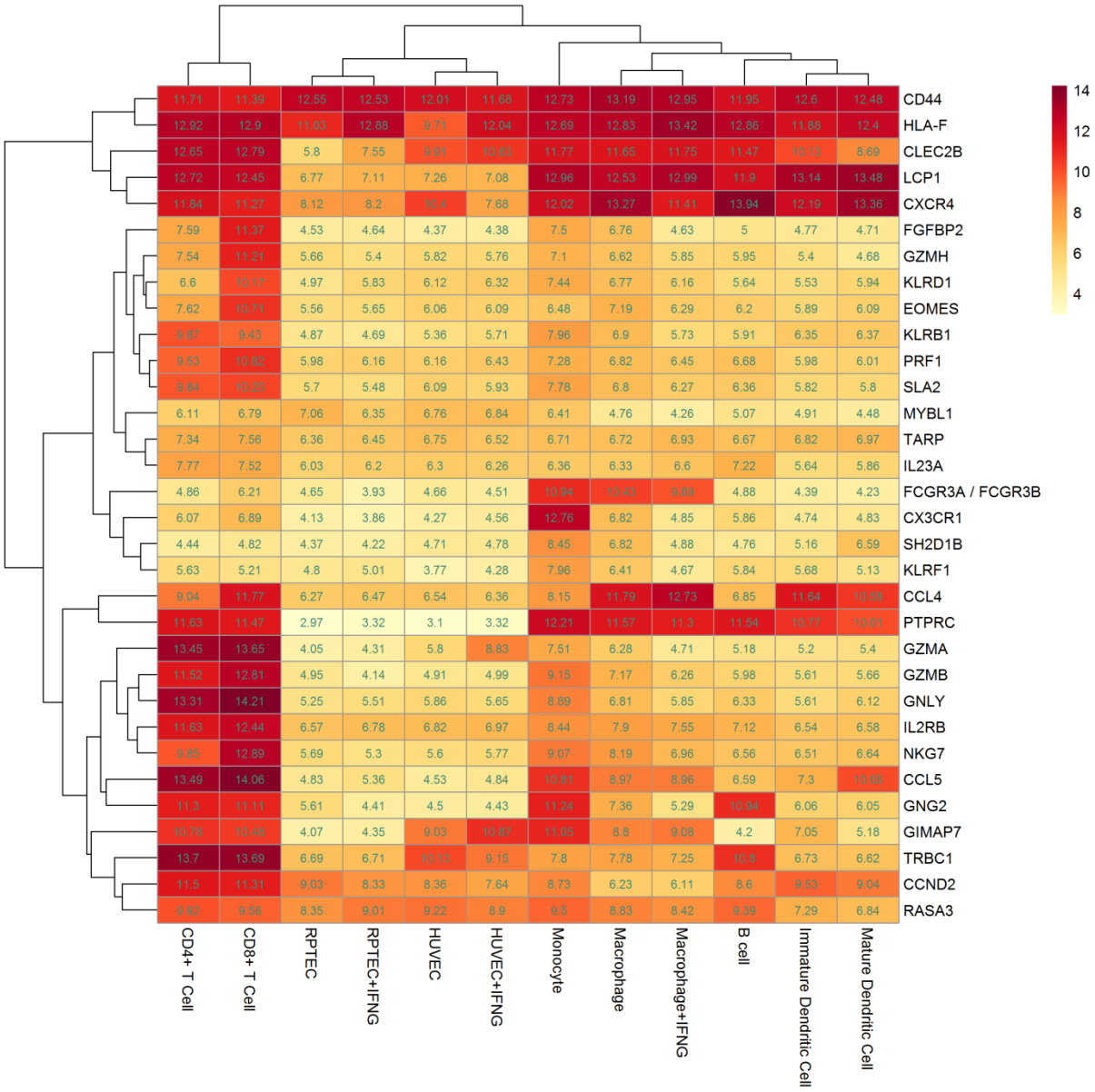

Figure 5.4 – Extended human cell panel expression of the top 30 most highly expressed resting NK cell transcripts and DSA-selective NK transcripts. Geometric mean expression for each transcript's representative probe set was calculated for each cell type. Geometric mean expression values are given in base-2 logarithmic format in each heatmap cell. Color is mapped to the logarithmic geometric mean expression values. Clustering was calculated using a Euclidean distance matrix. NK cell data is not shown, as the gene expression data for NK cells was obtained on a different chip platform (PrimeView™) than the cells shown in this figure (HG-U133™).

Table 5.4 – Characteristics of the most strongly ABMR-associated transcripts from the top 30 CD16a-inducible NK cell transcript list

Gene Symbol	Gene Title	Alias	Fold Change (Stim. vs. Unstim. NK Cells)	P Value (ABMR vs. Everything Except TCMR, Mixed)	Cells with >200 Expression*
CCL4	Chemokine (C-C motif) ligand 4/ 4-like 1 / 4-like 2	MIP-1B	43.4	7.97×10^{-25}	NK, DC, T4, T8, MC, MP
CD160	CD160 molecule	BY55	9.6	1.64×10^{-19}	NK
CCL3	Chemokine (C-C motif) ligand 3/ 3-like 1 / 3-like 3	MIP-1A	23.1	1.09×10^{-15}	NK, DC, T4, T8, MC, MP
XCL1	Chemokine (C motif) ligand 1	LTN	14.4	1.93×10^{-14}	NK, T4, T8
CRTAM	Cytotoxic and regulatory T cell molecule	CD355	164.7	6.89×10^{-11}	NK, T8, MP
FCRL3	Fc receptor-like 3	CD307c	9.3	1.30×10^{-10}	NK, B, T4, T8
TNFRSF9	Tumor necrosis factor receptor superfamily, member 9	4-1BBR	90.1	1.34×10^{-8}	NK, MP
STARD4	StAR-related lipid transfer (START) domain containing 4	-	5.9	3.10×10^{-8}	NK, B, DC, T4, T8, MP, HUVEC, RPTEC

*Based on the extended cell panel shown in Figure 4.
Abbreviations: B - B cells; DC - dendritic cells; HUVEC - human ubilical vein endothelial cells; MC - monocytes; MP - macrophages; NK - CD16a-stimulated NK cells; T4 - allostimulated CD4+ T cells; T8 - allostimulated CD8+ T cells; RPTEC - renal proximal tubule epithelial cells

CHAPTER 6
Molecular Overlap between NK cells, T cells, ABMR, and TCMR

6.1 Overview

CD3ζ is utilized by both CD16a and the TCR, inviting the possibility that activation of NK cells through CD16a results in some of the same gene expression changes as T cell activation through the TCR. The fact that NK cells and T cells are phenotypically similar probably poses an obstacle to interpreting the molecular signature of these cells in ABMR and TCMR, but this overlap has not yet been studied in the context of rejection pathogenesis. To effectively interpret molecular signatures in biopsies from organs undergoing rejection, it is important to understand which transcripts are induced following stimulation in both NK cells and effector T cells. Establishing a parallel between these two cells may also invite new opportunities for dual immunosuppression against ABMR and TCMR.

We hypothesized that some of the molecular features of CD16a-mediated NK cell activation and TCR-mediated CD8 T cell activation are shared, and are associated with both ABMR and TCMR as the result of this overlap. We cultured unstimulated and CD3-stimulated primary human CD8 T cells for 4 hours and assessed global gene expression changes. We asked how many transcripts were highly inducible by both CD16a triggering in NK cells and TCR/CD3 stimulation in

T cells. We also studied how the top 30 CD16a-inducible NK cell transcripts from earlier in this study were expressed in unstimulated and stimulated CD8 T cells, and compared soluble mediator production between CD16a-stimulated NK cells and CD3-stimulated T cells using a 30-plex platform. Finally, we examined expression of the top CD16a-inducible transcripts in TCMR compared to other diagnoses, postulating that CD16a-inducible transcripts that are also CD3-inducible in CD8 T cells will be associated not only with ABMR, but with TCMR.

6.2 Shared gene expression changes in stimulated NK cells and CD8 T cells

We asked which transcripts are highly inducible by CD16a triggering in NK cells and by CD3/TCR triggering in CD8 T cells. Primary human CD8 T cells were freshly isolated and cultured for 4 hours with or without CD3 stimulation. Stimulation was achieved by cross-linking anti-CD3 murine IgG antibodies (clone OKT3) to the culture plate with plate-bound goat anti-mouse IgG $F(ab')_2$. Three replicate cultures were established. Supernatants were harvested for IFNG and TNF ELISAs to verify activation. Total RNA was harvested for analysis on PrimeView™ gene chips.

The algorithm used to determine which transcripts are highly inducible (FC>2 vs. unstimulated) in both CD16a-stimulated NK cells and TCR/CD3-stimulated CD8 T cells is illustrated in **Figure 6.1.** As for the NK cell microarray data, we removed T cell transcripts that showed >500 expression in normal nephrectomies and were increased more than two-fold in IFNG-stimulated

monocyte cultures. We identified transcripts that were increased more than two-fold in CD3-stimulated versus unstimulated CD8 T cells, and looked for overlap with transcripts that were increased more than two-fold in CD16a-stimulated NK cells. Of 896 transcripts that were TCR/CD3-inducible in CD8 T cells and 455 transcripts that were CD16a-inducible in NK cells, we identified 239 that were inducible in both conditions. Summarily, NK cells and T cells increase expression of a generous number of overlapping transcripts following stimulation through these antigen recognition systems.

Next, we asked if any of the top 30 CD16a-inducible NK cell transcripts described in the previous chapter were inducible by TCR/CD3 stimulation of CD8 T cells. We looked up expression of the top 30 in the microarray results from both unstimulated and TCR/CD3 stimulated CD8 T cells, and calculated the fold change in stimulated over unstimulated T cells (**Table 6.1**). Of the 30 CD16a-inducible NK cell transcripts, 25 increased more than two-fold in TCR/CD3-stimulated CD8 T cells. *BIRC3, FAM3C, RILPL2, TBC1D4,* and *GPR18* were the only top 30 CD16a-inducible transcripts that were not increased more than two-fold in stimulated T cells. However, despite the fact that many CD16a-inducible transcripts also had high fold changes in T cells, several were not strongly expressed by T cells. *SPRY2, CD72, FEZ1, NR4A3, RRAD,* and *FAM3C* all had expression values under 200 in stimulated CD8 T cells. *RGS16, NAB2, CD160, FCRL3, STARD4,* and *RILPL2* were all under 500 in stimulated CD8 T cells. Many of the most highly CD16a-inducible transcripts were also very highly expressed by stimulated T cells. *CRTAM, IFNG,*

TNFRSF9, CCL4, CCL3, IRF4, and *MYC* had over 2000 expression in stimulated T cells. *IFNG* was by far the most pronounced with an expression signal of 10800 in stimulated T cells and a fold change of 259.2 over unstimulated T cells.

In chapter 5, we presented evidence that portrayed *CD160* as the most NK-selective CD16a-inducible transcripts we identified, because it was not expressed in other cells in a primary human cell panel (see **Figure 5.3**). Notably, in the extended cell panel *CD160* was not expressed in CD8 T cells, but **Table 6.1** shows that there was some expression by CD3-stimulated CD8 T cells *in vitro* (expression = 52 in **Figure 5.3** versus 407 in **Table 6.1**). **Figure 5.3** was based on U133 chip data and those T cells were stimulated by mixed lymphocyte culture, whereas the CD8 T cell data presented in **Table 6.1** was obtained with PrimeView chips and stimulation was achieved with anti-CD3 antibodies. These differences contribute to the discrepancy between expression values reported for CD8 T cells in **Figure 5.3** and **Table 6.1**.

6.3 Shared transcripts are associated with both ABMR and TCMR

We reasoned that transcripts that are both CD16a-inducible in NK cells and TCR/CD3-inducible in CD8 T cells would be associated not only with ABMR, but also with TCMR. We studied fold change and association of the top 30 CD16a-inducible transcripts with TCMR compared to all other diagnoses except ABMR and mixed rejection (**Figure 6.2**). ABMR and mixed rejection were excluded because inclusion would impact the p value of transcripts that are both CD16a-inducible in

NK cells in ABMR and TCR/CD3-inducible in effector T cells in TCMR. Sixteen of the top CD16a-inducible transcripts were strongly associated with TCMR ($p < 5x10^{-6}$), including *TNFRSF9, CRTAM, CCL4, XCL1, CCL3, FCRL3,* and *CD160,* which were all transcripts that were also strongly associated with ABMR. Other transcripts such as *IFNG* were strongly associated with TCMR but not ABMR.

6.4 NK cells and CD8 T cells share effector potential

Given the overlap between transcripts inducible by CD16a in NK cells and TCR/CD3 in CD8 T cells, we asked whether soluble mediators produced by each cell type are comparable, as soluble mediators are a significant component of immune system-mediated disease pathogenesis. We cultured primary human NK cells and CD8 T cells for 2, 4, 8, and 24 hours at a concentration of 500,000 cells/mL. NK cells and T cells were left unstimulated or stimulated respectively with anti-CD16a or anti-CD3 antibodies. Cell-free supernatants were harvested at each time point and analyzed for production of 30 different chemokines, cytokines, and growth factors. **Figure 6.3** shows soluble mediators that fell within or exceeded the upper detection range of their standard curves. Of the 30 mediators on the panel, only CCL3, CCL4, TNF, IFNG, and CSF2 were appreciably produced by either cell type. Strikingly, all five of these mediators were produced by both cell types following stimulation. These data illustrate that, of the 30 analytes tested, CD16a-stimulated NK cells and TCR/CD3-stimulated CD8 T cells produce a limited number of shared soluble mediators.

FIGURES & TABLES

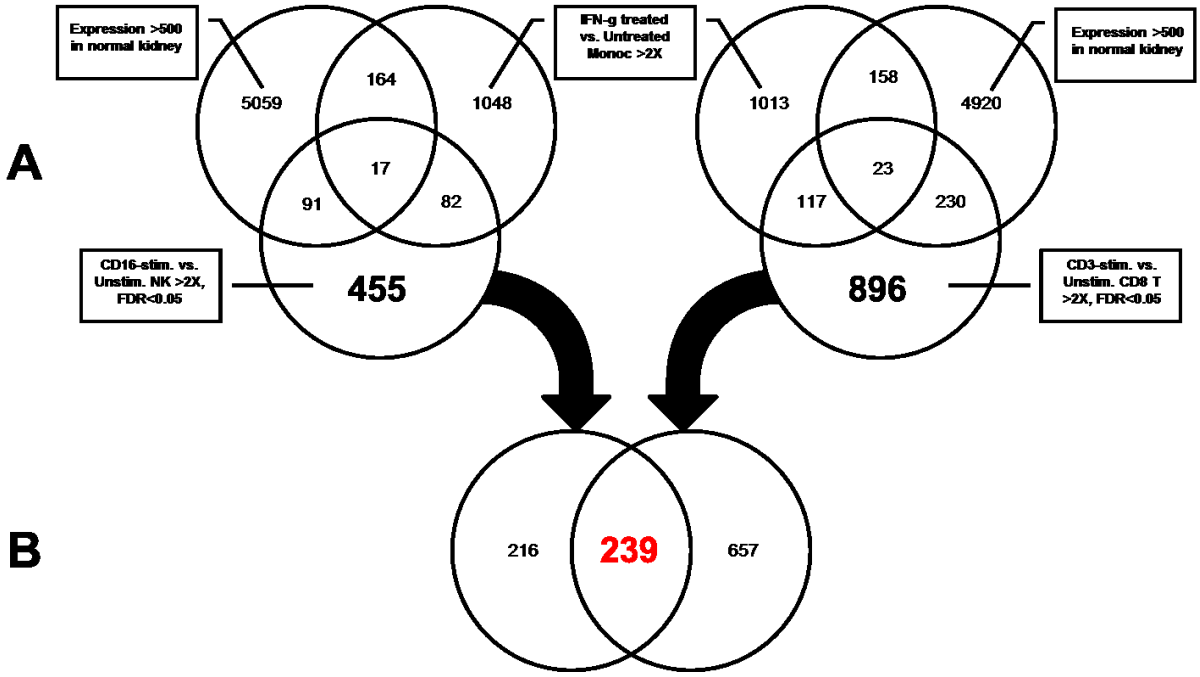

Figure 6.1 – Algorithm used to identify transcripts that are both CD16a-inducible in NK cells and TCR/CD3-inducible in CD8 T cells. Gene expression data was averaged over three independent samples from three different donors for each cell type. (A) Pre-filtering to exclude transcripts that are highly expressed in nephrectomies and IFNG-inducible in monocytes. CD16a-inducible and TCR/CD3-inducible transcripts were identified independently of one another. (B) The 455 CD16a-inducible NK cell transcripts and 896 TCR/CD3-inducible CD8 T cell transcripts were compared to identify overlap.

Table 6.1 – CD8 T cells' expression of the top 30 CD16a-inducible NK cell transcripts, sorted by decreasing fold change in stimulated versus unstimulated NK cells

Gene Symbol	Gene Title	Alias	Unstimulated CD8+ T Cells, Raw Expression	CD3-Stimulated CD8+ T Cells, Raw Expression	Fold Change (Stimulated vs. Unstimulated)
IFNG	Interferon, gamma	-	42	10800	259.2
CCL4	Chemokine (C-C motif) ligand 4/ 4-like 1 / 4-like 2	MIP-1B	98	8176	83.5
IRF4	Interferon regulatory factor 4	LSIRF	298	5600	18.8
CRTAM	Cytotoxic and regulatory T cell molecule	CD355	728	5427	7.5
MYC	V-myc myelocytomatosis viral oncogene homolog (avian)	MRTLC	2071	4555	2.2
TNFRSF9	Tumor necrosis factor receptor superfamily, member 9	4-1BBR	79	2933	37.1
CCL3	Chemokine (C-C motif) ligand 3/ 3-like 1 / 3-like 3	MIP-1A	130	2354	18.2
XCL1	Chemokine (C motif) ligand 1	LTN	8	1875	242.9
GPR18	G protein-coupled receptor 18	-	830	1686	2.0
NR4A2	Nuclear receptor subfamily 4, group A, member 2	NOT	134	1178	8.8
CSF2	Colony stimulating factor 2 (granulocyte-macrophage)	GM-CSF	29	1152	40.1
PTPN6	Protein tyrosine phosphatase, non-receptor type 6	SHP1	414	1129	2.7
BIRC3	Baculoviral IAP repeat containing 3	c-IAP2	775	1109	1.4
TBC1D4	TBC1 domain family, member 4	-	571	961	1.7
ZBED2	Zinc finger, BED-type containing 2	-	12	959	79.7
TRAF1	TNF receptor-associated factor 1	-	184	689	3.7
SERPINE2	Serpin peptidase inhibitor, clade E (nexin, plasminogen activator inhibitor type 1), member 2	GDN	47	659	13.9
SPRY1	Sprouty homolog 1, antagonist of FGF signaling (Drosophila)	-	28	501	17.7
RGS16	Regulator of G-protein signaling 16	RGSR	47	468	9.9
FCRL3	Fc receptor-like 3	CD307c	161	449	2.8
CD160	CD160 molecule	BY55	43	407	9.5
RILPL2	Rab interacting lysosomal protein-like 2	RLP2	213	325	1.5
STARD4	StAR-related lipid transfer (START) domain containing 4	-	73	248	3.4
NAB2	NGFI-A binding protein 2 (EGR1 binding protein 2)	YGL122C	66	217	3.3
FAM3C	Family with sequence similarity 3, member C	ILEI	109	188	1.7
NR4A3	Nuclear receptor subfamily 4, group A, member 3	CHN	20	155	7.6
RRAD	Ras-related associated with diabetes	RAD	57	118	2.1
FEZ1	Fasciculation and elongation protein zeta 1 (zygin I)	-	18	92	5.1
CD72	CD72 molecule	LYB2	14	68	5.0
SPRY2	Sprouty homolog 2 (Drosophila)	IGAN3	15	47	3.3

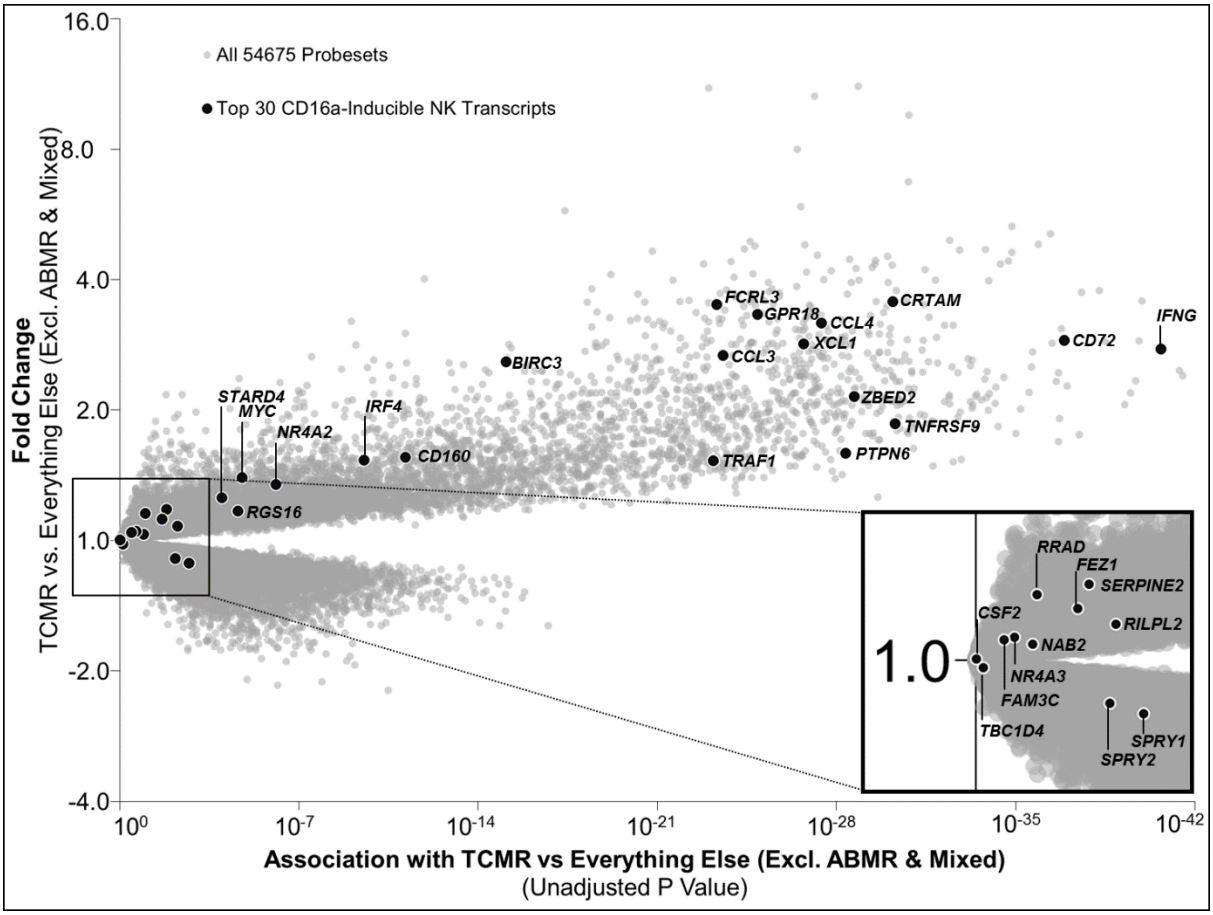

Figure 6.2 – Association of the top 30 CD16a-inducible NK cell transcripts with histologically classified TCMR versus all other diagnoses except ABMR and mixed rejection. Probe sets are plotted by fold change and association with 67 histologically classified TCMR biopsies versus 498 biopsies without histologically classified ABMR or mixed rejection.

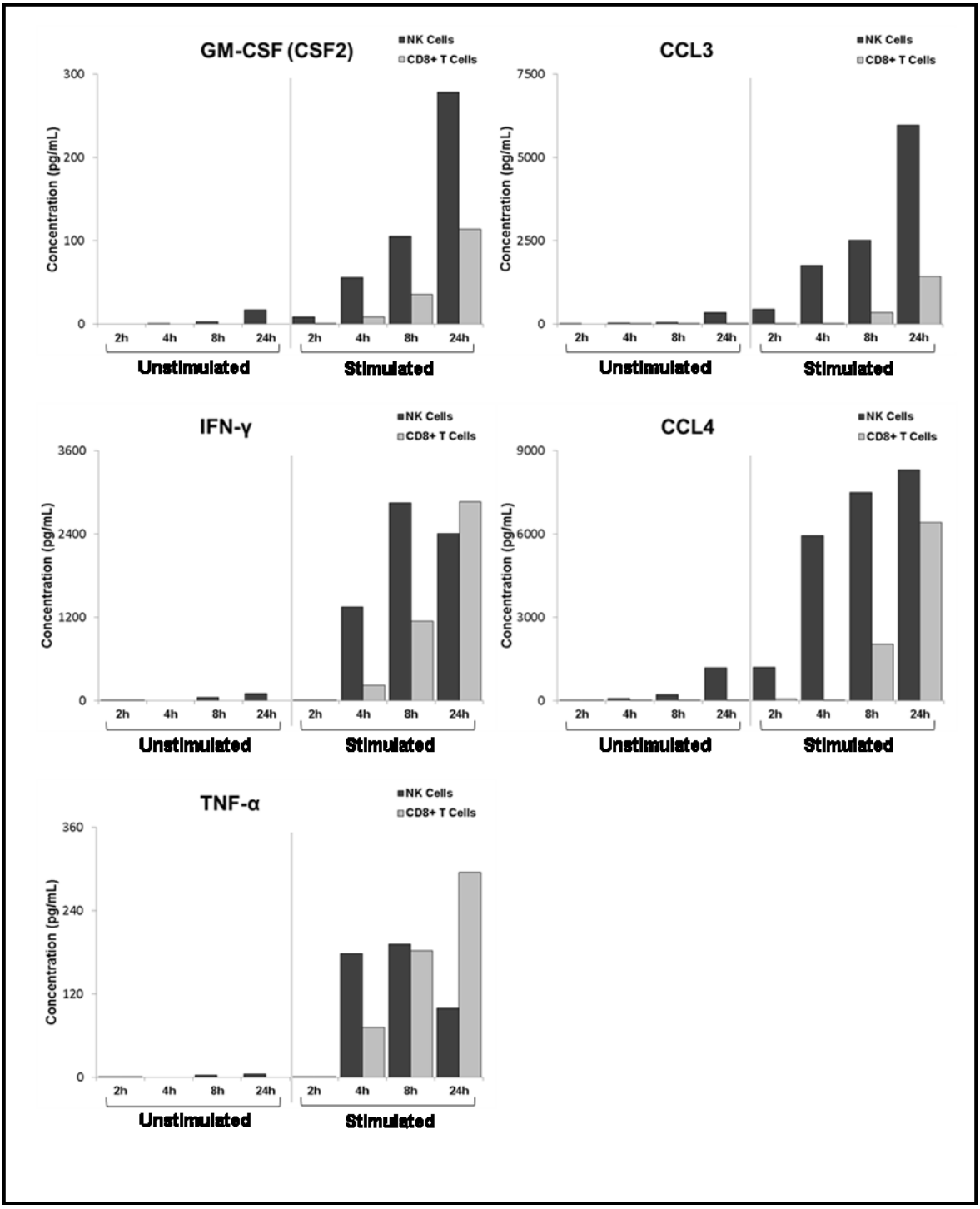
GM-CSF (CSF2)
NK Cells
CD8+ T Cells
Concentration (pg/mL)
300
200
100
0
2h
4h
8h
24h
Unstimulated
Stimulated
CCL3
7500
5000
2500
IFN-γ
3600
2400
1200
CCL4
9000
6000
3000
TNF-α
360
240
120

Figure 6.3 (previous page) – Multiplex analysis of soluble mediators produced by CD16a-stimulated NK cells and TCR/CD3-stimulated CD8 T cells. Positive readouts from a 30-plex analysis of cytokines and chemokines of culture supernatants are depicted. Positive readouts are defined as readouts well within the limits of or exceeding the detection range of the standard curve for each molecule. All other molecules were negligibly produced, and therefore not shown. Concentration is given in pg/mL. All cells were cultured for 2, 4, 8, and 24 hours with 200U/10^6 cells recombinant human IL2, with a density of 500,000 cells/mL medium at harvest. Black bars: NK cells. Light grey bars: CD8 T cells. Only one trial was performed with each cell type.

CHAPTER 7
Discussion

7.1 Summary of Results

Antibody-mediated rejection (ABMR) is the principle cause of allograft failure, and we previously showed that NK cells are involved in ABMR (2). However, the nature of NK cell involvement in ABMR pathogenesis is not known. We theorized that NK cells in ABMR are stimulated through their CD16a IgG Fc receptors by donor-specific antibodies (DSA), and hypothesized that some CD16a-inducible NK cell transcripts are differentially expressed in ABMR and can provide evidence of CD16a triggering in ABMR. Given similarities between the CD16a pathway in NK cells and the TCR/CD3 pathway in CD8 effector T cells that play a key role in T cell-mediated rejection (TCMR), this study sought answers to three outstanding questions:

1) What gene expression changes are CD16a-inducible in NK cells?
2) Are CD16a-inducible NK cell gene expression changes associated with ABMR?
3) Which CD16a-inducible NK cell transcripts, if any, are also TCR/CD3-inducible in CD8 effector T cells in TCMR?

Prior to this study, CD16a-mediated gene expression changes in NK cells had not been broadly characterized in the context of ABMR. Using an *in vitro* model of primary human cell stimulation, we addressed the first question by identifying transcripts that were CD16a-inducible in NK cells. We also identified transcripts that were constitutively high in both unstimulated and stimulated NK cells, but not necessarily CD16a inducible. Some of the most highly CD16a-inducible transcripts encoded proinflammatory chemokines and cytokines, as well as molecules known to influence NK cell cytotoxicity and IFNG production. Cytolysins were equally highly expressed in both stimulated and unstimulated NK cells; that is, they were not CD16a-inducible.

To address the second question, we studied expression of the top 30 CD16a-inducible and top 30 highly expressed NK cell transcripts in 703 histologically diagnosed human kidney transplant biopsies, and found that 8 CD16a-inducible transcripts were highly associated with ABMR compared to other diagnoses ($p < 5x10^{-6}$), whereas 22 of the top highly expressed transcripts were highly associated with ABMR. By examining transcript expression in a cell panel of other cell types encountered in biopsies, we determined that two of the 8 ABMR-associated CD16a-inducible transcripts were selective for NK cells in the context of ABMR and provide compelling evidence of CD16a activation in ABMR. Several highly expressed non-CD16a-inducible NK cell transcripts were also highly associated with ABMR, indicating increased NK cell burden in ABMR compared to other diagnoses.

In the third phase of this project, we asked whether the similarities between NK cells and CD8 effector T cells extend to gene expression changes induced by cognate antigen recognition events in ABMR and TCMR. We cultured primary human CD8 T cells with TCR/CD3 stimulation and compared gene expression changes with NK cells stimulated through CD16a. Many transcripts were highly inducible under both conditions. Furthermore, 25 of the top 30 CD16a-inducible NK cell transcripts were also TCR/CD3-inducible in CD8 T cells. We compared expression of the top 30 CD16a-inducible NK cell transcripts in biopsies with TCMR against other diagnoses, and found that 16 were associated not only with ABMR, but with TCMR as well. We also studied *in vitro* production of 30 different chemokines, cytokines, and growth factors by CD16a-stimulated NK cells and TCR/CD3-stimualted T cells, and found that both cell types produced the same five mediators.

Taken together, these data suggest that CD16a-mediated NK cell activation occurs in ABMR, and that NK cells stimulated this way have potential to orchestrate the immune response in ABMR through proinflammatory chemokines and cytokines. Strikingly, but not surprisingly, this study demonstrates that the effector potential of NK cells and CD8 T cells overlaps, and many shared gene expression changes in CD16a-stimulated NK cells and TCR/CD3-stimulated T cells are associated with both ABMR and TCMR. While this is not the first study aimed at studying NK cell involvement in ABMR using gene expression analysis, it is the first to examine the specificities of CD16a-inducible genes in a panel of other cell

types, and is the first to directly compare TCR and CD16a activation in T and NK cells, respectively, in the context of rejection (111).

7.2 CD16a-inducible transcript expression in cultured NK cells

CD16a-inducible soluble mediators

Some of the most highly CD16a-inducible transcripts in NK cells were chemokines and cytokines. Histologic examination of renal transplant biopsies with ABMR reveals monocytes/macrophages, neutrophils, and NK cells in inflammatory compartments, and our data revealed CD16a-inducible chemokines that recruit these types of cells (112). CCL3 and CCL4 (MIP-1A and MIP-1B) recruit monocytes and macrophages (113), and the growth factor CSF2 (GM-CSF) encourages macrophage activation (114). CCL3, CCL4, and XCL1 (lymphotactin) attract NK cells (115-117) and T cells (118;119), although T cells do not participate in ABMR to the same extent as TCMR and mixed rejection. Some of the chemokines and cytokines we observed in this study influence one another. In acute viral infection, neutrophils primed with IFNG respond to CCL3, and such chemotaxis may be involved in some cases of rejection as well (120). IFNG and TNF are potent proinflammatory cytokines that synergize in activating many cell types including monocytes, macrophages, and endothelial cells (121-123). Together, TNF and IFNG induce expression of various genes in target cells, including *CXCL9, CCL5,* and *IRF1* (123). TNF-mediated cytotoxicity is also enhanced by IFNG (124-126). TNF was not on our final top 30 list of CD16a-inducible NK cell transcripts because it

was highly IFNG-inducible in monocytes and was therefore eliminated in the transcript filtering process; nevertheless, TNF was highly expressed and strongly induced by CD16a stimulation in NK cells, and production was confirmed by ELISA and multiplex analysis.

NK cells are restricted to the microcirculation lumen in ABMR. This is surprising because the default behavior of NK cells in many diseases is to infiltrate interstitia (127;128). Interaction between CD16a, DSA, and donor endothelial cells may be responsible for retaining NK cells in the microcirculation lumen, generating the microvascular inflammation that is typical of ABMR. While lack of an appropriate animal model for human NK cell CD16a activation precludes direct study of the NK-endothelium synapse *in vivo,* gene expression microarray analysis of kidney transplant biopsies reveals ABMR-associated chemokines, cytokines, and membrane proteins that could enhance localization of circulating NK cells in a manner responsive to the proinflammatory mediators induced by CD16a triggering of NK cells. CCL3, CCL4, and XCL1 attract NK cells to inflamed sites (115-117), and physical interaction between DSA and CD16a could help maintain the NK cell-endothelium synapse. CD16a-inducible cytokines promote expression of additional molecules on endothelial cells that could enhance the synapse. On its own or in concert with TNF, IFNG stimulates endothelial cell expression of donor class I and class II HLA molecules for additional DSA binding (129;130), chemokine/adhesive molecules such as CX3CL1 (fractalkine) (131-133), and chemokines such as CCL2 (MCP1), CCL5 (RANTES), CXCL10 (IP-10), and CXCL11 (9;134-137).

CD16a-inducible regulatory receptors

Several CD16a-inducible transcripts encoded receptors known to regulate various effector functions of immune cells. This project was not concerned with the non-trivial matter of understanding these receptors' relevance to rejection pathogenesis, but their induction in NK cells reinforces the notion that the effector functions of NK cells in ABMR are highly regulated. CD160 is essential for IFNG production by NK cells (138), and triggers TNF and IL-6 secretion by peripheral blood NK cells upon binding class Ia and Ib MHC ligands (139). Specifically, CD160 preferentially binds HLA-C and soluble HLA-G. It also binds HLA-A2, HLA-B7, and HLA-E, albeit more weakly (140). CD160 ligation by HLA-C, but not HLA-G or HLA-E, triggers cytotoxicity. Furthermore, inhibitory KIR2DL2 against HLA-C on target cells is able to slightly attenuate CD160-mediated cytotoxicity (141). Interestingly, in the presence of IL-15 the GPI-anchored CD160 is released from the NK cell plasma membrane by metalloproteases, diminishing surface expression despite persistence of high *CD160* transcript levels. These functions may be relevant in kidney ABMR, as kidney proximal tubule cells and kidney epithelial cell lines express IL-15 mRNA. IFNG-stimulated monocytes and macrophages also express IL-15 (142). In its soluble form, CD160 may interact with non-endogenous HLA-C to inhibit CD160-mediated NK cell cytotoxicity in the absence of HLA-C-specific DSA (which would block this interaction) (143). On the other hand, in the presence of soluble CD160 in ABMR, matching HLA-C expression between a donor and recipient in the presence of DSA against other mismatched HLA alleles could

potentially intensify rejection. Speculatively, in such a scenario soluble CD160 might block HLA-C targets that could otherwise be recognized by inhibitory KIR2DL2 on host NK cells, potentially enhancing their activation by CD16a/DSA interactions. The role of CD160 in ABMR and the factors that influence its functions is a topic for further study.

CRTAM may affect cytotoxicity and/or IFNG production by stimulated NK cells. Little is known about the functional role of CRTAM in NK cells, but it may promote NK cell cytotoxicity in ABMR if its ligand CADM1 (NECL2) is accessible by NK cells. *CADM1* is moderately expressed in the kidney biopsies we examined, but we did not have data about its tissue restriction within the kidneys. CADM1 mediates epithelial cell junctions, playing an important role in maintaining the organization of epithelial cell layers (144). It is also ubiquitous in endothelial cells and vascular smooth muscle, and may therefore be accessible to NK cells in ABMR (145). The ability of CRTAM to promote NK cell cytotoxicity is likely context-dependent, as some but not all studies observed this effect in response to CADM1-bearing target cells (144;146). One study showed that CADM1 expression on tumor cells led to more rapid lysis by NK cells expressing CRTAM (144). In ABMR, CRTAM may enhance NK cell activation against endothelial cells coated with DSA.

On the other hand, CD72 could play an inhibitory role in ABMR. CD72 was traditionally considered a B cell molecule, but recent evidence supports an inhibitory role for CD72 in NK cells. Unlike CD160 and CRTAM, CD72 inhibits IFNG expression by NK cells but it does not affect cytotoxicity (147). Given the

variety of receptors with potential to influenceCD16a-triggered NK cell effector mechanisms, achieving a finely tuned understanding of how they relate to ABMR is not a straightforward matter, but the possibility that they affect ABMR pathogenesis cannot be ruled out.

7.3 Non-CD16a-inducible transcript expression in cultured NK cells

Cytolysins

Cytolysins *GNLY, GZMA, GZMB, GZMH,* and *PRF1* were highly expressed in NK cells but were not CD16a-inducible. For the most part, their expression levels were static between unstimulated and stimulated NK cells (*GZMH* expression modestly decreased following CD16a stimulation). NK cells contain pre-formed cytolysins in granules whose contents can be rapidly exocytosed following target recognition. A key branch of the CD16a signaling cascade is dedicated to granule exocytosis. Granule exocytosis proceeds in four steps. First, target recognition initiates actin rearrangements which form the lytic synapse. Microtubule organizing centers direct lytic granules to the synapse in the second step, and in the third step the granules harbor at the plasma membrane. In the fourth and final phase, the granules fuse with the plasma membrane and release cytolysins into the synapse, killing the target in a directed manner. In the present study, constitutive high expression of cytolysin transcripts aligns with this "pre-primed" state where NK cells do not have to wait for cytolysin gene transcription to occur in order to initiate ADCC. It is possible that CD16a triggering of NK cells in ABMR leads to

directed endothelial cell lysis through ADCC, but it should be noted that endothelial cell lysis is generally not observed upon histologic examination of transplant biopsies diagnosed with ABMR (44;45). There may be additional requirements for initiating ADCC that are not met in ABMR, because while CD16a can induce granule exocytosis against antibody-opsonized targets *in vitro*, it is not responsible for granule polarization to the synapse, which is a crucial step leading to granule exocytosis (148).

DSA-selective NK cell transcripts

In 2010, Hidalgo *et al.* published six DSA-selective transcripts (DSASTs) that implicated NK cells in ABMR. Biopsies with ABMR scored highly for DSASTs, implying a preponderance of NK cells in ABMR compared to non-ABMR, but the study did not establish whether these transcripts were CD16a-inducible in NK cells. Our results showed that these six DSASTs (*GNLY, MYBL1, FGFBP2, SH2D1B, CX3CR1,* and *KLRF1*) were highly expressed but not highly CD16a-inducible in NK cells, raising the question of why the DSAST study did not uncover evidence of NK cell involvement in the form of CD16a-inducible transcripts. The DSASTs were originally obtained by selecting transcripts differentially expressed in biopsies from patients with serologically confirmed DSA. Transcripts that were associated with TCMR were eliminated by the algorithm used in that study. Based on the results of the present study, we now know that many of the most highly increased and highly expressed CD16a-inducible transcripts in NK cells are also TCR/CD3-indcible in T cells. Excluding TCMR-related transcripts ruled out many CD16a-inducible

transcripts because of the overlap. This phenomenon feeds into our rationale behind comparing ABMR-diagnosed biopsies to all other diagnoses except TCMR and mixed rejection in order to find evidence of CD16a activation in ABMR. The p-values of CD16a-inducible NK cell transcripts that are also TCR/CD3-inducible in T cells in TCMR would be weakened if TCMR and mixed rejection were included in the comparator, making it more difficult to distinguish these transcripts in ABMR.

7.4 NK cell transcript expression in biopsies diagnosed with ABMR

Top ABMR-associated CD16a-inducible transcripts: evidence of CD16a-mediated NK cell activation in ABMR

A large number of transcripts gained in expression following NK cell CD16a stimulation, but the majority were not selectively expressed by NK cells. Of the eight CD16a-inducible NK cell transcripts identified in this study as being highly associated with ABMR (*CCL4, CCL3, CD160, XCL1, CRTAM, FCRL3, STARD4,* and *TNFRSF9*), *CD160* and *XCL1* could be considered NK selective in the context of ABMR; therefore, they strongly support CD16a triggering of NK cells in ABMR. Although we reported similar fold changes for *CD160* in stimulated versus unstimulated NK cells and CD8 T cells (9.6 and 9.5, respectively), *CD160* expression in stimulated NK cells was 11.3 times higher than its expression in TCR/CD3-stimulated CD8 T cells and *CD160* expression in stimulated CD8 T cells was below the levels found in unstimulated NK cells. Thus *CD160* is reasonably selective for CD16a-stimulated NK cells. Because *CD160* and *XCL1* are both

expressed by stimulated NK cells and CD8 T cells (but not other cells), the assumption about their selectivity for NK cells would not be valid in diseases with extensive T cell involvement, but the assumption is justified in ABMR because T cells are underrepresented in ABMR. Previous studies showed that T cell transcripts that are overwhelmingly associated with TCMR (e.g. *CTLA4, ICOS, CD8A*) are negligibly associated with ABMR (9;88). Given that *CD160* and *XCL1* are strongly associated with ABMR, but key T cell transcripts such as *CTLA4, ICOS,* and *CD8A* are not, it suggests that T cells contribute little to the p-values observed when comparing *CD160* and *XCL1* expression in ABMR to other phenotypes.

By the same criterion, *CSF2* and *ZBED2* could also be considered NK-selective, yet they were not associated with ABMR (p = 0.59 and 0.87, respectively). *ZBED2* was weakly expressed by stimulated NK cells, possibly explaining why it was not robust in biopsies. Weakly expressed transcripts are difficult to distinguish in ABMR over other diagnoses because the molecular signature of NK cells is not especially strong compared to signals from more ubiquitous cells (e.g. endothelial cells, epithelial cells). Compared to stimulated NK cells, TCR/CD3-stimulated CD8 T cells expressed *ZBED2* almost three-fold more intensely. This translated into a much higher association with TCMR ($p = 2.03 \times 10^{-29}$ in TCMR vs. p = 0.87 in ABMR) compounded by the fact that the T cell burden in TCMR is considerably greater than the NK cell burden in ABMR. *CSF2* was expressed in ABMR and its protein product was produced by stimulated NK cells *in vitro,* but it was not differentially

expressed in ABMR relative to other diagnoses. A possible explanation is that CSF2 is inducible by proinflammatory cytokines such as TNF that are present in other diagnoses but were not examined in our *in vitro* studies (149). Thus, while CSF2 may be an important growth factor in ABMR, other modes of induction in tissue injury make its expression in ABMR indistinguishable from its expression in other pathologies. *CSF2* was no more strongly associated with TCMR despite the fact that it is also produced by TCR/CD3-stimulated CD8 T cells ($p = 0.97$).

The CD16a-inducible transcripts *CCL4, CCL3, CRTAM, FCRL3, TNFRSF9,* and *STARD4* were highly associated with ABMR but were not selectively expressed by stimulated NK cells in ABMR. Therefore, their association with ABMR may reflect interaction between CD16a-stimulated NK cells and other cells in the inflammatory compartment in ABMR. *STARD4* was highly IFNG-inducible in endothelial cells (HUVECs), explaining why it was strongly associated with ABMR despite its widespread expression in all cell types on the extended cell panel. This is compatible with the previous finding that IFNG-inducible transcripts are among the most prominent in ABMR (9). *FCRL3* was highly expressed by B cells. *CRTAM* expression was moderately IFNG-inducible in macrophages, which have contributed to its p value in ABMR. *TNFRSF9* decreased in IFNG-stimulated versus unstimulated macrophages, possibly explaining why its p value was lower than most other CD16a-inducible transcripts that were highly associated with ABMR. *CCL3* and *CCL4* were not as selective for NK cells as were *CD160* and *XCL1*, yet they were at least as highly associated with ABMR. Because *CCL3* and *CCL4* were

somewhat IFNG-inducible in monocytes and macrophages, it is likely that IFNG from CD16a-stimulated NK cells stimulates additional CCL3 and CCL4 production by monocytes in ABMR, strengthening their p-values in ABMR compared to other diagnoses. Stimulated monocytes and NK cells may augment one another's expression of *CCL3*, *CCL4*, and possibly other soluble and membrane-linked immune response mediators. Along these lines, a study by Bluman *et al.* found that monocyte-derived cytokines—particularly IL-12 and IL-15—can affect CCL3 production by NK cells (150). Additional studies on the interactions between monocytes and NK cells in the microcirculation in ABMR are necessary to understand the impact on transcripts associated with ABMR. TCR/CD3-stimulated CD8 T cells also expressed *CCL3* and *CCL4*, but they are not as strongly associated with TCMR (88). The reason for the weaker association with TCMR is puzzling considering that macrophages are an important player in TCMR and T cells produce rich supplies of IFNG. It is possible that the localization of monocytes and NK cells in the microcirculation is more conducive to augmented *CCL3* and *CCL4* expression in ABMR than the spatial situation of macrophages and T cells in TCMR, but this hypothesis can only be supported with additional studies.

Our finding that NK cells signal through CD16a in ABMR may have grave consequences for DSA-positive solid organ transplant recipients who are infected with cytomegalovirus (CMV). CMV alone increases patient morbidity and mortality. In addition to causing inflammation in transplanted tissues, it is also associated with increased vascular thrombosis and post-transplant lymphoproliferative

disorder. Donor-positive/recipient-negative pairs carry as high as 47% chance of developing CMV disease in the first year following transplantation, although this number depends on risk factors such as the type of organ transplant and level of immunosuppression (151). It was recently discovered that human CMV infection is associated with incidence of an NK cell phenotype characterized by FcεRIγ deficiency alongside normal levels of CD3ζ, caused by epigenetic silencing of the FcεRIγ gene by methylation (152). These NK cells react more aggressively to CD16a stimulation than normal $CD56^{dim}$/CD16a+ NK cells from peripheral blood (153). This may be because CD3ζ contains three ITAMs, whereas FcεRIγ only encodes one. As reviewed in Chapter 1, CD16a signals through homodimers of FcεRIγ or CD3ζ, or heterodimers of the two. In the absence of FcεRIγ, CD16a would signal through CD3ζ homodimers containing six ITAMs as opposed to the two or four ITAMs present in configurations involving FcεRIγ. This could provide maximum space for recruitment of downstream activation molecules which may intensify NK cell activation. In ABMR coinciding with CMV infection, the FcεRIγ deficient phenotype could result in more aggressive rejection and reduced graft survival.

CD16a-inducible transcripts not strongly associated with ABMR

Many CD16a-inducible transcripts that were promiscuously expressed by cell types other than NK cells weakly associated with ABMR, with the exception of those that were IFNG-inducible in other cells (e.g. *STARD4, BIRC3*). Transcripts that were IFNG-inducible had stronger associations with ABMR than non-IFNG-inducible transcripts, even if they were expressed by other cell types. Transcripts that were CD16a-inducible in NK cells but also expressed in HUVECs and RPTECs

were some of the most strongly expressed transcripts in biopsies because of the ubiquity of endothelial cells and epithelial cells relative to other cell types. For example, *SERPINE2* expression in unstimulated HUVECs was 9674, and it was not strongly expressed by other cell types. Its mean expression in ABMR biopsies was 3468 compared to 3319 in all other biopsies combined. In contrast, *CD160* expression was restricted to NK cells and its expression was 144 in ABMR compared to 88 in all other diagnoses. Thus, relative cell burden in biopsies has a major impact on transcript expression in ABMR, and CD16a-inducible transcript signals from NK cells in ABMR can be easily overshadowed by signals from other cells that express the same transcripts.

CD16a-inducible NK cell transcripts that were also expressed in B cells comprise an interesting subset that tended to have moderate associations with ABMR. Little is known about the contribution of B cells to ABMR pathogenesis. B cells are the source of DSA in transplant recipients. One study found that, even in the absence of detectable DSA in the serum before and after kidney transplantation, recipients with stable graft function exhibited increased frequencies of class I HLA-specific plasmablasts in peripheral blood by eight weeks post-transplant (154). This finding suggests that B cells are more involved with transplants than previously appreciated. Our results show that CD16a-inducible NK cell transcripts such as *FCRL3, GPR18,* and *CD72* were strongly expressed by B cells in the extended cell panel. Given the complexity of gene expression *in vivo* and the fact that the present study was not designed to study B cells in rejection, we cannot exclude the

possibility that B cells affected these transcripts' p-values in ABMR; however, this argument is diminished by the fact that other B cell-associated transcripts such as *BTLA* and *MS4A1* (CD20) are not associated with ABMR (respectively, p = 0.18 and p = 0.46 in ABMR versus all other diagnoses except TCMR and mixed rejection).

Non-CD16-inducible NK cell transcripts and DSASTs in ABMR

The DSA-selective NK cell transcripts previously identified by Hidalgo *et al.* (*GNLY, FGFBP2, MYBL1, CX3CR1, KLRF1,* and *SH2D1B*) were among the most highly ABMR-associated transcripts despite the fact that they were not CD16a-inducible. Their strong association with ABMR may reflect the ability of CD16a to enhance NK cell localization through physical interactions with DSA and induction of chemokines such as XCL1. Like the DSASTs, many other transcripts were highly expressed in NK cells but not CD16a-inducible. These included cytolysins *GZMA, GZMB, GZMH, GNLY,* and *PRF1*. *CD44* and *HLA-F* were two highly expressed but non-CD16a-inducible NK cell transcripts that underscore the importance of IFNG in ABMR. Both were highly expressed in all cells on the extended cell panel; however, whereas *CD44* decreased slightly in response to IFNG treatment, *HLA-F* increased following IFNG treatment. *HLA-F* was strongly associated with ABMR, but *CD44* was not. In both cases, the contribution of NK cells to these transcripts' overall expression in biopsies is likely obscured by expression in other cell types, but these other cells' reactions to IFNG probably explain the p-values for *CD44* and *HLA-F* in ABMR. Thus, the non-CD16a-inducible transcripts and DSASTs demonstrate two important concepts. Firstly, they suggest increased NK cell

localization in ABMR, which may be enhanced by CD16a engagement with DSA on endothelium. Secondly, they corroborate our previous findings that the effects of IFNG are prominent in ABMR (9).

7.5 The curious case of IFNG

Paradoxically, despite the repeated observation that IFNG-inducible transcripts were strongly associated with ABMR regardless of whether or not they were CD16a-inducible in NK cells, IFNG itself was only mildly associated with ABMR. There are several possible explanations. IFNG is highly regulated *in vivo*, and some regulatory mechanisms may be in play in kidney transplants undergoing ABMR but could not be modelled by our *in vitro* system of NK cell stimulation. Examples include the CD16a-inducible receptors CD160 and CD72. As previously discussed, CD160 is necessary for IFNG production by NK cells, whereas CD72 inhibits *IFNG* expression. Stimulation of murine NK cells with monoclonal antibodies against the CD16a-inducible receptor TNFRSF9 (4-1BB) has been shown to induce IFNG secretion, but in contrast, studies have also shown that tumors expressing TNFSF9 (4-1BBL) actually impaired IFNG secretion (155). IFNG production in ABMR cannot be demystified until a complete understanding of the numerous regulatory mechanisms that influence it is achieved (a distant accomplishment, to say the least). Another possible explanation for the mild association of IFNG with ABMR relates to the concept that small quantities of IFNG could be sufficient to generate strong responses in target cells. IFNG-

inducible endothelial transcripts including *PLA1A1* and *CXCL11* are the molecular hallmarks of ABMR (9;45;156). The influence of IFNG on proximal cells in ABMR may be amplified by CD16a-mediated NK cell localization at sites of DSA binding on the microcirculation endothelium. A third explanation is that IFNG is present in the diagnoses that we compared ABMR and TCMR against. However, this does not appear to be the case, as the mean expression of *IFNG* across all non-rejection biopsies was low. In biopsies without major histologic abnormalities mean *IFNG* expression was equal to control nephrectomies. Relative to the other diagnoses, *IFNG* expression in ABMR was slightly increased (mean expression = 56 in ABMR versus 49 in biopsies without rejection), but the minimal increase suppressed its p-value in ABMR. Raw *IFNG* expression was also relatively low in biopsies with TCMR (mean expression = 128), but this was sufficient to generate *IFNG* the single strongest p-value of any transcript in TCMR compared to other diagnoses ($p = 2.14x10^{-41}$). Ultimately, investigating the details of IFNG production and release in ABMR will require the creation of novel *in vitro* models that better incorporate the immunologic complexities that are thought to occur in ABMR.

7.6 Proposed model of NK cell involvement in ABMR

Based on the results of the present study, we propose a model of ABMR wherein NK cell localization and activation at the microcirculation endothelium is mediated by CD16a engagement to DSA, creating the pathogenic environment of ABMR, illustrated in part by **Figure 7.1**. CD16a triggers NK cells to secrete

inflammatory cytokines and chemokines (e.g. CCL3, CCL4, XCL1, CSF2, IFNG and TNF), and stimulates increased expression of molecules that regulate proliferation, cytotoxicity, and soluble mediator production (e.g. CD160, CD72, TNFRSF9, and CRTAM). These chemokines and cytokines could encourage margination and proliferation of other leukocytes: CCL3 and CCL4 are potent chemoattractants for monocytes and macrophages (113), CSF2 is a growth factor that encourages macrophage activation and proliferation (114), and XCL1 attracts additional NK cells to sites of inflammation (117). IFNG and TNF activate many cell types including monocytes, macrophages, and endothelial cells (121-123), and could also mediate cytotoxic effects in ABMR (126). On its own or in concert with TNF, IFNG facilitates NK cell localization by stimulating endothelial cells to increase expression donor class I and class II HLA molecules for additional DSA binding (129;130). IFNG-stimulated endothelial cells produce chemokines (e.g. CX3CL1, CCL2, CCL5, CXCL10, CXCL11) and adhesion molecules (e.g. CX3CL1, selectins) that recruit and retain monocytes and NK cells (9;131-137), and initiate injury-repair responses that culminate in endothelial dedifferentiation and loss of function. In this model, monocytes recruited by stimulated NK cells produce chemokines CCL3, CCL4, and CCL5. Monocytes may also engage DSA directly through their own Fc receptors, further enhancing their cytotoxic effects. CD16a-stimulated NK cells may cause some microvascular damage directly through ADCC, although it should be noted that endothelial cell remodelling and injury response—potentially related to angiogenesis—is probably the principal determinant of graft dysfunction

following NK cell interaction with endothelium in ABMR, as endothelial cell lysis is uncommon in histologic examination of biopsies diagnosed with ABMR (44;45).

We cannot rule out the possibility that DSA could block interactions between HLA and inhibitory NK cell receptors, potentially further encouraging NK cell activation in ABMR. The ligand specificities of different inhibitory KIR alleles, for example, have not been fully characterized (157). Therefore, it is possible that DSA could be generated against a non-endogenous HLA allele that is recognized by an inhibitory NK cell receptor on host NK cells. In this case, the DSA could block interactions between the inhibitory receptor and the HLA. Notably, DSA is not generated against self-MHC; therefore, if the donor and recipient share certain alleles, these might raise the threshold of NK cell activation by DSA against non-self MHC, Other activating receptors may aggravate rejection; for instance, while the biological functions of HLA-F are not well known, it is a ligand for the activating KIR3DS1 receptor (158). HLA-F expression is IFNG-inducible in ABMR, and may further enhance the inflammatory responses from NK cells that express KIR3DS1.

7.7 Transcript sharing between T cells in TCMR and NK cells in ABMR

Evidence of shared effector functions between T cells and NK cells

We previously demonstrated that the transcriptomes of T cells and NK cells closely resemble one another (91). In keeping with the fact that CD16a and TCR both also

engage comparable signaling cascades via CD3ζ, the present study found that many CD16a-inducible transcripts in NK cells were also TCR/CD3-inducible in CD8 T cells. Many of the transcripts that were both CD16a-inducible and CD3/TCR-inducible were associated with both ABMR and TCMR. Multiplex analysis of 30 chemokines, cytokines, and growth factors revealed that stimulated NK cells and CD8 T cells produced the same succinct list of soluble mediators (CCL3, CCL4, IFNG, TNF, CSF2). Combined with the gene expression data from *in vitro* stimulation experiments with T cells and NK cells, the multiplex data suggest that NK cells and CD8 T cells share effector potential in rejection. The CSF2 receptor is expressed on myeloid cells and endothelial cells, and promotes activation and proliferation of monocytes, macrophages, neutrophils, dendritic cells, and others. It also enhances antigen presentation, cytokine production, phagocytic activity, chemotaxis, and adhesion in these cells (159). IFNG also enhances antigen presentation and monocyte/macrophage activity. In macrophages, it induces iNOS and stimulates respiratory burst activity, which may contribute to graft destruction in ABMR and TCMR (160). As previously discussed, CCL3 and CCL4 are chemotactic for various cells including monocytes, macrophages, IFNG-stimulated neutrophils, T cells, and NK cells. They also encourage transendothelial migration of monocytes, neutrophils, and T cells—an important characteristic in TCMR, which is focused in interstitial spaces (116). While the multiplex data is intriguing, it is the result of only a single trial with each type of cell. These data must be replicated through repeat trials. Nonetheless, the multiplex data gain reliability from the fact that they

corroborate the gene expression data from NK cell and T cell cultures, and they mirror the findings of many prior studies (160-165).

While many CD16a-inducible transcripts that were associated with both ABMR and TCMR were highly expressed in T cells following TCR/CD3 activation, some CD16a-inducible transcripts that were associated with both types of rejection were not strongly expressed in CD8 T cells. *CD72* expression was almost negligible in stimulated and unstimulated CD8 T cells, yet it was the second most highly TCMR-associated transcript of the 30 we studied ($p = 1.30x10^{-34}$). Likewise, *FCRL3* expression was modest in stimulated CD8 T cells but its association with TCMR was stronger than expected given such mild expression in T cells ($p = 4.91x10^{-24}$). The high expression of *CD72* and *FCRL3* in B cells is the unifying characteristic that could explain their association with TCMR. We did not observe the same effect on p-values in ABMR, suggesting that the p-values of *CD72* and *FCRL3* were due to expression in NK cells and not B cells. As previously discussed, B cell associated transcripts *BTLA* and *MS4A1* (CD20) were not associated with ABMR; however, they were strongly associated with TCMR ($p= 2.28x10^{-36}$ and $p = 1.24x10^{-12}$, respectively). Notably, our data from the extended cell panel (data not shown) indicates that *BTLA* is expressed at low levels by T cells, but *MS4A1* is not, potentially explaining the large difference in p-values between these two transcripts in TCMR. These data corroborate a previous study's finding that CD20+ B cell infiltrates are associated with TCMR but not ABMR. On the other hand, the same study found that CD20-/CD138+ plasma cell infiltrates are associated with ABMR

(166). It is worth noting, however, that B cell and plasma cell infiltrates are not always observed in TCMR and ABMR (167), and their presence is tied to the age of the transplanted organ (168).

Implications for diagnosis and management of rejection

This study provided evidence that CD16a-stimulated NK cells and TCR/CD3-stimulated CD8 T cells share effector potential. Overlapping gene expression and soluble mediator production *in vitro* was reflected in biopsies, where shared transcripts were often highly associated with both ABMR and TCMR. In light of the extensive similarities between T cells and NK cells that respond to their cognate antigens in rejection, differences in pathology between TCMR and ABMR are best explained by differences in effector cell localization. Whereas T cells infiltrate the interstitium in TCMR, NK cells are restricted to the microvascular lumen in ABMR. This corresponds to typical histology in TCMR and ABMR: interstitial inflammation in the former and microvascular inflammation in the latter.

The similarity between effector T cells and NK cells in rejection has exciting implications for diagnosis and management of rejection. Presently, TCMR can be effectively managed with immunosuppression, but the same strategies are not often reliable against ABMR in the long term. Current strategies to prevent and/or manage ABMR include DSA removal (e.g. plasmapheresis, immunoadsorption), complement inhibition (e.g. anti-C5), anti-B cell agents (e.g. rituximab), proteasome inhibitors (e.g. bortezomib), intravenous immunoglobulin, and splenectomy in

severe cases (112). The parallel between the NK CD16a and effector T cell TCR/CD3 alloantigen recognition systems presents opportunities for developing immunosuppressive agents that target both T cells and NK cells. For instance, although it is considered an agent that controls TCMR, antithymocyte globulin targets diverse antigens on T cells, B cells, and NK cells (169). Its potential to suppress NK cells and attenuate active ABMR should be explored. Moreover, its inclusion in induction therapy given at the time of transplant appears to reduce incidence of *de novo* DSA, which may be an added benefit (170).

Besides preventing rejection, a major challenge in transplantation is differentiating ABMR and TCMR. Molecular diagnosis promises to improve upon traditional histologic diagnosis of rejection, which is often unreliable. Although TCMR has a robust and distinct molecular signature, the molecular phenotype of ABMR is less crystallized. *CD160* and *XCL1* were unable to distinguish ABMR from TCMR because of their shared expression in T cells and NK cells, but they are selective for CD16a-stimulated NK cells in the absence of T cells, and may be useful for diagnosing ABMR when TCMR has already been ruled out. CD16a-inducible transcripts may have prognostic value as a measure of NK cell activity in biopsies with confirmed ABMR, for example, by testing levels of CD160 on peripheral blood NK cells in transplant patients with rejection by flow cytometry.

FIGURES & TABLES

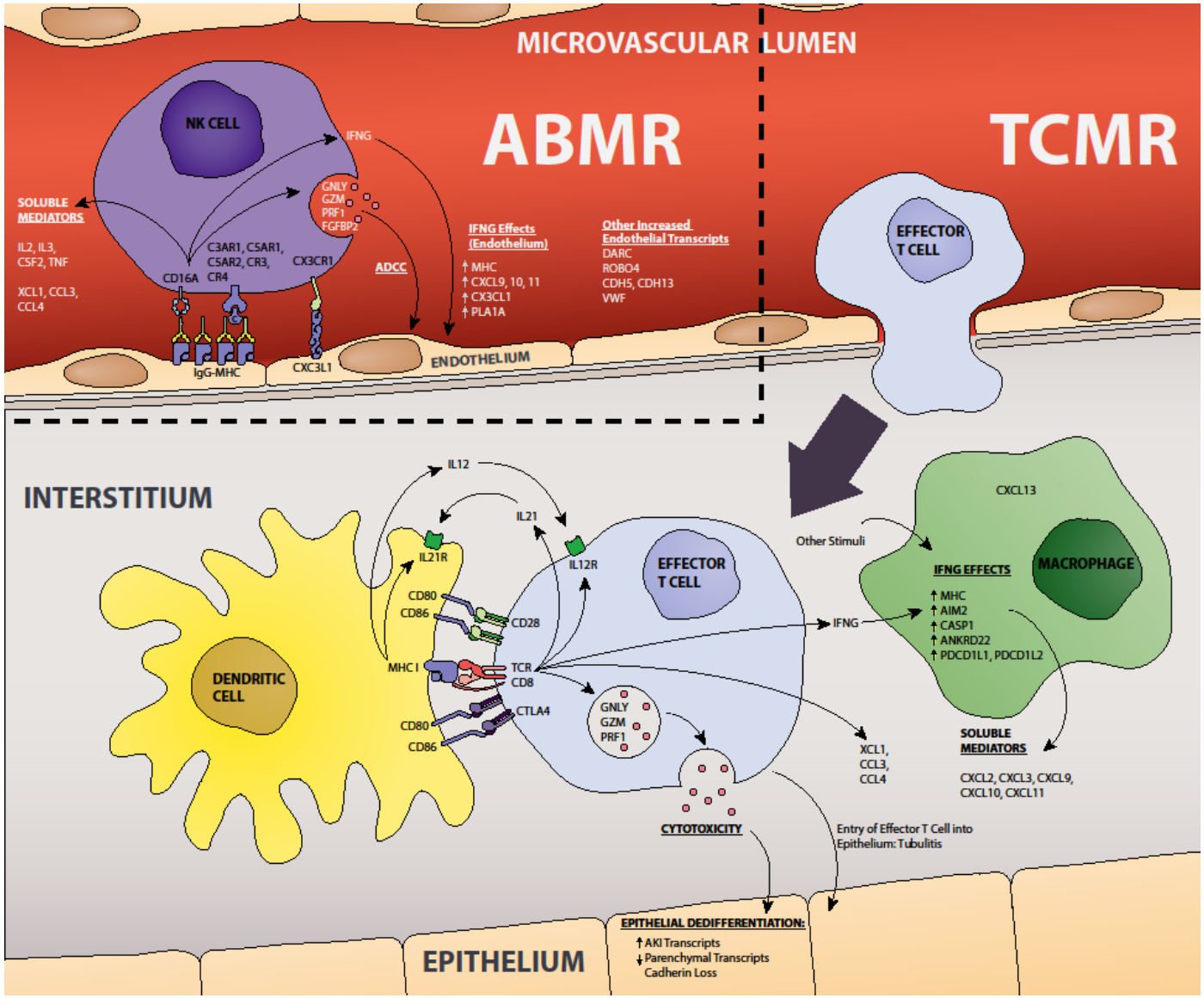

Figure 7.1—NK cell and T cell involvement in different compartments depending on the type of rejection.

Reference List

(1) Einecke G, Sis B, Reeve J, Mengel M, Hidalgo L, Kaplan B, et al. Antibody Mediated Microcirculation Damage Is the Major Cause of Late Kidney Transplant Loss. American Journal of Transplantation 9[s2], 383. 2009. Ref Type: Abstract

(2) Hidalgo LG, Sis B, Sellares J, Campbell PM, Mengel M, Einecke G, et al. NK cell transcripts and NK cells in kidney biopsies from patients with donor-specific antibodies: evidence for NK cell involvement in antibody-mediated rejection. Am J Transplant 2010;10(8):1812-22.

(3) Akiyoshi T, Hirohashi T, Alessandrini A, Chase CM, Farkash EA, Neal SR, et al. Role of complement and NK cells in antibody mediated rejection. Hum Immunol 2012 Jul 28;73(12):1226-32.

(4) Kiessling R, Klein E, Pross H, Wigzell H. "Natural" killer cells in the mouse. II. Cytotoxic cells with specificity for mouse Moloney leukemia cells. Characteristics of the killer cell. Eur J Immunol 1975 Feb;5(2):117-21.

(5) Lash GE, Robson SC, Bulmer JN. Review: Functional role of uterine natural killer (uNK) cells in human early pregnancy decidua. Placenta 2010 Mar;31 Suppl:S87-S92.

(6) Schroder K, Hertzog PJ, Ravasi T, Hume DA. Interferon-{gamma}: an overview of signals, mechanisms, and functions. J Leukoc Biol 2003 Oct 2.

(7) Kruse PH, Matta J, Ugolini S, Vivier E. Natural cytotoxicity receptors and their ligands. Immunol Cell Biol 2014 Mar;92(3):221-9.

(8) Mandelboim O, Lieberman N, Lev M, Paul L, Arnon TI, Bushkin Y, et al. Recognition of haemagglutinins on virus-infected cells by NKp46 activates lysis by human NK cells. Nature 2001 Feb 22;409(6823):1055-60.

(9) Venner JM, Hidalgo LG, Famulski KS, Chang J, Halloran PF. The molecular landscape of antibody-mediated kidney transplant rejection: Evidence for NK involvement through CD16a Fc receptors. Am J Transplant 2015;15(5):1336-48.

(10) Karre K, Ljunggren HG, Piontek G, Kiessling R. Selective rejection of H-2-deficient lymphoma variants suggests alternative immune defence strategy. Nature 1986 Feb 20;319(6055):675-8.

(11) Alcami A, Koszinowski UH. Viral mechanisms of immune evasion. Immunol Today 2000 Sep;21(9):447-55.

(12) Chervenak R, Wolcott RM. Target cell expression of MHC antigens is not (always) a turn-off signal to natural killer cells. J Immunol 1988 Jun 1;140(11):3712-6.

(13) Lanier LL. Up on the tightrope: natural killer cell activation and inhibition. Nat Immunol 2008 May;9(5):495-502.

(14) Raulet DH, Vance RE, McMahon CW. Regulation of the natural killer cell receptor repertoire. Annu Rev Immunol 2001;19:291-330.

(15) Lanier LL. NK cell recognition. Annu Rev Immunol 2005;23:225-74.

(16) Cheent KS, Jamil KM, Cassidy S, Liu M, Mbiribindi B, Mulder A, et al. Synergistic inhibition of natural killer cells by the nonsignaling molecule CD94. Proc Natl Acad Sci U S A 2013 Oct 15;110(42):16981-6.

(17) Nielsen N, Pascal V, Fasth AE, Sundstrom Y, Galsgaard ED, Ahern D, et al. Balance between activating NKG2D, DNAM-1, NKp44 and NKp46 and inhibitory CD94/NKG2A receptors determine natural killer degranulation towards rheumatoid arthritis synovial fibroblasts. Immunology 2014 Aug;142(4):581-93.

(18) Sasaki H, Xu XC, Mohanakumar T. HLA-E and HLA-G expression on porcine endothelial cells inhibit xenoreactive human NK cells through CD94/NKG2-dependent and -independent pathways. J Immunol 1999 Dec 1;163(11):6301-5.

(19) Kraemer T, Celik AA, Huyton T, Kunze-Schumacher H, Blasczyk R, Bade-Doding C. HLA-E: Presentation of a Broader Peptide Repertoire Impacts the Cellular Immune Response-Implications on HSCT Outcome. Stem Cells Int 2015;2015:346714.

(20) Waggoner SN, Kumar V. Evolving role of 2B4/CD244 in T and NK cell responses during virus infection. Front Immunol 2012;3:377.

(21) Eissmann P, Beauchamp L, Wooters J, Tilton JC, Long EO, Watzl C. Molecular basis for positive and negative signaling by the natural killer cell receptor 2B4 (CD244). Blood 2005 Jun 15;105(12):4722-9.

(22) Sivori S, Falco M, Marcenaro E, Parolini S, Biassoni R, Bottino C, et al. Early expression of triggering receptors and regulatory role of 2B4 in human natural killer cell precursors undergoing in vitro differentiation. Proc Natl Acad Sci U S A 2002 Apr 2;99(7):4526-31.

(23) Mathew SO, Rao KK, Kim JR, Bambard ND, Mathew PA. Functional role of human NK cell receptor 2B4 (CD244) isoforms. Eur J Immunol 2009 Jun;39(6):1632-41.

(24) Lanier LL. Natural killer cell receptor signaling. Curr Opin Immunol 2003 Jun;15(3):308-14.

(25) Hecht ML, Rosental B, Horlacher T, Hershkovitz O, De Paz JL, Noti C, et al. Natural cytotoxicity receptors NKp30, NKp44 and NKp46 bind to different heparan sulfate/heparin sequences. J Proteome Res 2009 Feb;8(2):712-20.

(26) Arnon TI, Lev M, Katz G, Chernobrov Y, Porgador A, Mandelboim O. Recognition of viral hemagglutinins by NKp44 but not by NKp30. Eur J Immunol 2001 Sep;31(9):2680-9.

(27) Augugliaro R, Parolini S, Castriconi R, Marcenaro E, Cantoni C, Nanni M, et al. Selective cross-talk among natural cytotoxicity receptors in human natural killer cells. Eur J Immunol 2003 May;33(5):1235-41.

(28) van de Winkel JGJ, Capel PJA. Human IgG Fc receptor heterogeneity: molecular aspects and clinical implications. Immunol Today 1993;14:215-21.

(29) Bruhns P, Iannascoli B, England P, Mancardi DA, Fernandez N, Jorieux S, et al. Specificity and affinity of human Fcgamma receptors and their polymorphic variants for human IgG subclasses. Blood 2009 Apr 16;113(16):3716-25.

(30) Lanier LL, Yu G, Phillips JH. Analysis of Fc gamma RIII (CD16) membrane expression and association with CD3 zeta and Fc epsilon RI-gamma by site-directed mutation. J Immunol 1991 Mar 1;146(5):1571-6.

(31) Li X, Baskin JG, Mangan EK, Su K, Gibson AW, Ji C, et al. The unique cytoplasmic domain of human FcgammaRIIIA regulates receptor-mediated function. J Immunol 2012 Nov 1;189(9):4284-94.

(32) Ting AT, Dick CJ, Schoon RA, Karnitz LM, Abraham RT, Leibson PJ. Interaction between lck and syk family tyrosine kinases in Fc gamma receptor-initiated activation of natural killer cells. J Biol Chem 1995 Jul 7;270(27):16415-21.

(33) Wang H, Kadlecek TA, Au-Yeung BB, Goodfellow HE, Hsu LY, Freedman TS, et al. ZAP-70: an essential kinase in T-cell signaling. Cold Spring Harb Perspect Biol 2010 May;2(5):a002279.

(34) Cassatella MA, Anegon I, Cuturi MC, Griskey P, Trinchieri G, Perussia B. Fc-Gamma-R(Cd16) Interaction with Ligand Induces Ca-2+ Mobilization and Phosphoinositide Turnover in Human Natural-Killer Cells - Role of Ca-2+ in Fc-Gamma-R(Cd16)-Induced Transcription and Expression of Lymphokine Genes. J Exp Med 1989 Feb 1;169(2):549-67.

(35) Aramburu J, Azzoni L, Rao A, Perussia B. Activation and expression of the nuclear factors of activated T cells, NFATp and NFATc, in human natural killer cells: regulation upon CD16 ligand binding. J Exp Med 1995;182:801-10.

(36) Kolch W. Meaningful relationships: the regulation of the Ras/Raf/MEK/ERK pathway by protein interactions. Biochem J 2000 Oct 15;351 Pt 2:289-305.

(37) Milella M, Gismondi A, Roncaioli P, Bisogno L, Palmieri G, Frati L, et al. CD16 cross-linking induces both secretory and extracellular signal-regulated kinase (ERK)-dependent cytosolic phospholipase A2 (PLA2) activity in human natural killer cells: involvement of ERK, but not PLA2, in CD16-triggered granule exocytosis. J Immunol 1997 Apr 1;158(7):3148-54.

(38) Foletta VC, Segal DH, Cohen DR. Transcriptional regulation in the immune system: all roads lead to AP-1. J Leukoc Biol 1998 Feb;63(2):139-52.

(39) Rao A, Luo C, Hogan PG. Transcription factors of the NFAT family: regulation and function. Ann Rev Immunol 1997;15:707-47.

(40) Jovanovic V, Dai X, Lim YT, Kemeny DM, Macary PA. Fc gamma receptor biology and systemic lupus erythematosus. Int J Rheum Dis 2009 Dec;12(4):293-8.

(41) Galandrini R, Palmieri G, Piccoli M, Frati L, Santoni A. Role for the Rac1 exchange factor Vav in the signaling pathways leading to NK cell cytotoxicity. J Immunol 1999 Mar 15;162(6):3148-52.

(42) Galandrini R, Micucci F, Tassi I, Cifone MG, Cinque B, Piccoli M, et al. Arf6: a new player in FcgammaRIIIA lymphocyte-mediated cytotoxicity. Blood 2005 Jul 15;106(2):577-83.

(43) Lanier LL, Ruitenberg JJ, Phillips JH. Functional and Biochemical-Analysis of Cd16 Antigen on Natural-Killer Cells and Granulocytes. Journal of Immunology 1988 Nov 15;141(10):3478-85.

(44) Sis B, Campbell PM, Mueller T, Hunter C, Cockfield SM, Cruz J, et al. Transplant glomerulopathy, late antibody-mediated rejection and the

ABCD tetrad in kidney allograft biopsies for cause. Am J Transplant 2007 Jul;7(7):1743-52.

(45) Sis B. Endothelial Molecules Decipher the Mechanisms and Functional Pathways in Antibody-Mediated Rejection. Hum Immunol 2012;73(12):1218-25.

(46) Mengel M, Sis B, Haas M, Colvin RB, Halloran PF, Racusen LC, et al. Banff 2011 Meeting Report: New Concepts in Antibody-Mediated Rejection. Am J Transplant 2012 Feb 2;12(3):563-70.

(47) Reeve J, Sellares J, Mengel M, Sis B, Skene A, Hidalgo L, et al. Molecular diagnosis of T cell-mediated rejection in human kidney transplant biopsies. Am J Transplant 2013;13(3):645-55.

(48) Reeve J, Einecke G, Mengel M, Sis B, Kayser N, Kaplan B, et al. Diagnosing rejection in renal transplants: a comparison of molecular- and histopathology-based approaches. Am J Transplant 2009 Aug;9(8):1802-10.

(49) Gould DS, Auchincloss H, Jr. Direct and indirect recognition: the role of MHC antigens in graft rejection. Immunology Today 1999 Feb;20(2):77-82.

(50) Zou GM, Tam YK. Cytokines in the generation and maturation of dendritic cells: recent advances. Eur Cytokine Netw 2002 Apr;13(2):186-99.

(51) Garcia KC, Degano M, Stanfield RL, Brunmark A, Jackson MR, Peterson PA, et al. An ab T cell receptor structure at 2.5 Å and its orientation in the TCR-MHC complex. Science 1996;274:209-19.

(52) Clevers H, Alarcon B, Wileman T, Terhorse C. The T-cell receptor/CD3 complex: a dynamic protein ensemble. Ann Rev Immunol 1988;6:629-62.

(53) Sussman JJ, Bonifacino JS, Lippincott-Schwartz J, Weissman AM, Saito T, Klausner RD, et al. Failure to synthesize the T cell CD3-zeta chain: structure and function of a partial T cell receptor complex. Cell 1988 Jan 15;52(1):85-95.

(54) Belz GT, Carbone FR, Heath WR. Cross-presentation of antigens by dendritic cells. Crit Rev Immunol 2002;22(5-6):439-48.

(55) Heath WR, Carbone FR. Cross-presentation, dendritic cells, tolerance and immunity. Annu Rev Immunol 2001;19:47-64.

(56) Bennett SR, Carbone FR, Karamalis F, Flavell RA, Miller JF, Heath WR. Help for cytotoxic-T-cell responses is mediated by CD40 signalling. Nature 1998 Jun 4;393(6684):478-80.

(57) Valenzuela J, Schmidt C, Mescher M. The roles of IL-12 in providing a third signal for clonal expansion of naive CD8 T cells. Journal of Immunology 2002 Dec 15;169(12):6842-9.

(58) Williams MA, Bevan MJ. Effector and memory CTL differentiation. Annu Rev Immunol 2007;25:171-92.

(59) Zhai Y, Meng L, Gao F, Busuttil RW, Kupiec-Weglinski JW. Allograft rejection by primed/memory CD8+ T cells is CD154 blockade resistant: therapeutic implications for sensitized transplant recipients. J Immunol 2002 Oct 15;169(8):4667-73.

(60) Wang B, Maile R, Greenwood R, Collins EJ, Frelinger JA. Naive CD8+ T cells do not require costimulation for proliferation and differentiation into cytotoxic effector cells. J Immunol 2000 Feb 1;164(3):1216-22.

(61) Sun JC, Bevan MJ. Defective CD8 T cell memory following acute infection without CD4 T cell help. Science 2003 Apr 11;300(5617):339-42.

(62) Kreisel D, Krupnick AS, Gelman AE, Engels FH, Popma SH, Krasinskas AM, et al. Non-hematopoietic allograft cells directly activate CD8+ T cells and trigger acute rejection: an alternative mechanism of allorecognition. Nat Med 2002 Mar;8(3):233-9.

(63) Rose ML. Endothelial cells as antigen-presenting cells: role in human transplant rejection. Cell Mol Life Sci 1998 Sep;54(9):965-78.

(64) Piotti G, Palmisano A, Maggiore U, Buzio C. Vascular endothelium as a target of immune response in renal transplant rejection. Front Immunol 2014;5:505.

(65) Savage CO, Hughes CC, Pepinsky RB, Wallner BP, Freedman AS, Pober JS. Endothelial cell lymphocyte function-associated antigen-3 and an unidentified ligand act in concert to provide costimulation to human peripheral blood CD4+ T cells. Cell Immunol 1991 Oct 1;137(1):150-63.

(66) Adams PW, Lee HA, Waldman J, Sedmak DD, Morgan CJ, Ward JS, et al. Alloantigenicity of human endothelial cells: I. Frequency and phenotype of human T helper lymphocytes that can react to endothelial cells. Journal of Immunology 1992;148:3753.

(67) Page C, Thompson C, Yacoub M, Rose M. Human endothelial stimulation of allogeneic T cells via a CTLA-4 independent pathway. Transpl Immunol 1994 Dec;2(4):342-7.

(68) Kreisel D, Krasinskas AM, Krupnick AS, Gelman AE, Balsara KR, Popma SH, et al. Vascular endothelium does not activate CD4+ direct allorecognition in graft rejection. J Immunol 2004 Sep 1;173(5):3027-34.

(69) Lagaaij EL, Cramer-Knijnenburg GF, van Kemenade FJ, van Es LA, Bruijn JA, van Krieken JH. Endothelial cell chimerism after renal transplantation and vascular rejection. Lancet 2001 Jan 6;357(9249):33-7.

(70) Ayasoufi K, Fan R, Fairchild RL, Valujskikh A. CD4 T Cell Help via B Cells Is Required for Lymphopenia-Induced CD8 T Cell Proliferation. J Immunol 2016 Apr 1;196(7):3180-90.

(71) Jones ND, Van MA, Hara M, Spriewald BM, Witzke O, Morris PJ, et al. CD40-CD40 ligand-independent activation of CD8+ T cells can trigger allograft rejection. J Immunol 2000 Jul 15;165(2):1111-8.

(72) Pietra BA, Wiseman A, Bolwerk A, Rizeq M, Gill RG. CD4 T cell-mediated cardiac allograft rejection requires donor but not host MHC class II. J Clin Invest 2000 Oct;106(8):1003-10.

(73) Bumgardner GL, Gao D, Li J, Baskin JH, Heininger M, Orosz CG. Rejection responses to allogeneic hepatocytes by reconstituted SCID mice, CD4, KO, and CD8 KO mice. Transplant 2000 Dec 27;70(12):1771-80.

(74) Newell KA, He G, Guo Z, Kim O, Szot GL, Rulifson I, et al. Cutting edge: blockade of the CD28/B7 costimulatory pathway inhibits intestinal allograft rejection mediated by CD4+ but not CD8+ T cells. J Immunol 1999 Sep 1;163(5):2358-62.

(75) Trambley J, Bingaman AW, Lin A, Elwood ET, Waitze SY, Ha J, et al. Asialo GM1(+) CD8(+) T cells play a critical role in costimulation blockade-resistant allograft rejection. J Clin Invest 1999 Dec;104(12):1715-22.

(76) Williams MA, Trambley J, Ha J, Adams AB, Durham MM, Rees P, et al. Genetic characterization of strain differences in the ability to mediate CD40/CD28-independent rejection of skin allografts. Journal of Immunology 2000 Dec 15;165(12):6849-57.

(77) Hwang KW, Sweatt WB, Brown IE, Blank C, Gajewski TF, Bluestone JA, et al. Cutting edge: targeted ligation of CTLA-4 in vivo by membrane-bound anti-CTLA-4 antibody prevents rejection of allogeneic cells. J Immunol 2002 Jul 15;169(2):633-7.

(78) Kirk AD, Harlan DM, Armstrong NN, Davis TA, Dong Y, Gray GS, et al. CTLA4-Ig and anti-CD40 ligand prevent renal allograft rejection in primates. Proc Natl Acad Sci USA 1997;94:8789-94.

(79) Ville S, Poirier N, Blancho G, Vanhove B. Co-Stimulatory Blockade of the CD28/CD80-86/CTLA-4 Balance in Transplantation: Impact on Memory T Cells? Front Immunol 2015;6:411.

(80) Krummey SM, Cheeseman JA, Conger JA, Jang PS, Mehta AK, Kirk AD, et al. High CTLA-4 expression on Th17 cells results in increased sensitivity to CTLA-4 coinhibition and resistance to belatacept. Am J Transplant 2014 Mar;14(3):607-14.

(81) Fox WM, III, Hameed A, Hutchins GM, Reitz BA, Baumgartner WA, Beschorner WE, et al. Perforin expression localizing cytotoxic lymphocytes in the intimas of coronary arteries with transplant-related accelerated arteriosclerosis. Hum Pathol 1993 May;24(5):477-82.

(82) Zheng L, Ben LH, Pober JS, Bothwell AL. Porcine endothelial cells, unlike human endothelial cells, can be killed by human CTL via Fas ligand and cannot be protected by Bcl-2. J Immunol 2002 Dec 15;169(12):6850-5.

(83) Sleater M, Diamond AS, Gill RG. Islet allograft rejection by contact-dependent CD8+ T cells: perforin and FasL play alternate but obligatory roles. Am J Transplant 2007 Aug;7(8):1927-33.

(84) Einecke G, Fairhead T, Hidalgo LG, Sis B, Turner P, Zhu LF, et al. Tubulitis and Epithelial Cell Alterations in Mouse Kidney Transplant Rejection Are Independent of CD103, Perforin or Granzymes A/B. Am J Transplant 2006;6(9):2109-20.

(85) Bruewer M, Utech M, Ivanov AI, Hopkins AM, Parkos CA, Nusrat A. Interferon-gamma induces internalization of epithelial tight junction proteins via a macropinocytosis-like process. FASEB J 2005 Jun;19(8):923-33.

(86) Koh KP, Wang Y, Yi T, Shiao SL, Lorber MI, Sessa WC, et al. T cell-mediated vascular dysfunction of human allografts results from IFN-gamma dysregulation of NO synthase. J Clin Invest 2004 Sep;114(6):846-56.

(87) Sprague AH, Khalil RA. Inflammatory cytokines in vascular dysfunction and vascular disease. Biochem Pharmacol 2009 Sep 15;78(6):539-52.

(88) Venner JM, Famulski K, Badr D, Hidalgo LG, Chang J, Halloran PF. Molecular landscape of T cell-mediated rejection in human kidney transplants: Prominence of CTLA4 and PD ligands. Am J Transplant 2014;14(11):2565-76.

(89) Halloran PF, Miller LW, Urmson J, Ramassar V, Zhu LF, Kneteman NM, et al. IFN-gamma alters the pathology of graft rejection: protection from early necrosis. Journal of Immunology 2001 Jun 15;166(12):7072-81.

(90) Miura M, Morita K, Kobayashi H, Hamilton TA, Burdick MD, Strieter RM, et al. Monokine induced by IFN-gamma is a dominant factor directing T cells into murine cardiac allografts during acute rejection. Journal of Immunology 2001 Sep 15;167(6):3494-504.

(91) Hidalgo LG, Einecke G, Allanach K, Halloran PF. The transcriptome of human cytotoxic T cells: similarities and disparities among allostimulated CD4(+) CTL, CD8(+) CTL and NK cells. Am J Transplant 2008 Mar;8(3):627-36.

(92) Watzl C, Long EO. Signal transduction during activation and inhibition of natural killer cells. Curr Protoc Immunol 2010 Aug;Chapter 11:Unit.

(93) Chu DH, Morita CT, Weiss A. The Syk family of protein tyrosine kinases in T-cell activation and development. Immunol Rev 1998 Oct;165:167-80.

(94) Macian F, Lopez-Rodriguez C, Rao A. Partners in transcription: NFAT and AP-1. Oncogene 2001 Apr 30;20(19):2476-89.

(95) Ponti C, Gibellini D, Boin F, Melloni E, Manzoli FA, Cocco L, et al. Role of CREB transcription factor in c-fos activation in natural killer cells. Eur J Immunol 2002 Dec;32(12):3358-65.

(96) Kaiser M, Wiggin GR, Lightfoot K, Arthur JS, Macdonald A. MSK regulate TCR-induced CREB phosphorylation but not immediate early gene transcription. Eur J Immunol 2007 Sep;37(9):2583-95.

(97) Zhou J, Zhang J, Lichtenheld MG, Meadows GG. A role for NF-kappa B activation in perforin expression of NK cells upon IL-2 receptor signaling. J Immunol 2002 Aug 1;169(3):1319-25.

(98) Sica A, Dorman L, Viggiano V, Cippitelli M, Ghosh P, Rice N, et al. Interaction of NF-kappaB and NFAT with the interferon-gamma promoter. J Biol Chem 1997 Nov 28;272(48):30412-20.

(99) Young HA. Regulation of interferon-gamma gene expression. J Interfer Cytokine Res 1996 Aug;16(8):563-8.

(100) Tsai EY, Jain J, Pesavento PA, Rao A, Goldfeld AE. Tumor necrosis factor alpha gene regulation in activated T cells involves ATF-2/Jun and NFATp. Mol Cell Biol 1996 Feb;16(2):459-67.

(101) Falvo JV, Tsytsykova AV, Goldfeld AE. Transcriptional control of the TNF gene. Curr Dir Autoimmun 2010;11:27-60.

(102) Haas M, Sis B, Racusen LC, Solez K, Glotz D, Colvin RB, et al. Banff 2013 Meeting Report: Inclusion of C4d-Negative Antibody-Mediated Rejection and Antibody-Associated Arterial Lesions. Am J Transplant 2014;14(2):272-83.

(103) Sis B, Halloran PF. Endothelial transcripts uncover a previously unknown phenotype: C4d-negative antibody-mediated rejection. Curr Opin Organ Transplant 2010 Feb;15(1):42-8.

(104) Salazar ID, Merino LM, Chang J, Halloran PF. Reassessing the Significance of Intimal Arteritis in Kidney Transplant Biopsy Specimens. J Am Soc Nephrol 2015 Dec;26(12):3190-8.

(105) Reeve J, Chang J, Salazar IDR, Lopez MM, Halloran PF. Using molecular phenotyping to guide improvements in the histologic diagnosis of T cell-mediated rejection. Am J Transplant 2016;16(4):1183-92.

(106) Halloran PF, Merino LM, Barreto PA. Identifying Subphenotypes of Antibody-Mediated Rejection in Kidney Transplants. Am J Transplant 2016 Mar;16(3):908-20.

(107) Sellares J, Reeve J, Loupy A, Mengel M, Sis B, Skene A, et al. Molecular diagnosis of antibody-mediated rejection in human kidney transplants. Am J Transplant 2013;13(4):971-83.

(108) Halloran PF, Pereira AB, Chang J, Matas A, Picton M, De Freitas D, et al. Microarray diagnosis of antibody-mediated rejection in kidney transplant biopsies: an international prospective study (INTERCOM). Am J Transplant 2013;13(11):2865-74.

(109) Goes N, Urmson J, Ramassar V, Halloran PF. Ischemic acute tubular necrosis induces an extensive local cytokine response: evidence for induction of interferon-g, transforming growth factorb-1, granulocyte-macrophage colony-stimulating factor, interleukin-2 and interleukin-10. Transplant 1995;59:565-72.

(110) Halloran PF, Famulski K, Reeve J. The molecular phenotypes of rejection in kidney transplant biopsies. Current Opinion In Organ Transplantation 2015;20(3):359-67.

(111) Suviolahti E, Ge S, Nast CC, Mirocha J, Karasyov K, White M, et al. Genes associated with antibody-dependent cell activation are overexpressed in

renal biopsies from patients with antibody-mediated rejection. Transpl Immunol 2015;32(1):9-17.

(112) Djamali A, Kaufman DB, Ellis TM, Zhong W, Matas A, Samaniego M. Diagnosis and management of antibody-mediated rejection: current status and novel approaches. Am J Transplant 2014 Feb;14(2):255-71.

(113) Maurer M, von SE. Macrophage inflammatory protein-1. Int J Biochem Cell Biol 2004 Oct;36(10):1882-6.

(114) Hamilton JA. Colony-stimulating factors in inflammation and autoimmunity. Nat Rev Immunol 2008 Jul;8(7):533-44.

(115) Robertson MJ. Role of chemokines in the biology of natural killer cells. J Leukoc Biol 2002 Feb;71(2):173-83.

(116) Menten P, Wuyts A, Van DJ. Macrophage inflammatory protein-1. Cytokine Growth Factor Rev 2002 Dec;13(6):455-81.

(117) Hedrick JA, Saylor V, Figueroa D, Mizoue L, Xu Y, Menon S, et al. Lymphotactin is produced by NK cells and attracts both NK cells and T cells in vivo. J Immunol 1997 Feb 15;158(4):1533-40.

(118) Castellino F, Huang AY, tan-Bonnet G, Stoll S, Scheinecker C, Germain RN. Chemokines enhance immunity by guiding naive CD8+ T cells to sites of CD4+ T cell-dendritic cell interaction. Nature 2006 Apr 13;440(7086):890-5.

(119) Kennedy J, Kelner GS, Kleyensteuber S, Schall TJ, Weiss MC, Yssel H, et al. Molecular cloning and functional characterization of human lymphotactin. J Immunol 1995 Jul 1;155(1):203-9.

(120) Bonville CA, Percopo CM, Dyer KD, Gao J, Prussin C, Foster B, et al. Interferon-gamma coordinates CCL3-mediated neutrophil recruitment in vivo. BMC Immunol 2009;10:14.

(121) Schroder K, Hertzog PJ, Ravasi T, Hume DA. Interferon-gamma: an overview of signals, mechanisms and functions. J Leukoc Biol 2004 Feb;75(2):163-89.

(122) Matsumiya T, Ota K, Imaizumi T, Yoshida H, Kimura H, Satoh K. Characterization of synergistic induction of CX3CL1/fractalkine by TNF-alpha and IFN-gamma in vascular endothelial cells: an essential role for TNF-alpha in post-transcriptional regulation of CX3CL1. J Immunol 2010 Apr 15;184(8):4205-14.

(123) Ohmori Y, Schreiber RD, Hamilton TA. Synergy between interferon-gamma and tumor necrosis factor-alpha in transcriptional activation is mediated by cooperation between signal transducer and activator of transcription 1 and nuclear factor kappaB. J Biol Chem 1997 Jun 6;272(23):14899-907.

(124) Pukel C, Baquerizo H, Rabinovitch A. Destruction of rat islet cell monolayers by cytokines. Synergistic interactions of interferon-g, tumor necrosis factor, lymphotoxin, and interleukin 1. Diabetes 1988;37:133-6.

(125) Williamson BD, Carswell EA, Rubin BY, Prendergast JS, Old LJ. Human tumor necrosis factor produced by human B-cell lines: synergistic cytotoxic interaction with human interferon. Proc Natl Acad Sci U S A 1983 Sep;80(17):5397-401.

(126) Yui J, Garcia-Lloret M, Wegmann TG, Guilbert LJ. Cytotoxicity of tumour necrosis factor-alpha and gamma-interferon against primary human placental trophoblasts. Placenta 1994 Dec;15(8):819-35.

(127) Fogler WE, Volker K, McCormick KL, Watanabe M, Ortaldo JR, Wiltrout RH. NK cell infiltration into lung, liver, and subcutaneous B16 melanoma is mediated by VCAM-1/VLA-4 interaction. J Immunol 1996 Jun 15;156(12):4707-14.

(128) Glas R, Franksson L, Une C, Eloranta ML, Ohlen C, Orn A, et al. Recruitment and activation of natural killer (NK) cells in vivo determined by the target cell phenotype. An adaptive component of NK cell-mediated responses. J Exp Med 2000 Jan 3;191(1):129-38.

(129) Pober JS, Gimbrone Jr. MA, Lapierre LA, Mendrick DL, Fiers W, Rothlein R, et al. Overlapping patterns of activation of human endothelial cells by interleukin 1, tumor necrosis factor, and immune interferon. Journal of Immunology 1986;137:1893-6.

(130) Muczynski KA, Ekle DM, Coder DM, Anderson SK. Normal human kidney HLA-DR-expressing renal microvascular endothelial cells: characterization, isolation, and regulation of MHC class II expression. J Am Soc Nephrol 2003 May;14(5):1336-48.

(131) Imaizumi T, Matsumiya T, Fujimoto K, Okamoto K, Cui X, Ohtaki U, et al. Interferon-gamma stimulates the expression of CX3CL1/fractalkine in cultured human endothelial cells. Tohoku J Exp Med 2000 Oct;192(2):127-39.

(132) Imaizumi T, Yoshida H, Satoh K. Regulation of CX3CL1/fractalkine expression in endothelial cells. J Atheroscler Thromb 2004;11(1):15-21.

(133) Jones BA, Beamer M, Ahmed S. Fractalkine/CX3CL1: a potential new target for inflammatory diseases. Mol Interv 2010 Oct;10(5):263-70.

(134) Chui R, Dorovini-Zis K. Regulation of CCL2 and CCL3 expression in human brain endothelial cells by cytokines and lipopolysaccharide. J Neuroinflammation 2010;7:1.

(135) Marfaing-Koka A, Devergne O, Gorgone G, Portier A, Schall TJ, Galanaud P, et al. Regulation of the production of the RANTES chemokine by endothelial cells. Synergistic induction by IFN-gamma plus TNF-alpha and inhibition by IL-4 and IL-13. J Immunol 1995 Feb 15;154(4):1870-8.

(136) Kitaya K, Yasuo T, Yamaguchi T, Fushiki S, Honjo H. Genes regulated by interferon-gamma in human uterine microvascular endothelial cells. Int J Mol Med 2007 Nov;20(5):689-97.

(137) Luster AD, Unkeless JC, Ravetch JV. g-interferon transcriptionally regulates an early-response gene containing homology to platelet proteins. Nature 1985;315:672-6.

(138) Tu TC, Brown NK, Kim TJ, Wroblewska J, Yang X, Guo X, et al. CD160 is essential for NK-mediated IFN-gamma production. J Exp Med 2015 Mar 9;212(3):415-29.

(139) Barakonyi A, Rabot M, Marie-Cardine A, guerre-Girr M, Polgar B, Schiavon V, et al. Cutting edge: Engagement of CD160 by its HLA-C physiological ligand triggers a unique cytokine profile secretion in the cytotoxic peripheral blood NK cell subset. Journal of Immunology 2004 Nov 1;173(9):5349-54.

(140) Le BP, Tabiasco J, Polgar B, Kozma N, Giustiniani J, Siewiera J, et al. CD160: a unique activating NK cell receptor. Immunol Lett 2011 Aug 30;138(2):93-6.

(141) Le BP, Barakonyi A, Giustiniani J, Lenfant F, Marie-Cardine A, guerre-Girr M, et al. Engagement of CD160 receptor by HLA-C is a triggering mechanism used by circulating natural killer (NK) cells to mediate cytotoxicity. Proc Natl Acad Sci U S A 2002 Dec 24;99(26):16963-8.

(142) Fehniger TA, Caligiuri MA. Interleukin 15: biology and relevance to human disease. Blood 2001 Jan 1;97(1):14-32.

(143) Giustiniani J, Marie-Cardine A, Bensussan A. A soluble form of the MHC class I-specific CD160 receptor is released from human activated NK lymphocytes and inhibits cell-mediated cytotoxicity. J Immunol 2007 Feb 1;178(3):1293-300.

(144) Boles KS, Barchet W, Diacovo T, Cella M, Colonna M. The tumor suppressor TSLC1/NECL-2 triggers NK-cell and CD8+ T-cell responses through the cell-surface receptor CRTAM. Blood 2005 Aug 1;106(3):779-86.

(145) Tatsumi K, Taatjes DJ, Wadsworth MP, Bouchard BA, Bovill EG. Cell adhesion molecule 1 (CADM1) is ubiquitously present in the endothelium and smooth muscle cells of the human macro- and micro-vasculature. Histochem Cell Biol 2012 Nov;138(5):815-20.

(146) Arase N, Takeuchi A, Unno M, Hirano S, Yokosuka T, Arase H, et al. Heterotypic interaction of CRTAM with Necl2 induces cell adhesion on activated NK cells and CD8+ T cells. Int Immunol 2005 Sep;17(9):1227-37.

(147) Alcon VL, Luther C, Balce D, Takei F. B-cell co-receptor CD72 is expressed on NK cells and inhibits IFN-gamma production but not cytotoxicity. Eur J Immunol 2009 Mar;39(3):826-32.

(148) Topham NJ, Hewitt EW. Natural killer cell cytotoxicity: how do they pull the trigger? Immunology 2009 Sep;128(1):7-15.

(149) Lenhoff S, Olofsson T. Cytokine regulation of GM-CSF and G-CSF secretion by human umbilical cord vein endothelial cells (HUVEC). Cytokine 1996 Sep;8(9):702-9.

(150) Bluman EM, Bartynski KJ, Avalos BR, Caligiuri MA. Human natural killer cells produce abundant macrophage inflammatory protein-1 alpha in response to monocyte-derived cytokines. J Clin Invest 1996 Jun 15;97(12):2722-7.

(151) Ramanan P, Razonable RR. Cytomegalovirus infections in solid organ transplantation: a review. Infect Chemother 2013 Sep;45(3):260-71.

(152) Schlums H, Cichocki F, Tesi B, Theorell J, Beziat V, Holmes TD, et al. Cytomegalovirus infection drives adaptive epigenetic diversification of NK cells with altered signaling and effector function. Immunity 2015 Mar 17;42(3):443-56.

(153) Zhang T, Scott JM, Hwang I, Kim S. Cutting edge: antibody-dependent memory-like NK cells distinguished by FcRgamma deficiency. J Immunol 2013 Feb 15;190(4):1402-6.

(154) Lynch RJ, Silva IA, Chen BJ, Punch JD, Cascalho M, Platt JL. Cryptic B cell response to renal transplantation. Am J Transplant 2013 Jul;13(7):1713-23.

(155) Barao I. The TNF receptor-ligands 4-1BB-4-1BBL and GITR-GITRL in NK cell responses. Front Immunol 2012;3:402.

(156) Mueller TF, Einecke G, Reeve J, Sis B, Mengel M, Jhangri.G., et al. Microarray analysis of rejection in human kidney transplants using pathogenesis-based transcript sets. Am J Transplant 2007;7(12):2712-22.

(157) van BJ, Trowsdale J. Ligand specificity of Killer cell Immunoglobulin-like Receptors: a brief history of KIR. Front Immunol 2012;3:394.

(158) Garcia-Beltran WF, Holzemer A, Martrus G, Chung AW, Pacheco Y, Simoneau CR, et al. Open conformers of HLA-F are high-affinity ligands of the activating NK-cell receptor KIR3DS1. Nat Immunol 2016 Sep;17(9):1067-74.

(159) Shiomi A, Usui T. Pivotal roles of GM-CSF in autoimmunity and inflammation. Mediators Inflamm 2015;2015:568543.

(160) Boehm U, Klamp T, Groot M, Howard JC. Cellular responses to interferon-g. Ann Rev Immunol 1997;15:749-95.

(161) Oliva A, Kinter AL, Vaccarezza M, Rubbert A, Catanzaro A, Moir S, et al. Natural killer cells from human immunodeficiency virus (HIV)-infected individuals are an important source of CC-chemokines and suppress HIV-1 entry and replication in vitro. J Clin Invest 1998 Jul 1;102(1):223-31.

(162) Annunziato F, Galli G, Nappi F, Cosmi L, Manetti R, Maggi E, et al. Limited expression of R5-tropic HIV-1 in CCR5-positive type 1-polarized T cells explained by their ability to produce RANTES, MIP-1alpha, and MIP-1beta. Blood 2000 Feb 15;95(4):1167-74.

(163) Fauriat C, Long EO, Ljunggren HG, Bryceson YT. Regulation of human NK-cell cytokine and chemokine production by target cell recognition. Blood 2010 Mar 18;115(11):2167-76.

(164) Brehm MA, Daniels KA, Welsh RM. Rapid production of TNF-alpha following TCR engagement of naive CD8 T cells. J Immunol 2005 Oct 15;175(8):5043-9.

(165) Bryceson YT, March ME, Ljunggren HG, Long EO. Synergy among receptors on resting NK cells for the activation of natural cytotoxicity and cytokine secretion. Blood 2006 Jan 1;107(1):159-66.

(166) Carpio VN, Noronha IL, Martins HL, Jobim LF, Gil BC, Kulzer AS, et al. Expression patterns of B cells in acute kidney transplant rejection. Exp Clin Transplant 2014 Oct;12(5):405-14.

(167) Alegre ML, Florquin S, Goldman M. Cellular mechanisms underlying acute graft rejection: time for reassessment. Curr Opin Immunol 2007 Oct;19(5):563-8.

(168) Einecke G, Reeve J, Mengel M, Sis B, Bunnag S, Mueller TF, et al. Expression of B cell and immunoglobulin transcripts is a feature of inflammation in late allografts. Am J Transplant 2008 Jul;8(7):1434-43.

(169) Popow I, Leitner J, Grabmeier-Pfistershammer K, Majdic O, Zlabinger GJ, Kundi M, et al. A comprehensive and quantitative analysis of the major specificities in rabbit antithymocyte globulin preparations. Am J Transplant 2013 Dec;13(12):3103-13.

(170) Pascual J, Zuckermann A, Djamali A, Hertig A, Naesens M. Rabbit antithymocyte globulin and donor-specific antibodies in kidney transplantation - A review. Transplant Rev (Orlando) 2016 Feb 18.